Calhoun: The NPS Institutional Archive
DSpace Repository

Theses and Dissertations 1. Thesis and Dissertation Collection, all items

1971

Performance analysis of a turbo-type energy absorber for an aircraft carrier arresting gear.

Rolek, Leo Stanley.

Monterey, California ; Naval Postgraduate School

http://hdl.handle.net/10945/15851

Downloaded from NPS Archive: Calhoun

Calhoun is the Naval Postgraduate School's public access digital repository for research materials and institutional publications created by the NPS community. Calhoun is named for Professor of Mathematics Guy K. Calhoun, NPS's first appointed -- and published -- scholarly author.

Dudley Knox Library / Naval Postgraduate School
411 Dyer Road / 1 University Circle
Monterey, California USA 93943

http://www.nps.edu/library

PERFORMANCE ANALYSIS OF A TURBO-TYPE ENERGY ABSORBER FOR AN AIRCRAFT CARRIER ARRESTING GEAR

Leo Stanley Rolek

United States
Naval Postgraduate School

THESIS

PERFORMANCE ANALYSIS OF A TURBO-TYPE ENERGY ABSORBER FOR AN AIRCRAFT CARRIER ARRESTING GEAR

by

Leo Stanley Rolek, Jr.

T140751

June 1971

Approved for public release; distribution unlimited.

LIBRARY
NAVAL POSTGRADUATE SCHOOL
MONTEREY, CALIF. 93940

Performance Analysis of a Turbo-Type Energy Absorber for an Aircraft Carrier Arresting Gear

by

Leo Stanley Rolek, Jr.
Ensign, United States Navy
B.S.A.E., United States Naval Academy, 1970

Submitted in partial fulfillment of the
requirements for the degree of

MASTER OF SCIENCE IN AERONAUTICAL ENGINEERING

from the

NAVAL POSTGRADUATE SCHOOL
June 1971

Thesis
R58995
c.1

LIBRARY
NAVAL POSTGRADUATE SCHOOL
MONTEREY, CALIF. 93940

ABSTRACT

The increasing weight and speed of carrier based aircraft are taxing the limit of conventional piston type energy absorbers which are used for arresting gear. Turbo-type absorbers have been proposed as an alternative. This study investigates a turbo-type energy absorber for an aircraft arresting gear under development by the Naval Air Engineering Center. A mathematical analysis, computer simulation and performance prediction are given for each mode of operation. It was initially expected that the absorber could operate in just two modes, forward and reverse, but the analysis shows that four distinct modes are possible, since not only shaft rotation but the path of fluid flow can be reversed. Theoretical performance predictions are also compared with test data from an existing smaller scale version of the absorber. The agreement is excellent. An approximation of scaling effects on power absorption is also presented. It is concluded that the turbo-type absorber is basically adequate to meet the demands of carrier operation for the forseeable future.

TABLE OF CONTENTS

I. INTRODUCTION - 12

II. DESIGN VALUES AND CONSIDERATIONS - - - - - - - - - - - - - 15

III. ANALYSIS OF THE PROBLEM - - - - - - - - - - - - - - - - - 21

A. MODES OF OPERATION - - - - - - - - - - - - - - - - - - - 21

B. DIMENSIONAL ANALYSIS - - - - - - - - - - - - - - - - - - 29

C. ENERGY BALANCE AT EQUILIBRIUM - - - - - - - - - - - - - 31

D. MODEL TESTING - 34

E. ASSUMPTIONS AND LIMITATIONS OF THE ANALYSIS - - - - - 35

IV. RESULTS AND DISCUSSION - - - - - - - - - - - - - - - - - - 38

V. CONCLUSIONS AND RECOMMENDATIONS - - - - - - - - - - - - - 47

APPENDIX A Detailed Analysis of the Energy Absorber with the Fluid Circulating in the Normal Direction, Mode 1 and 2 - 48

APPENDIX B Detailed Analysis of the Energy Absorber with the Fluid Circulating in the Reverse Direction, Modes 1 and 2 - 82

APPENDIX C Program NORMAL - - - - - - - - - - - - - - - - - - - 88

APPENDIX D Program REVERSE - - - - - - - - - - - - - - - - - - 110

LIST OF REFERENCES - 129

INITIAL DISTRIBUTION LIST - - - - - - - - - - - - - - - - - - - 130

FORM DD 1473 - 131

LIST OF TABLES

Table		Page
I	Parameters of the Absorber	18
II	Modes of Operation	21
III	Detailed List of Results for All Modes of the Absorber	42
IV	Flow Chart for Computer Programs NORMAL and REVERSE	90

LIST OF FIGURES

Figure Page

1. Overall Schematic, Programmed Drum Arresting Gear - - - 14

2. Schematic of Energy Absorber - - - - - - - - - - - - - - 16

3. Diagram of Absorber Bladings - - - - - - - - - - - - - - 17

4. Velocity Diagrams for Mode 1 - - - - - - - - - - - - - - 23

5. Velocity Diagrams for Mode 2 - - - - - - - - - - - - - - 24

6. Velocity Diagrams for Mode 3 - - - - - - - - - - - - - - 25

7. Velocity Diagrams for Mode 4 - - - - - - - - - - - - - - 26

8. Total Enthalpy-Entropy Diagram for Modes 1 and 2 - - - 27

9. Total Enthalpy-Entropy Diagram for Modes 3 and 4 - - - 28

10. Energy Balance for Equilibrium for Normal Flow - - - - 32

11. Energy Balance for Equilibrium for Reverse Flow - - - 33

12. Power Coefficient versus Rotational Speed - - - - - - - 39

13. Power versus Shaft Speed - - - - - - - - - - - - - - - - 40

14. Maximum Power Coefficient versus Maximum Reynolds Number - 41

15. Estimate of Loss Coefficient ξ - - - - - - - - - - - - - 75

16. Estimated Channel Wall Friction Factor λ_f - - - - - - - - 77

TABLE OF SYMBOLS

Symbol	FORTRAN	Definition	Units
Latin			
a	- - - -	Opening at blade exit	ft
b	B	Blade height	ft
c_f	CF	Local skin friction coefficient	- - - -
c_ℓ	CL	Pressure loss coefficient for lower passage	- - - -
c_p	CP	Specific heat of fluid	BTU/lb/^{o}R
C_u	CU	Pressure loss coefficient for upper passage	- - - -
D_h	- - - -	Hydraulic diameter	ft
h	- - - -	Static enthalpy	ft-lb/slug
H	H	Total head	ft-lb/slug
H_T	- - - -	Total enthalpy	ft-lb/slug
i_R	IR	Rotor incidence angle	degree
i_S	IS	Stator incidence angle	degree
K_B	KB	Blockage factor	- - - -
L_ℓ	LL	Length of meridional contour of lower passage	ft
L_u	LU	Length of meridional contour of upper passage	ft
$\dot{m}$	- - - -	Mass flow rate	slugs/sec
M_f	- - - -	Frictional moment	lb-ft
p	SP	Static pressure	lb/ft^2
P_E	- - - -	Equivalent relative total enthalpy	ft^2/sec^2

Symbol	FORTRAN	Definition	Units
$\mathcal{P}$	- - - -	Power	lb-ft/sec
$\mathcal{P}_{ref}$	POWREF	Reference power	lb-ft/sec
P_T	TP	Total pressure	lb/ft^2
R	R	Radius	ft
r_i	RI	Radius of curvature of inner contour of passage	in
R_{Ne}	- - - -	Effective Reynolds number	- - - -
R_{Nl}	REL	Reynolds number lower passage	- - - -
R_{NR}	RER	Reynolds number rotor	- - - -
R_{NS}	RES	Reynolds number stator	- - - -
R_{Nu}	REU	Reynolds number upper passage	- - - -
$\mathscr{s}$	- - - -	Blade spacing	ft
r_o	- - - -	Radius of curvature of outer contour of passage	in
T_R	TORQUE	Torque exerted on fluid by rotor	lb-ft
T_{Rref}	TORREF	Reference torque	lb-ft
T_S	- - - -	Torque exerted on fluid by stator	lb-ft
u	- - - -	Internal energy	ft-lb/slug
U	- - - -	Peripheral velocity of blade	ft/sec
V	V	Absolute velocity	ft/sec
V'	- - - -	Useful absolute velocity	ft/sec
V_M	VM	Meridional component of absolute velocity	ft/sec
V_u	VU	Peripheral component of absolute velocity	ft/sec
W	W	Relative velocity	ft/sec
W'	- - - -	Useful relative velocity	ft/sec

Symbol	FORTRAN	Definition	Units
W_i	- - - -	Relative velocity lost due to incidence	ft/sec
W_u	WU	Peripheral component of relative velocity	ft/sec
Y_R	YR	Rotor blade loss factor	- - - -
Y_S	YS	Stator blade loss factor	- - - -
Greek			
α	ALPHA	Absolute flow angle	degree
α_{3B}	A3B	Tangent to stator blade mean camber line at station 3	degree
Λ_R	AAR	Aspect ratio of rotor	- - - -
Λ_S	ARS	Aspect ratio of stator	- - - -
α_{4B}	A4B	Tangent to stator blade mean camber line at station 4	degree
β	BETA	Relative flow angle	degree
β_{1B}	B1B	Tangent to rotor blade mean camber line at station 1	degree
β_{2B}	B2B	Tangent to rotor blade mean camber line at station 2	degree
Δ	DEL	Change	- - - -
ξ_ℓ	ZETAL	Channel bending loss coefficient for lower passage	- - - -
ξ_u	ZETAU	Channel bending loss coefficient for upper passage	- - - -
η_{Mu}	ETAMU	Friction efficiency for upper passage	- - - -
$\eta_{M\ell}$	ETAML	Friction efficiency for lower passage	- - - -
η_R	- - - -	Rotor efficiency	- - - -

Symbol	FORTRAN	Definition	Units
λ_f	LMBD	Wall friction factor in straight ducts	- - - -
λ_ℓ	LAMDAL	Friction coefficient for lower passage	- - - -
λ_u	LAMDAU	Friction coefficient for upper passage	- - - -
ν	NU	Kinematic viscosity	ft^2/sec
Π_H	- - - -	Dimensionless head	- - - -
$\Pi_{\mathcal{P}}$	PIPOWR	Reference power	lb-ft/sec
Π_T	PITORQ	Dimensionless Torque	- - - -
Π_ω	PIOM	Reference rotational speed	- - - -
ρ	RHO	Fluid density	$slugs/ft^3$
τ_R	TAUR	Dimensionless torque coefficient	- - - -
τ_o	- - - -	Wall shear stress	lb/ft^2
Φ	PHI	Flow coefficient used in Program NORMAL	- - - -
Φ'	PHI	Convenient flow coefficient used in program REVERSE	- - - -
Ψ	PSI	Velocity coefficient	- - - -
ω	OM	Rotational speed	rad/sec
ω_{ref}	OMREF	Reference rotational speed	rad/sec

Subscripts

R	Rotor
S	Stator
ℓ	Lower passage
u	Upper passage
o	Outer passage
i	Inner passage
TH	Theoretical
MAX	Maximum value
ref	Reference value
1	Rotor inlet
2	Rotor discharge
3	Stator inlet
4	Stator discharge

Superscript

$'$	Useful component

ACKNOWLEDGEMENTS

The author gratefully acknowledges the assistance provided in this investigation by the following persons:

Professor T. H. Gawain of the Naval Postgraduate School, the thesis advisor, whose understanding and patience made the learning process most gratifying. His insight and guidance insured the worth of this thesis.

Professor Michael H. Vavra of the Naval Postgraduate School who developed the original analysis of the absorber. Without his help and inspiration this thesis would not have been possible.

Mr. Wayne Gallant and the staff of Section SI of the Naval Air Engineering Center in Philadelphia, Pennsylvania. These men kindly provided the background material, supporting information on the M-21 absorber, test data, and the original computer simulation of the analysis. Their full cooperation was most beneficial.

I. INTRODUCTION

Over the years, the speed, size, and weight of carrier based aircraft have steadily increased, thus demanding an ever larger energy absorption capacity from the shipboard arresting gear. Up to now, design improvements to meet these increasing demands have been limited to mere enlargement of the basic linear hydraulic energy absorber, which has been of the piston type. Modern aircraft, however, have loaded this system to its upper limit, and make any further development along these lines impractical due to weight and space limitations. The need exists for a new concept which will minimize space and weight demands while providing the necessary increase in energy absorption capacity.

The solution proposed involves the use of a turbo-type rotary hydraulic energy absorber. In essence the fluid is put into motion by a suitably designed rotor and is retarded by a stator and by the resistance of the flow passage. The power input to the rotor is absorbed by the hydraulic resistance of the system, and is eventually dissipated as heat.

The energy absorber is directly coupled to a cable storage drum. The drum profile is programmed to match drum rotational velocity to that required for optimum retarder performance. A device of this type was introduced in 1968, and is known as the M-21 energy absorber. The initial design gives satisfactory performance, but is of rather limited capacity, thirty million ft.lbs. Therefore, a program has been undertaken to redesign the absorber to increase the capacity to fifty-five million ft.lbs.

A development program was initiated by the Naval Air Engineering Center (NAEC) (Ref. 1). A full scale test of the programmed drum coupled with the M-21 absorber was conducted to determine the feasibility of the overall concept and to obtain performance data needed in the redesign program. A schematic diagram of the proposed system is shown in Figure 1.

A theoretical approximation of the flow conditions in a machine of this type was derived by Professor Michael H. Vavra (Ref. 2). To facilitate investigation of the effects of various design parameters NAEC formulated a computer program. From the computer analysis, a workable combination of design parameters was chosen such that torque and energy requirements were satisfied at the design point, the condition at which the absorber is expected to perform most often.

Professor Vavra has also been commissioned to develop and test a flow model of the new design. This model will be useful for refining losses, checking for flow separation, and obtaining information that is not available from the mean streamline analysis.

In this paper, a theoretical simulation and performance analysis of the energy absorber in all modes of operation is presented in terms of dimensionless parameters that facilitate comparisons of various designs and interpretation of model tests. The retraction problem is also studied, and preliminary estimates of the power needed to retract the programmed drum are given.

A throttling system is incorporated into the design to aid in arresting aircraft of various sizes. The discussion and analysis presented here are concerned with the condition of open throttle only.

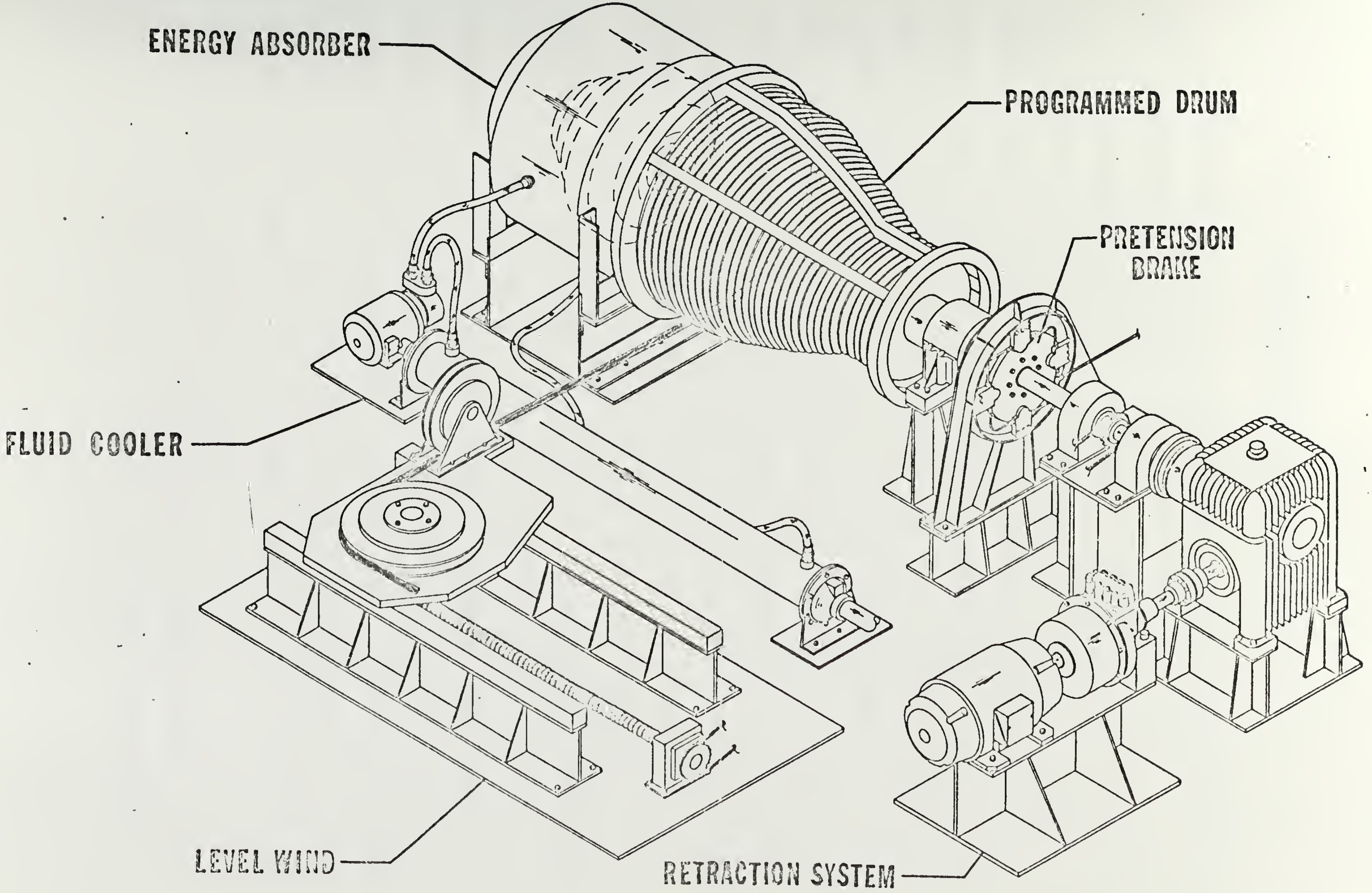

FIGURE I. PROGRAMMED DRUM ARRESTING GEAR

II. DESIGN VALUES AND CONSIDERATIONS

The main features of the energy absorber design that is analyzed here are summarized in Figures 2 and 3, and Table I.

The customary approach in the design of turbomachinery is first to optimize conditions with respect to a single specified design point. The resulting performance over a broad range of off-design conditions is then investigated to determine overall acceptability. The condition at which the absorber is expected to operate most often is naturally chosen as the design point. Specifically, a design torque of 340,000 ft.lbs. is required at a rotational speed of 76 rad./sec. The maximum rotational speed the cable will impart to the drum, and consequently to the rotor, is about 83 rad./sec. This limit is fixed by the allowable landing speed of the aircraft, and by drum design.

The mechanical power imparted to the rotor is continuously converted to thermal energy of the fluid. The temperature rise of the fluid is significant and imposes a constraint on the design. The temperature limit is the maximum allowable temperature the fluid may attain without causing cavitation. Obviously, heat must be removed to maintain equilibrium conditions. For this reason, provisions are made to bleed off a portion of the circulating fluid continuously and to replace it by fresh cool fluid. During a rapid series of arrests, the cooling problem is especially critical.

The fluid used in the absorber is an ethyl glycol mixture. This fluid is acceptable because it remains usable over a wide range of temperatures.

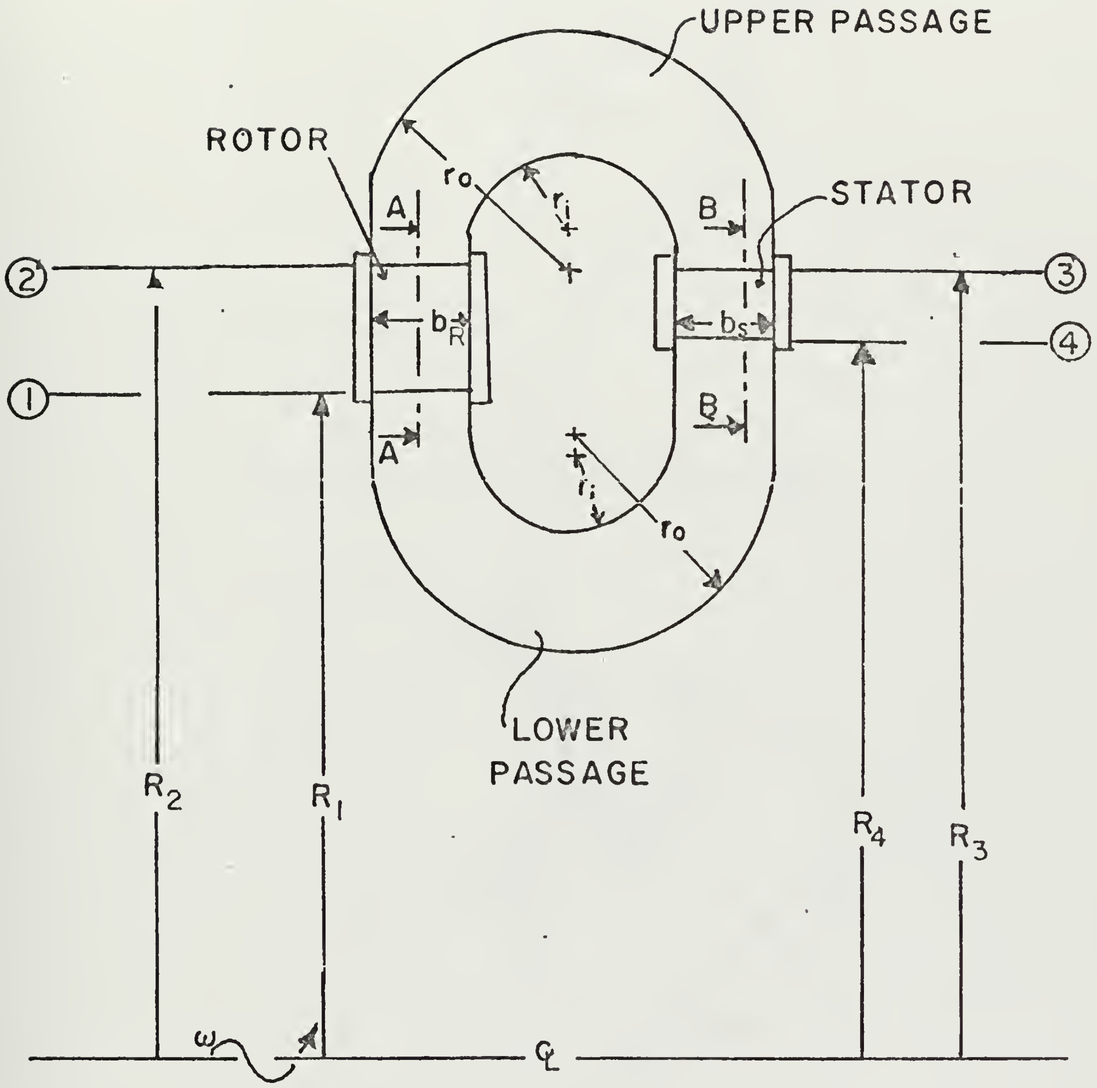

SCHEMATIC DIAGRAM OF ENERGY ABSORBER

FIGURE 2

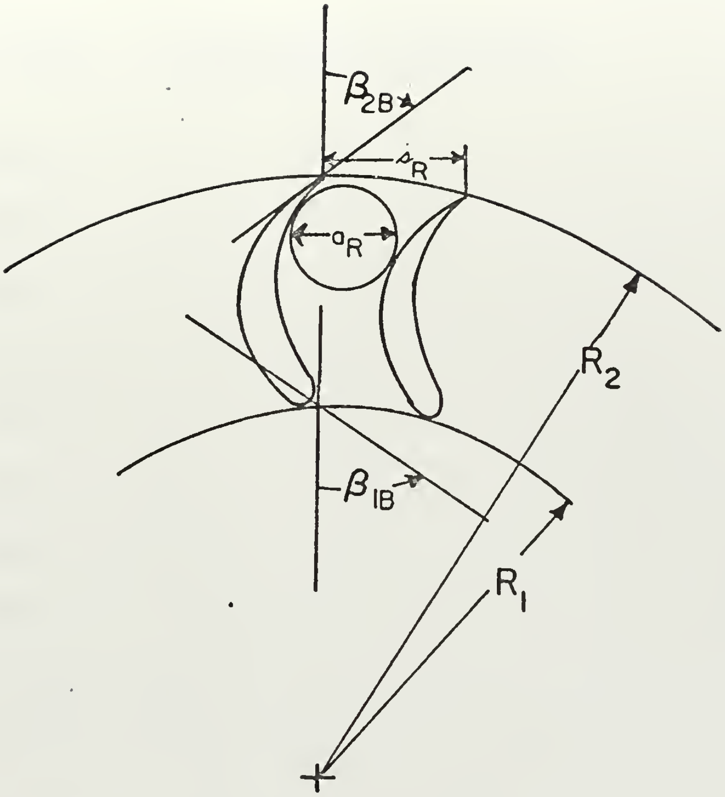

Section A-A of Figure 2 Through Rotor

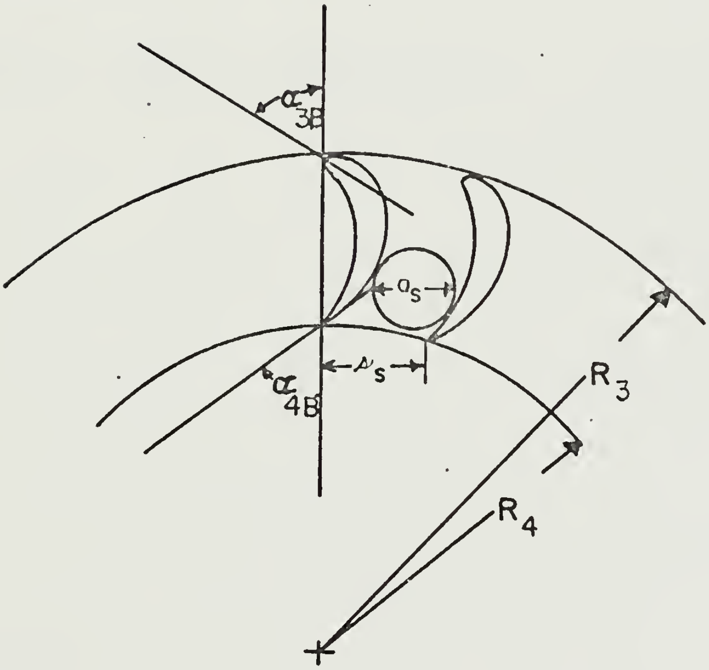

Section B-B of Figure 2 Through Stator

Figure 3 DIAGRAM OF ABSORBER BLADING

Table I PARAMETERS OF THE ABSORBER

$R_1 = 13.61$ inches

$R_2 = 16.25$ inches

$R_3 = 16.07$ inches

$R_4 = 14.93$ inches

$b_R = 2.02$ inches

$b_S = 2.02$ inches

$r_o = 4.18$ inches

$r_i = 2.02$ inches

$$\frac{(L_{ui} + L_{uo})}{2} = 10.26 \text{ inches}$$

$$\frac{(L_{\ell i} + L_{\ell o})}{2} = 10.26 \text{ inches}$$

Number of blades for rotor and stator: 72

$\beta_{1B} = 57^\circ$

$\beta_{2B} = 53^\circ$

$\alpha_{3B} = 57^\circ$

$\alpha_{4B} = 53^\circ$

$K_{B1} = .95$

$K_{B2} = .87$

$K_{B3} = .90$

$K_{B4} = .87$

$\omega_{MAX} = 83$ rad./sec.

Fluid properties:

$\rho = 2.095$ slugs/ft.^{2}	$c_f = .016$
$\nu = 3.76 \times 10^{-5}$ ft.^{2}/sec	$c_p = .7$

A detailed discussion of the effects of various parameters and loss coefficients is undertaken in the analysis section. A few words, however, are in order here. The radius of curvature r_i of the inner contour of both the upper and lower passage must not be smaller than the blade height. This insures that the flow does not separate, and it also increases absorption capacity. Estimates of losses in this machine are obtained through various empirical turbomachinery correlations as is shown in the analysis. Enthalpy losses in the passages are significant. Much of this loss is due to the bending of the passage with friction responsible for the remainder. However, a change in the coefficient of friction c_f which expresses the direct wall friction losses in the passages has little influence on overall performance. A value of $c_f = 0.016$ was chosen since it gives best agreement with M-21 test data.

The blade shapes first optimized by Professor Vavra from a performance standpoint were found by NAEC to be unacceptable on a stress basis. Blade thickness, spacing and angles were accordingly revised by NAEC, and a blade of sufficient strength was found; its characteristics are listed in Table 1.

The reliability of this analysis can only be judged experimentally by correlation with test data. The theory correlates very well with actual test results on the M-21 design. From this it appears that the theoretical analysis is reasonable and that the new design should be workable, if not optimum.

Naval carrier operations often require a series of rapid and repeated arrests. The drum must be retracted thus reversing the

rotational direction of the rotor. This process is investigated to obtain preliminary estimates of the power required to retract the absorber.

III. ANALYSIS OF THE PROBLEM

A. MODES OF OPERATION

The energy absorber is capable of operation in four modes. These modes are summarized in Table II.

Table II MODES OF OPERATION

Flow Direction	Shaft Rotation	
	Normal	Reverse
Normal	Mode 1	Mode 2
Reverse	Mode 3	Mode 4

Mode 1 corresponds to design point conditions. In this mode, the fluid passes successively through stations 1, 2, 3, 4 and back to 1, in that order. Note that the flow leaving the rotor at station 2 is moving radially outward. See Figures 2 and 3. For fluid circulation in this sense, conditions at stations 2 and 4 are particularly significant. At the rotor exit, station 2, the direction of the flow with respect to the rotor, is assumed to remain constant at all flow rates. At stator exit, station 4, the direction of the flow with respect to the stator is likewise assumed to remain constant. While this assumption of fixed relative and absolute flow directions is not exact, it represents an excellent approximation when the blades are closely spaced as in the present design.

In Mode 2, the sense of the fluid circulation is exactly as described above. However, the direction of shaft rotation is reversed.

Naturally, stations 2 and 4 are still governing in the sense that flow directions at these stations are known.

In Mode 3, the shaft rotation is the same as for Mode 1, but the direction of fluid circulation is reversed. Consequently, the fluid passes successively through stations 2, 1, 4, 3 and back to 1, in that order. Note that the rotor exit is now at station 1, and the direction of flow at this station is radially inward. In this case, stations 1 and 3, are controlling. The relative flow direction at rotor exit, station 1, and the absolute flow direction at stator exit, station 3, are now assumed to remain fixed.

In Mode 4, the sense of fluid circulation is the same as in Mode 3, but the direction of shaft rotation is reversed. Of course, stations 1 and 3 still govern flow direction as in the previous case.

The same set of equations describe Modes 1 and 2, but a separate set of equations is needed to describe the reverse flow Modes, 3 and 4. Note that only two sets of equations are needed for the four Modes, and each set is governed by the flow direction relative to the blade exits. Two separate computer programs are needed since one program will be used to solve each set of equations. Program Normal finds the solution for Modes 1 and 2, and program Reverse finds the solution for Modes 3 and 4. Both programs will be discussed in the appendix. All quantities and results discussed throughout the paper are obtained from these programs.

The velocity diagrams for each mode are presented in Figures 4, 5, 6, and 7. All angles and velocities are drawn to scale.

The thermodynamic processes in the absorber are shown on the enthalpy-entropy diagrams, Figures 8 and 9. The process for normal

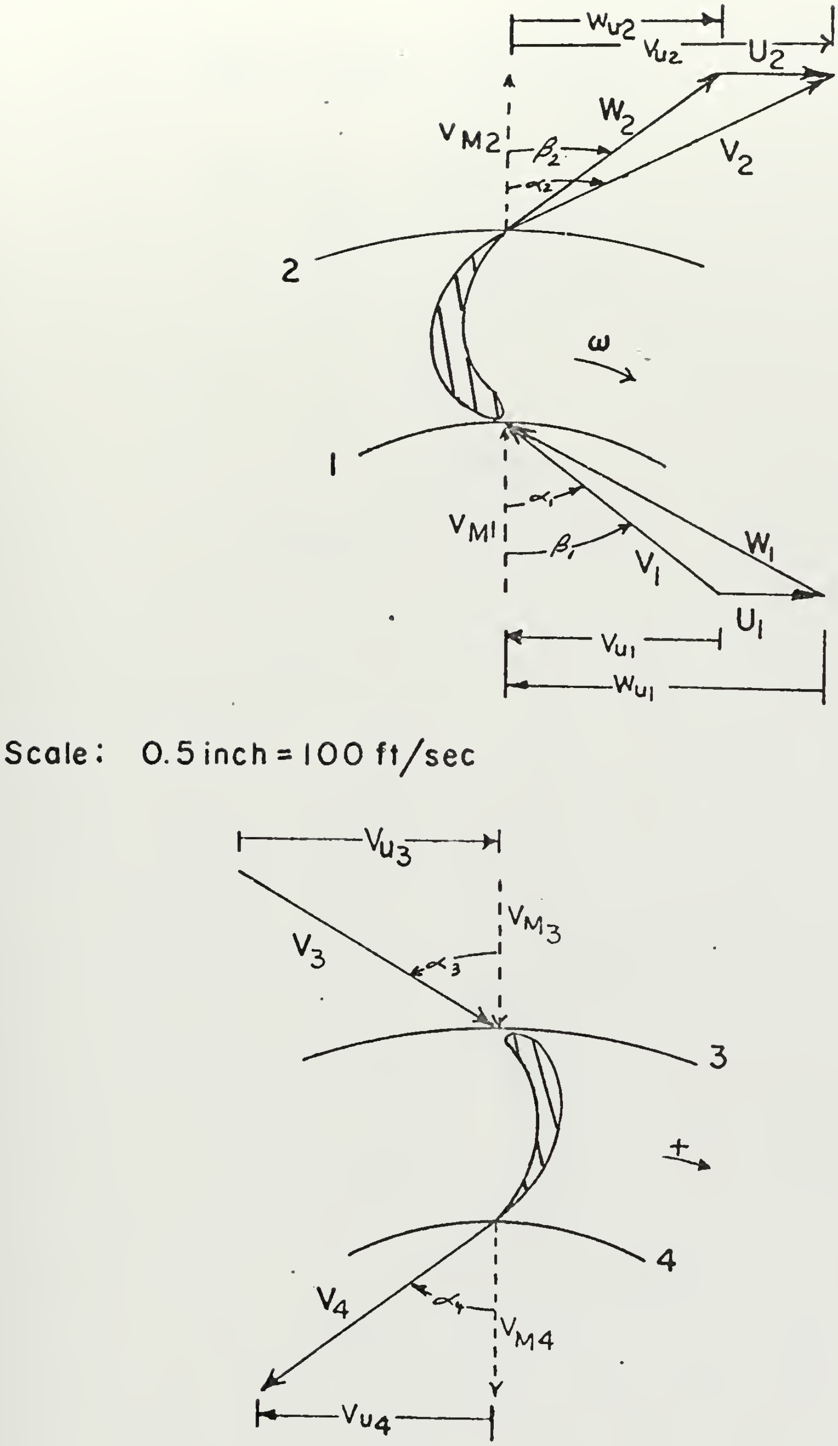

Figure 4 Velocity Diagrams for Mode 1 Operation at

$$R_{Ne} = \frac{\omega_{MAX} R_2^{2}}{\nu} = 4.8 \times 10^6$$

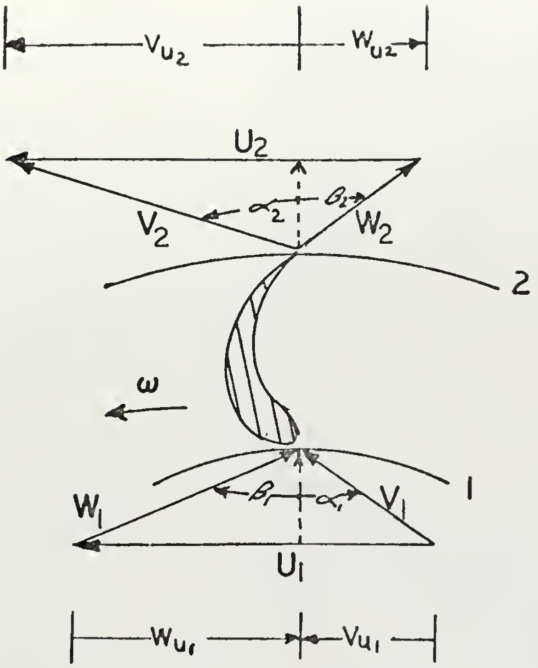

Scale: 0.5 inch = 25ft/sec

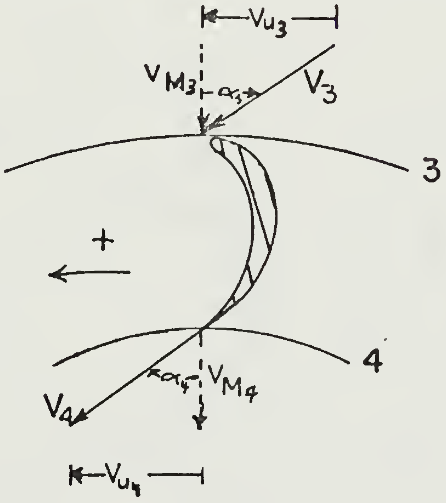

Figure 5 Velocity Diagrams for Mode 2 Operation at

$$R_{Ne} = \frac{\omega_{MAX} R_2^2}{\nu} = 4.8 \times 10^6$$

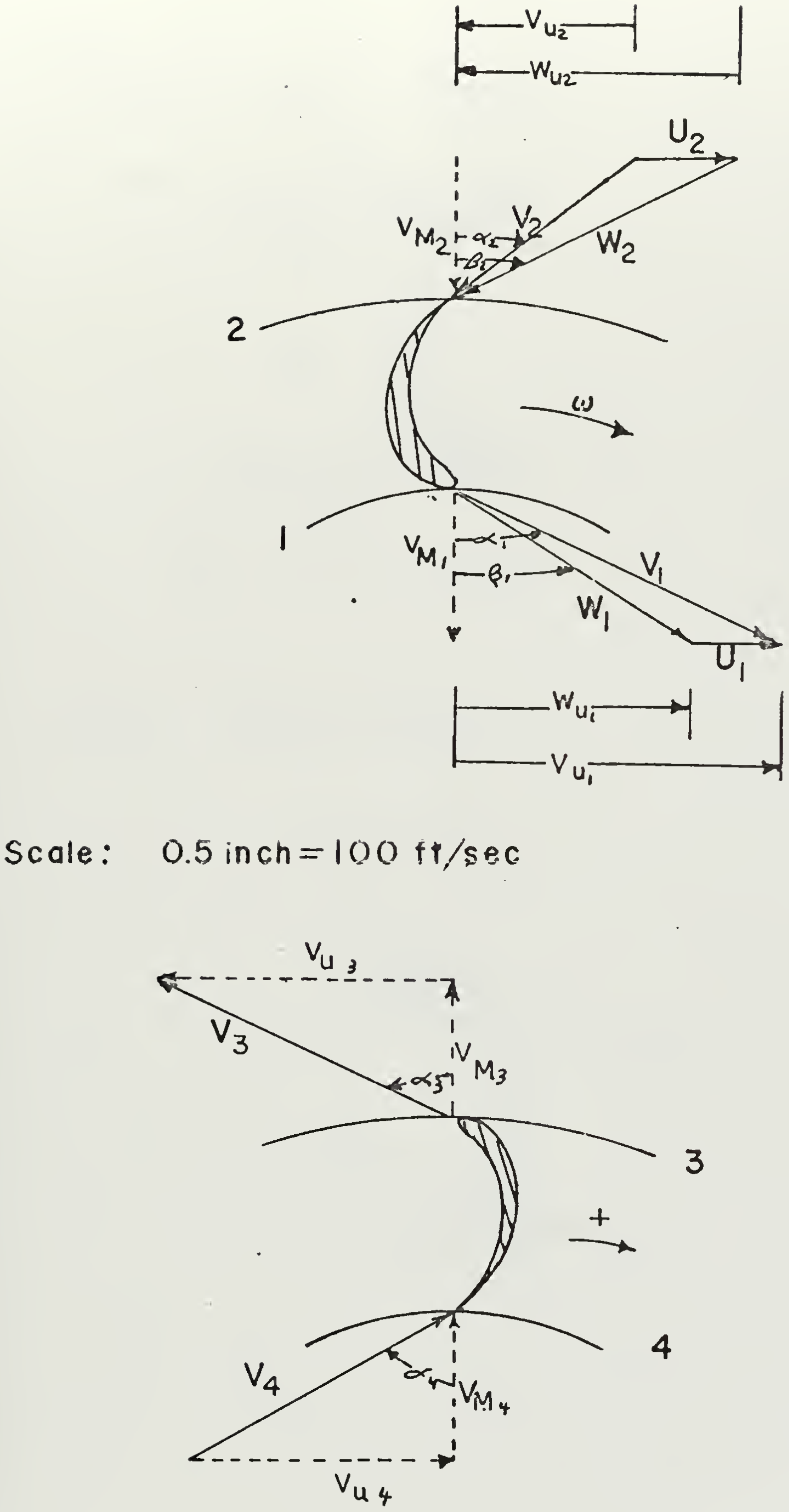

Figure 6 Velocity Diagrams for Mode 3 Operation at

$$R_{Ne} = \frac{\omega_{MAX} R_2^2}{\nu} = 4.8 \times 10^6$$

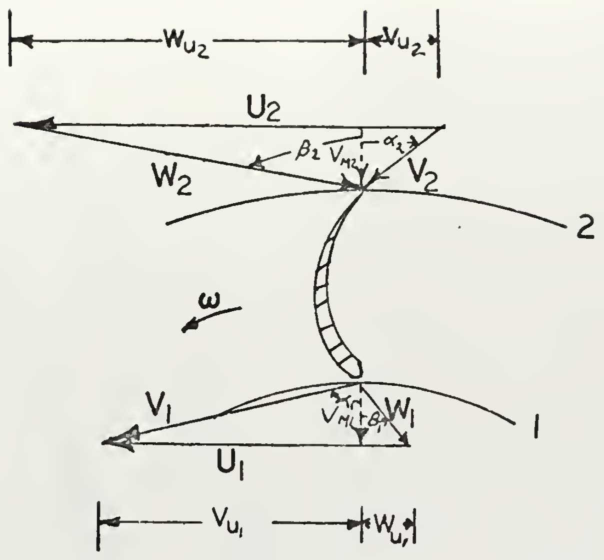

Scale: 0.5 inch = 25 ft/sec

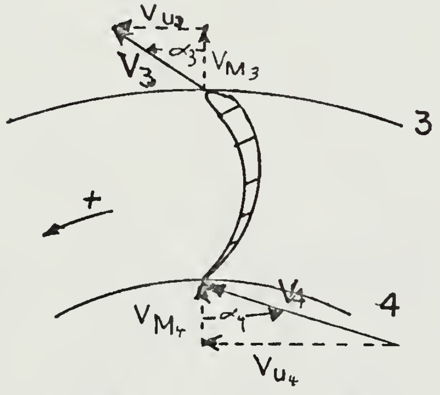

Figure 7 Velocity Diagrams for Mode 4 Operation at

$$R_{Ne} = \frac{\omega_{MAX} R_2^2}{\nu} = 4.8 \times 10^6$$

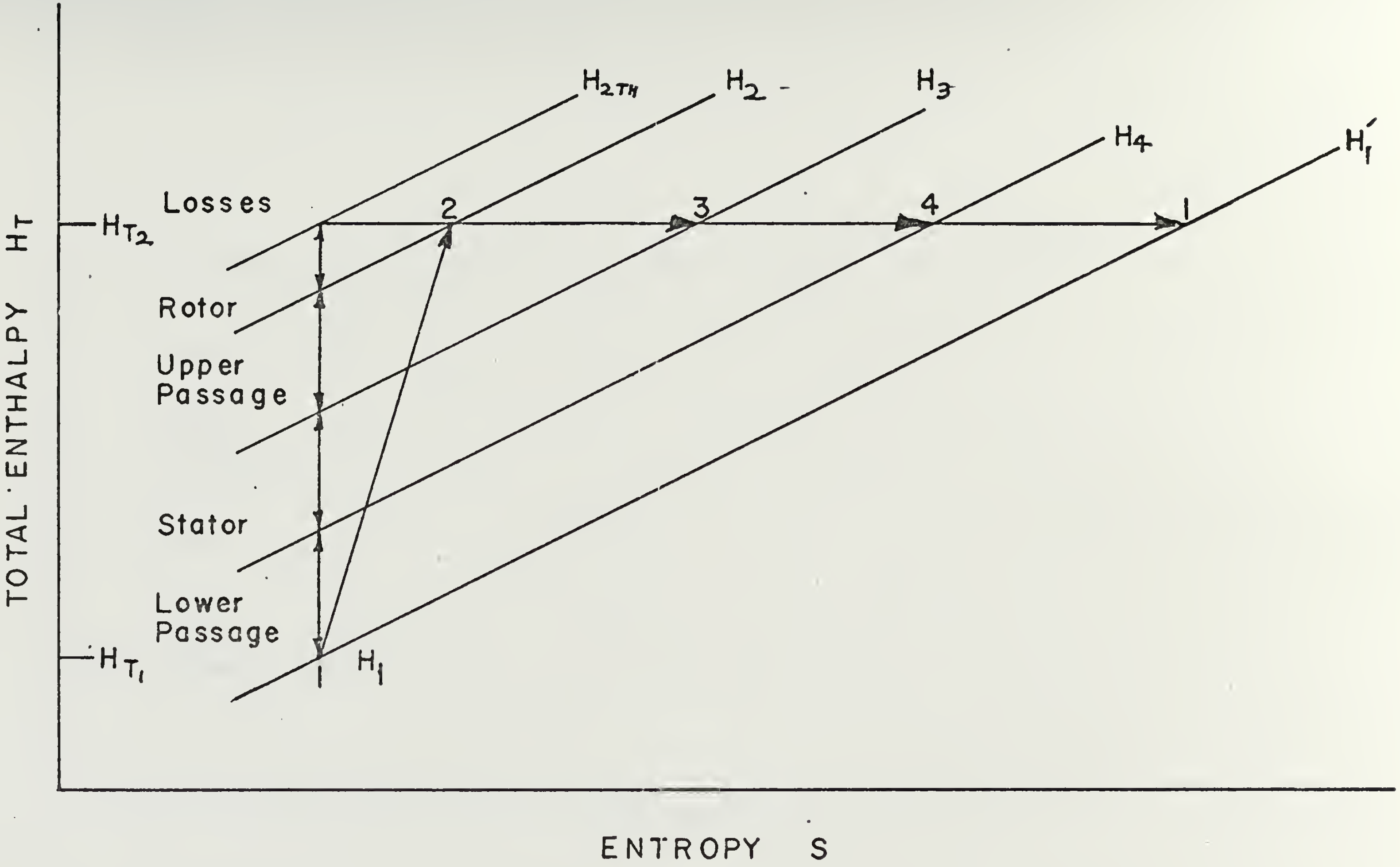

Figure 8 Total Enthalpy-Entropy Diagram of the Thermodynamic Process in the Absorber for Normal Circulation, Modes 1 and 2

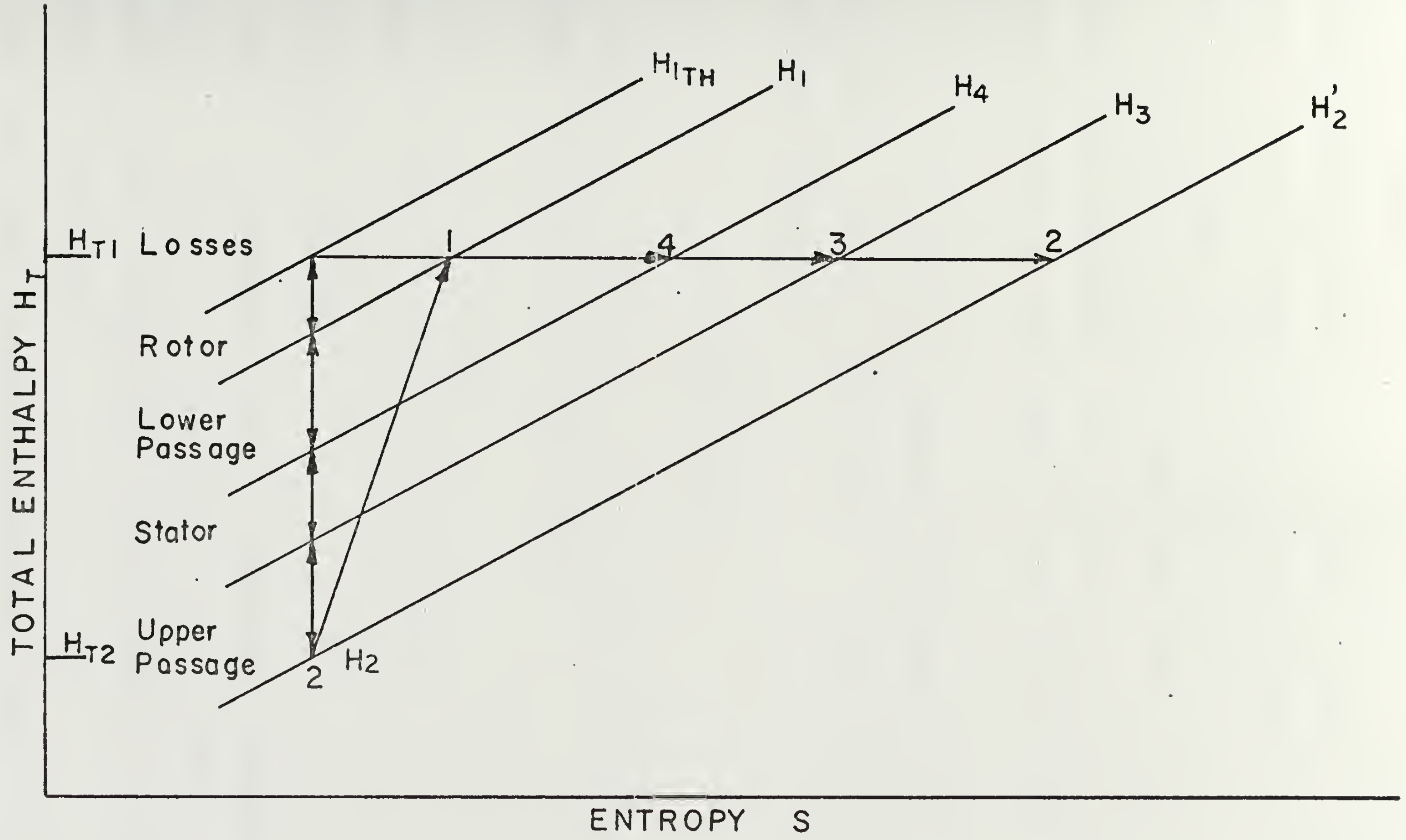

Figure 9 Total Enthalpy-Entropy Diagram of the Thermodynamic Process in the Absorber for Reverse Circulation, Modes 3 and 4

circulation, Modes 1 or 2, is shown in Figure 8, while that for reverse circulation, Modes 3 or 4, is shown in Figure 9. The direction of shaft rotation affects the exact quantitative enthalpy values. The graphs, however, are merely qualitative.

A "total head" H (per unit mass) is used which differs from the standard total enthalpy H_T. This is discussed in greater depth in the analysis section, but a few words are needed at this point to clarify the discussion.

The fluid is considered incompressible which allows the thermal and mechanical effects to be uncoupled. A "total head" is conveniently defined as

$$H = \frac{P_T}{\rho} = \frac{p}{\rho} + \frac{v^2}{2}$$

Henceforth H is referred to simply as head. The head and total enthalpy are linked by the simple relation

$$H = H_T - u$$

where u represents internal energy per unit mass.

B. DIMENSIONAL ANALYSIS

Results are presented in terms of appropriate dimensionless quantities. The use of non-dimensional terms simplifies the correlation of data, the comparison of various designs, and the interpretation of model tests.

The three quantities chosen as consistent dimensional reference parameters are the radius of the rotor outlet R_2, the fluid density ρ, and the shaft rotational speed ω or ω_{MAX}, whichever is appropriate.

Using these parameters, one defines the effective Reynolds number for this design to be

$$R_{N_e} = \frac{\omega R_2^{\,2}}{\nu}$$

where ν is the kinematic viscosity. And the dimensionless total head is

$$\Pi_H = \frac{H}{\omega^2 R_2^{\,2}}$$

In the discussion of results, it is convenient to define the flow coefficient Φ in the following specific way, namely,

$$\Phi = \frac{|V_{M2}|}{\omega R_2}$$

where the algebraic signs of ω and Φ are always positive for normal shaft rotation and negative for reversed shaft rotation. This sign convention for shaft rotation is maintained regardless of the direction of the fluid circulation, hence the use of the absolute magnitude $|V_{M2}|$ in the definition.

In the actual computer programs NORMAL and REVERSE, however, somewhat different sign conventions are more convenient. All equations are written in such a way that the three quantities V_{M2} ωR_2 and Φ are always positive. For this reason the four modes are computed as separate cases.

For comparison of various modes and designs the dimensionless torque, power and rotational speed coefficients are respectively

$$\Pi_T = \frac{T_R}{\omega^2_{MAX} R_2^{\,5} \rho}$$

$$\Pi_{\mathcal{P}} = \frac{\mathcal{P}}{\omega^3_{MAX} R_2^5 \rho}$$

$$\Pi_\omega = \frac{\omega}{\omega_{MAX}}$$

The detailed analysis considered later also uses various dimensionless quantities for convenience in the derivations. The parameters used to facilitate the non-dimensionalization in that case are not necessarily the same as introduced in the present section, and the separate cases should not be confused.

C. ENERGY BALANCE AT EQUILIBRIUM

In general the rotor adds energy to the fluid. In traveling through the passages and returning to its initial state the fluid dissipates this mechanical energy through various losses. Under equilibrium these losses exactly cancel the original energy input.

It turns out that the energy input of the rotor can be expressed in terms of the flow coefficient Φ in the form

$$\Delta H_{IN} = A + B\,\Phi$$

where A and B are true constants. The losses can be expressed as

$$\Sigma\Delta H_{LOSS} = A' + B'\,\Phi + C'\,\Phi^2$$

where A', B', and C' may be considered constant to a first approximation. Actually these quantities are weak functions of Φ, a fact which must be considered in the exact solution. The energy relations which fix the equilibrium state are shown in Figures 10 and 11. Figure 10 represents the two modes which correspond to normal flow direction.

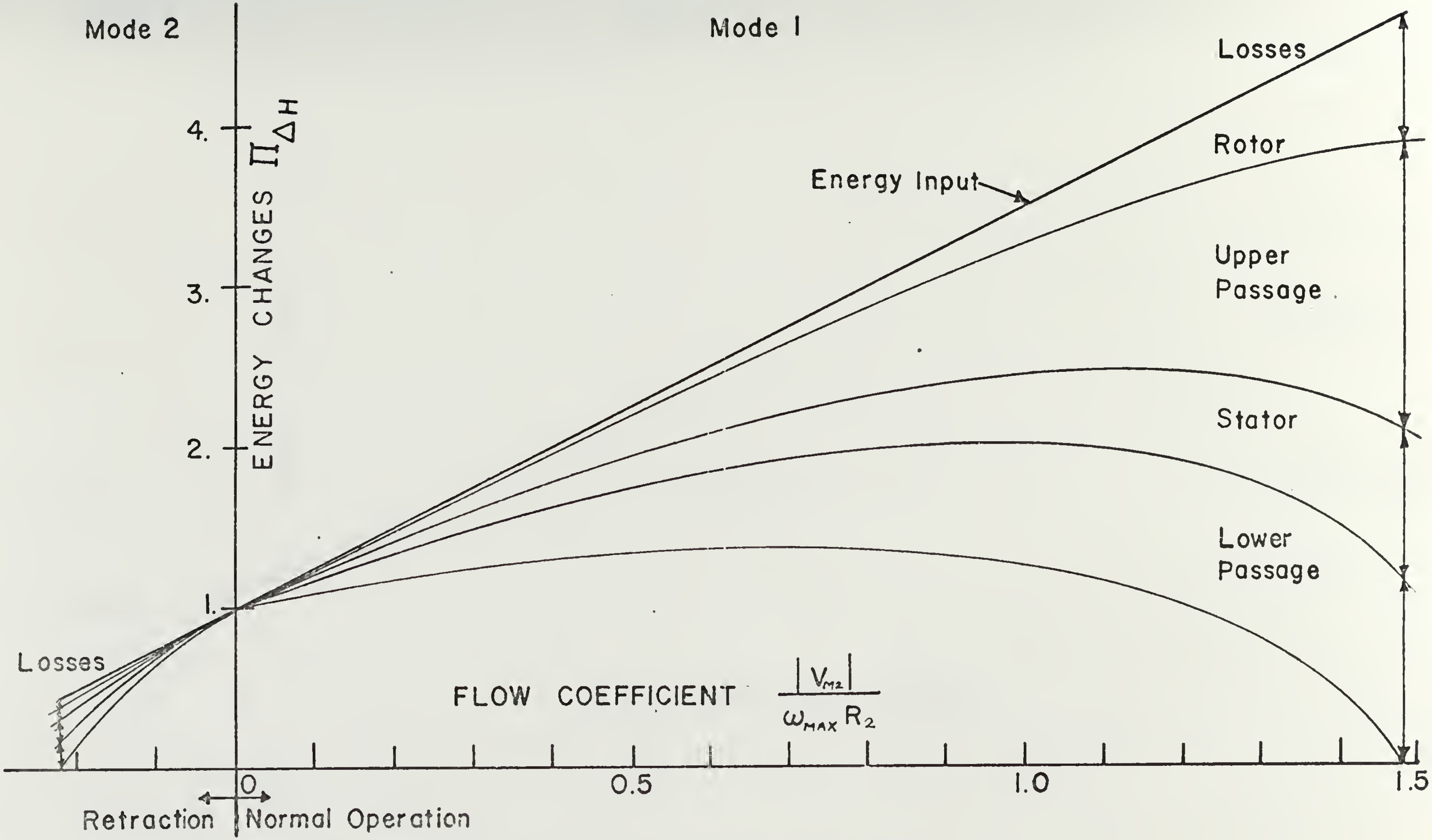

Figure 10 The Energy Balance for Equilibrium Under the Conditions of Normal Circulation at $R_{Ne} = \frac{\omega_{MAX} R_2^2}{\nu} = 4.8 \times 10^6$

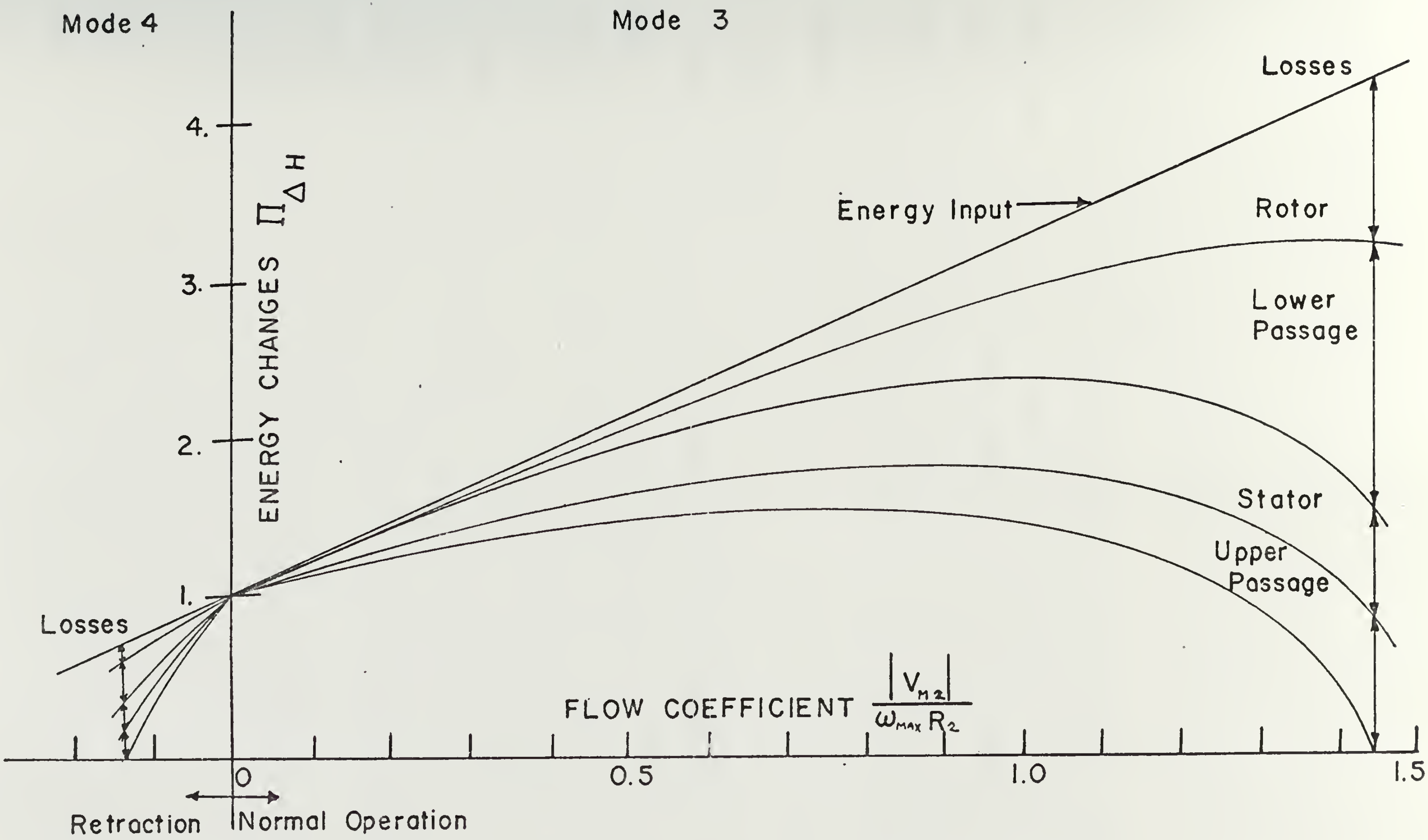

Figure 11 The Energy Balance for Equilibrium Under the Conditions of Reverse Circulation at $R_{Ne} = \frac{\omega_{MAX} R_2^2}{\nu} = 4.8 \times 10^6$

Figure 11 shows the two modes for reverse flow. These results are drawn to scale, except that the parabolic lines are only approximate. The final equilibrium points, where the losses balance the energy input, however, and the relative distribution of losses at these points are in correct scale.

Initially, it was thought that only two of the above four modes would prove to be physically possible, one corresponding to normal shaft rotation, the other corresponding to retraction. Surprisingly enough, the present analysis has demonstrated that operation in all four of the modes is theoretically possible. This point is clearly indicated in Figures 10 and 11.

D. MODEL TESTING

Professor Vavra has proposed that a model testing program be undertaken. The model will not be a true dynamic model, but will be a purely static device that uses air as the working fluid. Construction of the model will constrain the air flow to the normal direction only. However, the scale model should be useful in checking for flow separation through the passages and refining the loss coefficients for the analysis of the absorber. The effects of the tangential component of velocity will also be investigated.

The discussion of the above static model is not within the scope of this thesis. However, a hypothetical model is considered which is a true dynamic model of the actual full scale device. The size of the hypothetical model is taken as identical to that of the static model. The model is scaled to 0.569 of the size of the actual absorber. In both cases the fluid is air. When expressed in dimensionless terms,

the performance of the hypothetical model is basically the same as that of the full scale machine, except for Reynolds number effects. The full scale machine operates at a maximum Reynolds number, as defined above, of 4.88×10^6 while the maximum Reynolds number of the model is 3.70×10^5. The results for this model are presented along with the results for the real absorber.

E. ASSUMPTIONS AND LIMITATIONS OF THE ANALYSIS

A one-dimensional mean streamline analysis is obviously only a crude approximation of the actual performance of any turbomachine, but is a starting point necessary in most development programs. The validity of the assumptions used are very important to the reliability of the analysis. The primary assumptions used in this report are summarized below.

The fluid is treated as incompressible. This assumption is excellent as long as the provisions to maintian the fluid at a temperature lower than the cavitation temperature are adequate. This conveniently uncouples mechanical and thermal effects and allows a form of "total head" H to be defined which is independent of internal energy.

If the velocity distribution across every section were turly uniform, the meridional component $V_{M_{TH}}$ at the mean streamline could be computed simply from a continuity relation of the form

$$V_{M_{TH}} = \frac{Q}{A_M}$$

where Q is the volumetric flow rate and A_M is the meridional cross-section area. The actual velocity distribution, however, is non-

uniform because of the effect of streamline curvature, boundary layers and so on. To allow for these effects, approximately, the actual meridional velocity V_M is assumed to be governed by a relation of the form

$$V_M = K_B \frac{Q}{A_M}$$

where the so-called blockage factor K_B is treated as a constant. The blockage factors were extrapolated from M-21 test data. Their reliability in the reverse flow modes is doubtful, however, since all test data were obtained only from Mode 1 operation. An extension of these data to all modes would be very useful.

The present analysis treats operation of the absorber as a steady state phenomenon. Strictly speaking, the operation is actually unsteady. However, the arrest and retraction processes require a sufficient number of drum revolutions that the steady state assumption provides a fair approximation.

A major assumption is that the relative flow direction at the rotor outlet and the absolute flow direction at the stator outlet are constant. For the case of normal flow this is an excellent approximation. However, the validity is reduced for the reverse flow modes. In Modes 3 and 4, the flow encounters a sharp leading edge, and exits past a blunt trailing edge. The implication is that the flow is not as well guided as in the normal flow case. Thus the actual turning angle of the flow is undoubtedly less than predicted by the theoretical analysis. The power absorbed in both reverse flow modes would consequently be less than predicted.

Losses, in general, are approximated by various empirical correlations and are reasonable as shown by test results. They are discussed in depth in the detailed analysis section.

Incidence losses, however, pose a problem. The incidence loss approximations introduced in the analysis section are reasonable as long as the incidence angles remain small. This is obviously not the case for the retraction modes as shown in Figures 5 and 7. The approximations break down physically at these severe incidence angles.

It was thought earlier that two of the four theoretical modes might show themselves to be physically impossible. For example, a large incidence loss might conceivably preclude the attainment of the necessary energy balance. This has not proved to be the case, however. It appears from the present analysis that operation in all four modes remains possible physically. It is true, of course, that the predicted performance for the two retraction modes, Modes 2 and 4, will be inaccurate because of these large incidence effects, but this in itself does not eliminate the existance of these modes.

At extreme angles of incidence, a distinct possibility of stalling exists. In normal operation, this limits the attainable power absorption. In a retraction mode, however, stalling would not be totally undesirable. If the rotor stalls, the energy absorbed by the device is greatly reduced, and the power necessary to retract the rotor is minimal.

All of the foregoing assumtions are thought to be reasonable. Refinements of various points would be useful, especially for large incidence angles and blunt trailing edges.

IV. RESULTS AND DISCUSSION

The discussion of the problem up to this point has already included a number of significant results reached in the analysis as shown in Figures 4 through 11.

Additional detailed results for all modes of the absorber are presented in Figures 12, 13, 14, and in Table III. The results for Mode 1 of the dynamic model are also included.

The main results of this investigation are summarized concisely in Figure 12. This is a logarithmic plot of the dimensionless power Π as a function of the dimensionless shaft speed ω/ω_{MAX}. Performance of the proposed absorber, of the hypothetical model, and of the existing M-21 machine are compared on this graph. Note that the theoretically predicted performance of the M-21 version as shown by the continuous line is in excellent agreement with the actual measured performance as shown by the data points.

The actual horsepower is plotted as a function of absolute shaft speed for all four modes of the proposed absorber in Figure 13. The power absorbed during arrest and the power expended during retraction are presented for a range of possible operating speeds.

The maximum dimensionless power is also shown as a function of Reynolds number R_{N_e} in Figure 14. This graph, although based on only three computed points, does correctly portray, approximately, how scaling affects power absorption. It would be a simple matter to calculate additional points on this curve from program NORMAL.

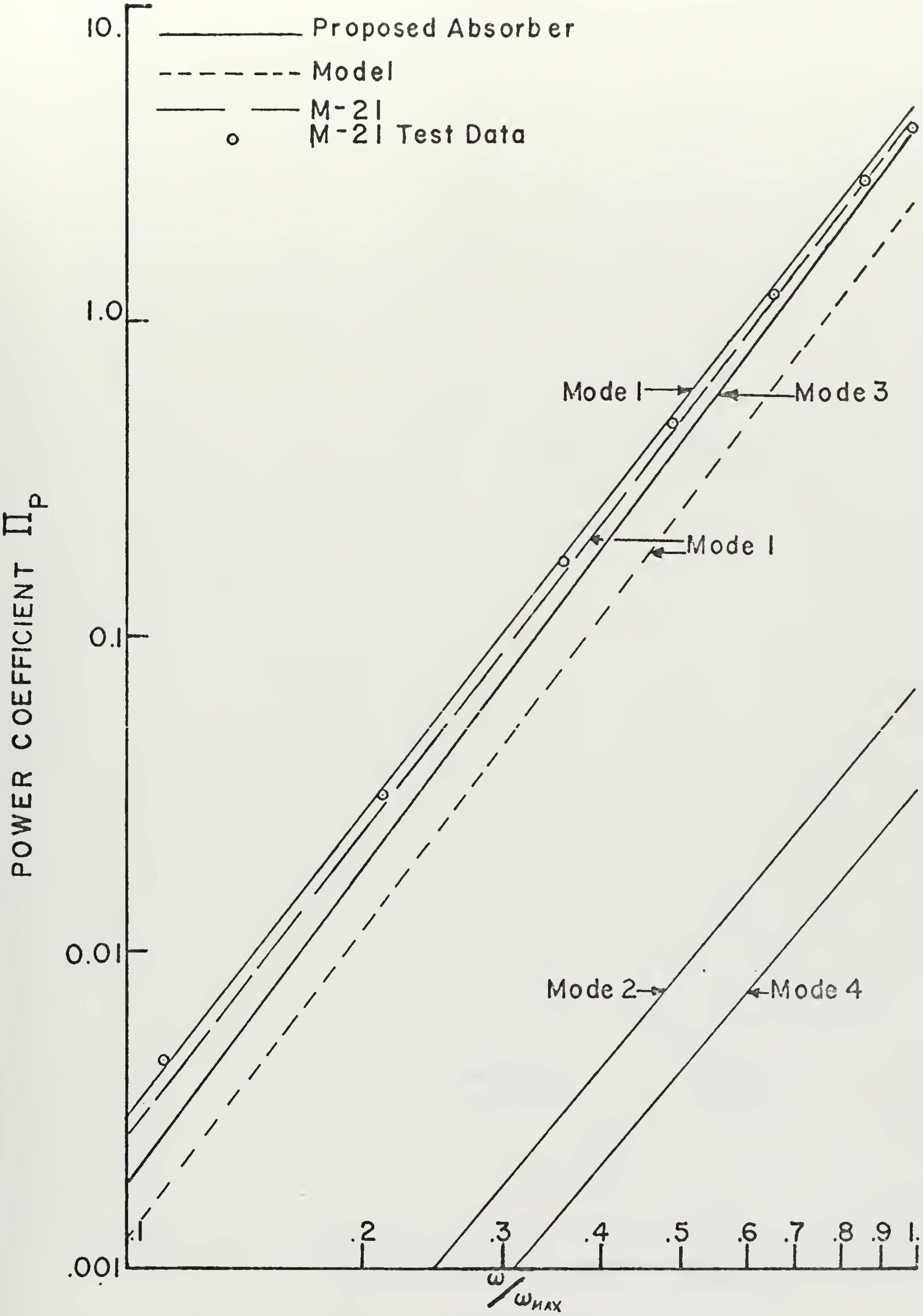

Figure 12 Non-dimensional Power vs. Non-dimensional Rotational Speed

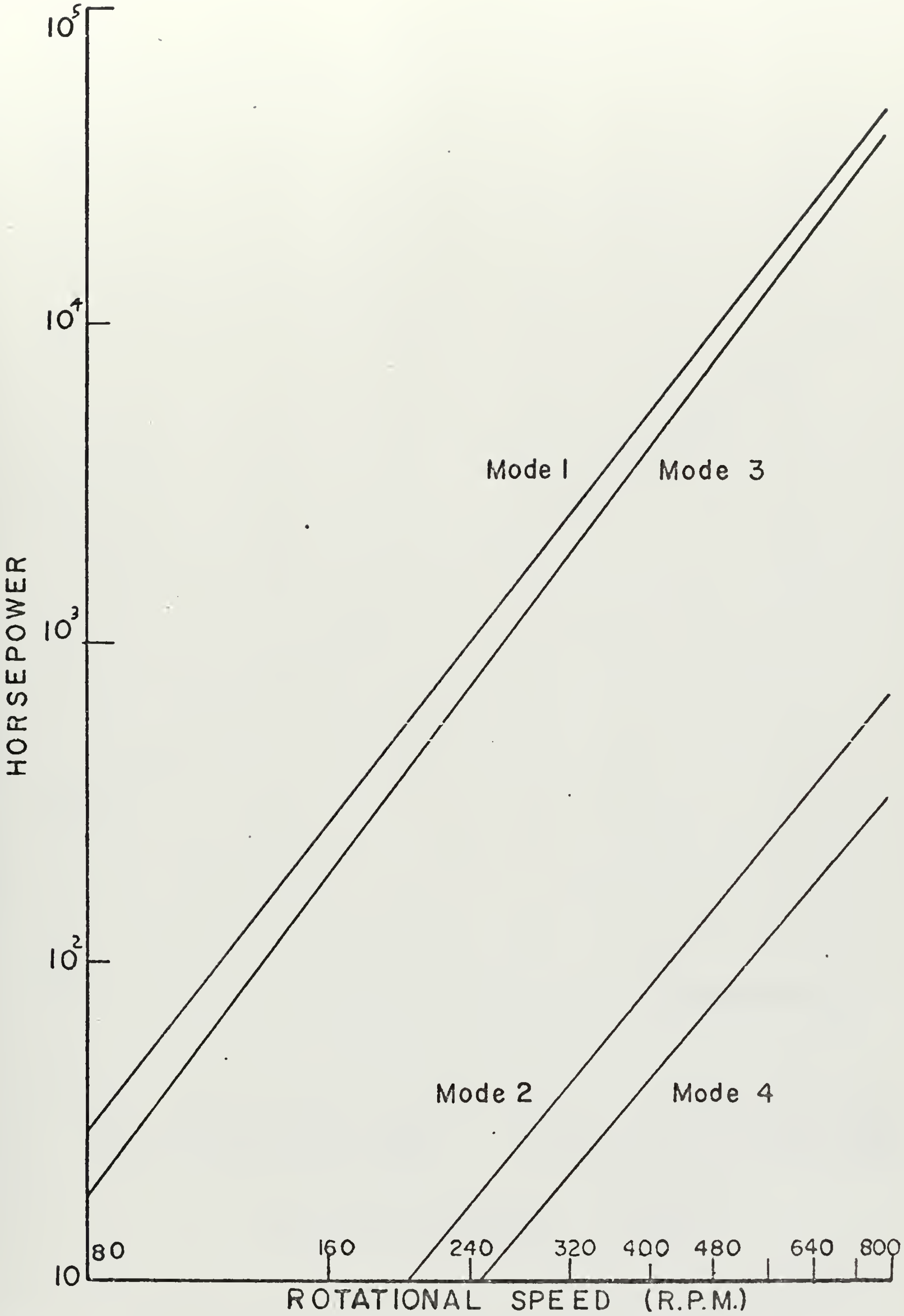

Figure 13 Absolute Power vs. Shaft Speed for the Four Operating Modes of the Proposed Energy Absorber

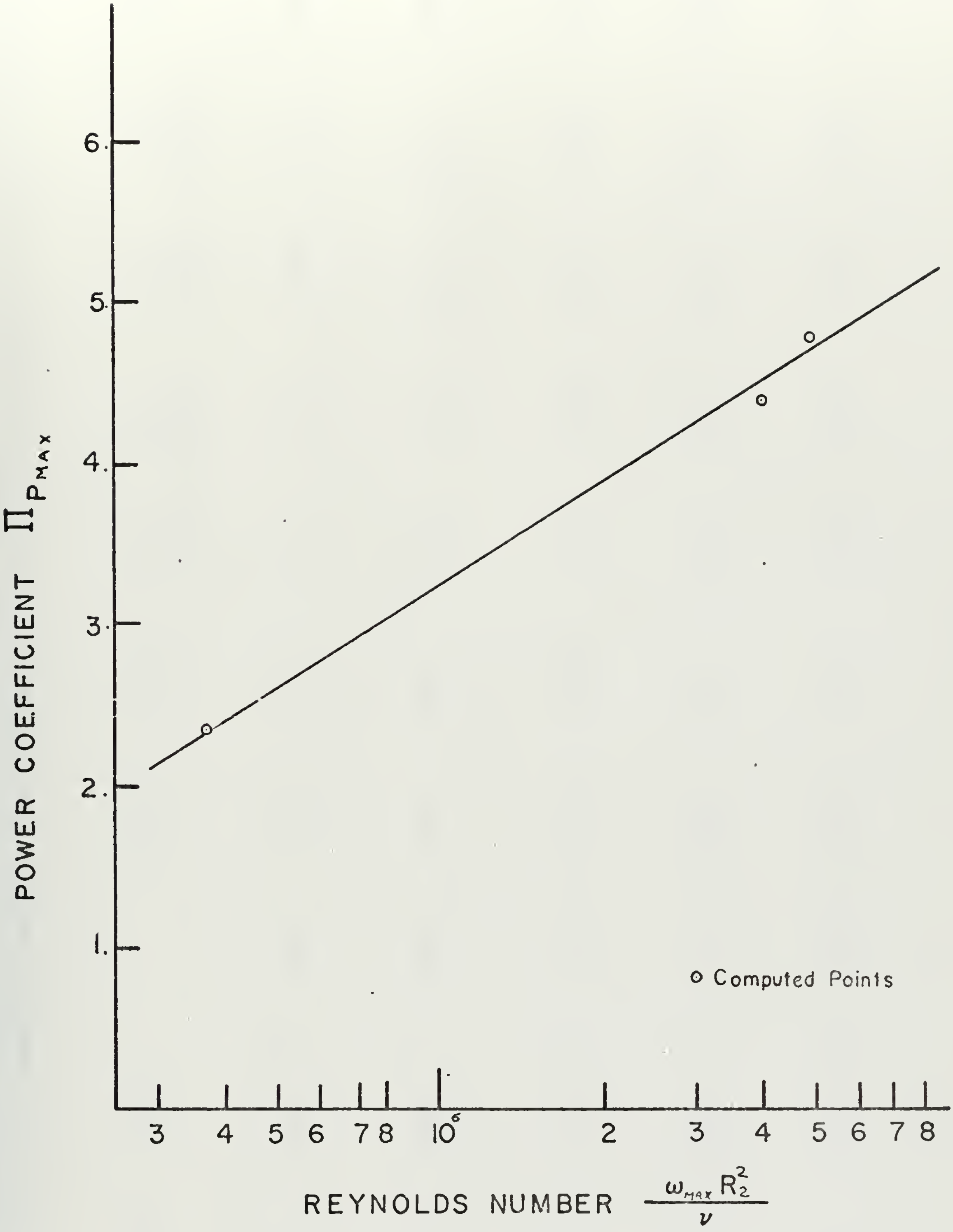

Figure 14 Maximum Power Coefficient vs. Maximum Reynolds Number for the 3 Designs Considered

Table III: Detailed results of the proposed energy absorber for the four modes and the dynamic model for Mode 1. All results are for the case of $\omega = \omega_{max}$.

Operating Mode	N_{Re}	ϕ	Torque (lb-ft)	Horsepower Absorbed	ΔH_R $\left(\frac{\text{ft-lbs}}{\text{slug}}\right)$	ΔH_u $\left(\frac{\text{ft-lbs}}{\text{slug}}\right)$	ΔH_S $\left(\frac{\text{ft-lbs}}{\text{slug}}\right)$	ΔH_1 $\left(\frac{\text{ft-lbs}}{\text{slug}}\right)$	$\Pi_{\wp}$
1	4.88×10^6	1.489	318730.	48551.	51313.	24304.	11658.	15351.	4.765
2	4.88×10^6	0.223	4512.	687.	4026.	2694.	981.	351.	0.067
3	4.88×10^6	1.450	271770.	41050.	41999.	10558.	8822.	22620.	4.063
4	4.88×10^6	0.136	2194.	334.	1895.	115.	1174.	607.	0.033
Model Mode 1	3.70×10^5	0.995	10.65	1.62	11054.	5315.	3715.	2475.	2.352

Table III. Continued

Operating Mode	Π_{T_R}	$\Pi_{\Delta H_{in}}$	i_R (degrees)	i_s (degrees)	$\Delta\beta_R$ (degrees)	$\Delta\alpha_s$ (degrees)	Y_R	Y_s	C_u	C_l	η_{Mu}
1	4.765	4.71	-3.73	2.26	113.7	-112.3	0.227	0.208	0.337	0.412	0.813
2	0.067	0.45	-122.3	113.2	12.3	-3.2	0.174	0.120	0.359	0.435	0.456
3	4.063	4.27	10.7	-6.3	120.7	-116.3	0.239	0.222	0.337	0.412	0.856
4	0.033	0.34	133.7	-126.0	23.7	-16.0	0.197	0.149	0.384	0.456	0.856
Model Mode 1	2.352	3.48	-6.88	5.1	116.9	0115.1	0.494	0.453	0.436	0.515	0.782

Table III. Continued

Operating Mode	η_{M_1}	R_{NR}	R_{NS}	R_{Nu}	R_{N1}
1	0.876	6.1×10^6	3.3×10^6	1.5×10^7	1.7×10^7
2	0.876	9.1×10^4	5.0×10^4	2.2×10^5	2.5×10^5
3	0.868	7.1×10^5	3.2×10^5	1.3×10^6	1.5×10^6
4	0.868	7.2×10^4	3.3×10^4	1.3×10^5	1.5×10^5
Model Mode 1	0.876	3.2×10^4	1.7×10^4	7.7×10^4	8.6×10^4

As mentioned earlier, the actual existence of four stable modes is a surprising result. The original expectation, based largely on intuition rather than analysis, was that only one mode would be possible for each direction of shaft rotation. But the absorber is an unusual machine which tends to confound intuitions based on experience with more conventional devices. Consider for example the fact that losses are necessary for the machine to absorb the mechanical energy input. The smaller the loss coefficients, the higher the final equilibrium flow rate will be, and the greater the energy absorption. Thus we are led to the seeming paradox that the lower the loss coefficients the higher the energy lost!

The power curves of Figures 12 and 13 are interesting and significant in that all curves have nearly constant and nearly equal slopes. The power can be expressed in the form

$$\Pi_{\mathcal{P}} = \Pi_{\mathcal{P}_{MAX}} \left(\frac{\omega}{\omega_{MAX}}\right)^{\eta}$$

where the slope of the curve is roughly $\eta \approx 3$ for all cases.

The horsepower curves of Figure 13 indicate that Mode 1, the design point mode, absorbs the greatest amount of energy. Mode 3, however, is a very close second. Refinement of the analysis should lower the predicted absorption of Mode 3 somewhat. Nevertheless, the favorable comparison of this mode to the design mode is interesting. Figure 13 also shows that the power needed to retract the rotor is reasonably small for Modes 2 and 4, especially in comparison to the power absorbed during arrest.

The question of which mode the absorber will actually operate in under various conditions of use is interesting, but by no means

completely clear at this time. It is thought possibly that if the absorber be started from rest with shaft rotation in the normal direction, Mode 1 should occur. If retraction follows immediately, the retraction mode will probably be Mode 2. This is based on the fact that during arrest the flow will build up a large momentum which will tend to persist in the same sense during the subsequent retraction. If retraction be started after the fluid motion ceased, however, the resulting mode of operation remains uncertain.

Some method of sensing and/or controlling flow direction would be useful to insure that Mode 1 was occurring on all arrests. Mode 3 operation might not have enough absorption capacity to handle large aircraft.

The general question of which mode occurs is an area for further study. Testing of the actual absorber with the idea of definitely determining the operating modes under various conditions would be extremely useful.

V. CONCLUSIONS AND RECOMMENDATIONS

The development of the problem and the exact solution of the two sets of equations describing normal and reverse flow conditions clearly show that four stable operating modes exist. The analysis adequately predicts the absorption capacity of the proposed device for Mode 1. However, the analysis is not as accurate for the reverse flow or retraction modes.

It is recommended that the retraction problem be further studied to refine loss coefficients and to more accurately predict the power necessary to retract the absorber. It is also recommended that further study be made into the question of predicting which mode occurs under various operating conditions. This study would encompass the unsteady phase of the problem. Actual testing of the absorber should also be conducted with the intention of determining which mode will occur. A method of flow control or sensing would also be useful to guarantee proper performance in that Mode 3 absorption capacity may be insufficient in certain cases.

This turbo-type of energy absorber appears to be completely adequate to meet the demand of carrier operations now and in the forseeable future. The potential for future development and enlargement is ample.

APPENDIX A

DETAILED ANALYSIS OF THE ENERGY ABSORBER WITH THE FLUID CIRCULATING IN THE NORMAL DIRECTION, MODES 1 AND 2.

A one dimensional mean streamline analysis after Vavra (Ref. 2) will be developed with the following assumptions:

β_2 = constant

α_2 = constant

Uniform flow at stations 1 to 4 except for blockage factors.

Blockage factors are independent of the flow.

The fluid is incompressible.

Steady state conditions exist.

1.0 Torque and Velocity Relations

The torque T_R exerted on the fluid by the rotor is positive when acting in the direction of rotation.

$$T_R = \dot{m} \left[R_2 V_{u_2} - R_1 V_{u_1}\right] \tag{1}$$

where $\dot{m}$ is the mass flow rate.

$$\begin{aligned} \dot{m} &= \rho A \overline{V}_m \\ &= \rho(2\pi R_1 b_R) V_{M_1} K_{B_1} \\ &= \rho(2\pi R_2 b_R) V_{M_2} K_{B_2} \end{aligned} \tag{2}$$

The quantity $2\pi R b_R$ is the flow area, V_{m1} and V_{m2} are the meridional velocities at the mean streamline, and K_{B1} and K_{B2} are blockage factors which are assumed to be independent of the flow.

By introducing a flow coefficient

$$\Phi = \frac{V_{M2}}{U_2} = \frac{V_{M2}}{\omega R_2} \tag{3}$$

all necessary velocity and thrust equations can be written in terms of known geometric parameters and the flow coefficient. An iteration technique is later employed in program NORMAL to calculate Φ. The following velocity relations are developed now in order to simplify the energy relationships which follow.

The sign convention used is that all peripheral velocity components are positive when in the direction of rotation. From Figures 4 or 5 simple geometric relations are obtained which become, using eq. 3.

$$W_2 = V_{M2}/\cos \beta_2 = \omega R_2 \Phi/\cos \beta_2 \tag{4}$$

$$W_{u2} = V_{M2} \operatorname{Tan} \beta_2 = \omega R_2 \Phi \operatorname{Tan} \beta_2 \tag{5}$$

$$V_{u2} = W_{u2} + \omega R_2 = \omega R_2 [1 + \Phi \operatorname{Tan} \beta_2] \tag{6}$$

Also

$$V_{u2} = V_{M2} \operatorname{Tan} \alpha_2 = \omega R_2 \Phi \operatorname{Tan} \alpha_2 \tag{7}$$

An expression for α_2 in terms of the known relative exit angle can be obtained by equating the previous two equations, or

$$\operatorname{Tan} \alpha_2 = \operatorname{Tan} \beta_2 + 1/\Phi \tag{8}$$

similarly at the rotor inlet

$$W_{u1} = V_{M1} \operatorname{Tan} \beta_1 \tag{9}$$

$$V_{u1} = V_{M1} \operatorname{Tan} \beta_1 + \omega R_1 \tag{10}$$

The mass flow equation and the definition of the flow coefficient yield

$$V_{M1} = \Phi \; \omega R_2 \frac{R_2}{R_1} \; \frac{K_{B2}}{K_{B1}} \tag{11}$$

and

$$V_{u1} = \Phi \; \omega R_2 \frac{R_2}{R_1} \; \frac{K_{B2}}{K_{B1}} \; \text{Tan} \; \beta_1 + \omega R_1 \tag{12}$$

The mass flow equations must be extended to include flow through the stator.

$$\begin{aligned} \dot{m} = 2\pi \; R_2 \; b_R \; \rho \; V_{M2} \; K_{B2} &= 2\pi \; R_3 \; b_s \; \rho \; V_{M3} \; K_{B3} \\ &= 2\pi \; R_4 \; b_s \; \rho \; V_{M4} \; K_{B4} \end{aligned} \tag{13}$$

From the above relations, the meridional velocity equations are developed.

$$\frac{V_{M1}}{V_{M2}} = \frac{R_2}{R_1} \; \frac{K_{B2}}{K_{B1}} \tag{14}$$

$$\frac{V_{M3}}{V_{M2}} = \frac{R_2}{R_3} \; \frac{K_{B2}}{K_{B3}} \; \frac{b_R}{b_s} \tag{15}$$

$$\frac{V_{M4}}{V_{M2}} = \frac{R_2}{R_4} \; \frac{K_{B2}}{K_{B4}} \; \frac{b_R}{b_s} \tag{16}$$

1.1 Frictional Losses in Upper Passage

Let M_{fu} be the frictional moment from forces along the walls of the upper passage from station 2 to 3, acting on the flow opposite to the direction of rotation.

$$\dot{m} \; R_3 \; V_{u3} = \dot{m} \; R_2 \; V_{u2} - M_{fu} \tag{17}$$

Setting $M_{fu} = \lambda_u \dot{m} R_2 V_{u2}$ (18)

and $\eta_{Mu} = (1 - \lambda_u)$ (19)

eq. 17 becomes

$$V_{u3} = \eta_{Mu} \frac{R_2}{R_3} V_{u2} \tag{20}$$

From the mass flow equation

$$V_{M3} = \Phi \, \omega R_2 \frac{R_2}{R_3} \frac{K_{B2}}{K_{B3}} \frac{b_R}{b_s} \tag{21}$$

1.2 Frictional Losses in Lower Passage

With $M_{f\ell}$ being the frictional moment caused by forces along the lower passage walls from station 4 to 1 acting on the flow opposite to the direction of rotation, the equations for the lower passage are developed in a manner similar to the previous development.

$$M_{f\ell} = \lambda_\ell \dot{m} R_4 V_{u4} \tag{22}$$

$$\eta_{M\ell} = 1 - \lambda_\ell \tag{23}$$

$$V_{u1} = \eta_{M\ell} V_{u4} \frac{R_4}{R_1} \tag{24}$$

$$V_{M4} = \Phi \, \omega \, R_2 \frac{R_2}{R_4} \frac{K_{B2}}{K_{B4}} \frac{b_R}{b_s} \tag{25}$$

From Figure 4 it can be seen that

$$V_{u4} = V_{M4} \operatorname{Tan} \alpha_4 \tag{26}$$

Using the previous three equations gives

$$V_{u1} = \eta_{M\ell} \, \Phi \, \omega \, R_2 \frac{R_2}{R_1} \frac{K_{B2}}{K_{B4}} \frac{b_R}{b_s} \operatorname{Tan} \alpha_4 \tag{27}$$

From Figures 4 or 5, one can relate the absolute inlet angle to absolute velocity components as

$$\text{Tan } \alpha_1 = \frac{V_{u1}}{V_{M1}} \tag{28}$$

Using the relations developed for the inlet velocity eqs. 11 and 27, the absolute inlet angle is

$$\text{Tan } \alpha_1 = \eta_{M\ell} \frac{b_R}{b_s} \frac{K_{B1}}{K_{B4}} \text{Tan } \alpha_4 \tag{29}$$

Similarly the relative inlet angle is

$$\text{Tan } \beta_1 = \frac{V_{u1} - \omega R_1}{V_{M1}}$$

$$= \text{Tan } \alpha_1 - \frac{\omega R_1}{V_{M1}}$$

Substituting for V_{M1} yields

$$\text{Tan } \beta_1 = \eta_{M\ell} \frac{b_R}{b_s} \frac{K_{B1}}{K_{B4}} \text{Tan } \alpha_4 - \left(\frac{R_1}{R_2}\right)^2 \frac{K_{B1}}{K_{B2}} 1/\Phi \tag{30}$$

The relative and absolute velocities can now be obtained from their respective components by employing the following general equations:

$$V^2 = V_M^2 + V_u^2 \tag{31}$$

$$W^2 = V_M^2 + W_u^2 \tag{32}$$

$$W = V_M/\cos \beta \tag{33}$$

1.3 Torque Relations

The torque as defined in eq. 1 can now be expressed in terms of known geometric parameters and the flow coefficient. Using eqs. 37, 6, and 12 in eq. 1 yields

$$T_R = 2\pi\, R_2^{\,5}\, \frac{b_R}{R_2}\, \rho\, K_{B2}\, \omega^2 \left[\Phi + \Phi^2 \left\{ \mathrm{Tan}\, \beta_2 - \eta_{M\ell}\, \frac{K_{B2}}{K_{B4}}\, \frac{b_R}{b_s}\, \mathrm{Tan}\, \alpha_4 \right\} \right] \qquad (34)$$

The non-dimensional torque coefficient τ_R is now introduced as

$$\tau_R = \frac{T_R}{2\pi (R_2)^5\, \frac{b_R}{b_s}\, \rho\, K_{B2} \omega^2} =$$

$$\Phi + \Phi^2 \left\{ \mathrm{Tan}\, \beta_2 - \eta_{M\ell}\, \frac{K_{B2}}{K_{B4}}\, \frac{b_R}{b_s}\, \mathrm{Tan}\, \alpha_4 \right\} \qquad (35)$$

The torque T_s which the stator exerts on the fluid is positive when acting in the direction opposite to rotation

$$T_s = \dot{m}\, (R_3\, V_{u3} - R_4\, V_{u4}) \qquad (36)$$

Substituting the values for the whirl components gives

$$T_s = 2\pi R_2^{\,5} \left(\frac{b_R}{R_2}\right) \rho\, \omega^2\, K_{B2} \Big[\eta_{Mu}\, \Phi (1 + \Phi \mathrm{Tan} \beta_2) - \Phi^2 \left(\frac{b_R}{b_s}\right) \frac{K_{B2}}{K_{B4}}\, \mathrm{Tan}\, \alpha_4$$

Again introducing a non-dimensional torque coefficient

$$\tau_s = \frac{T_s}{2\pi\, R_2^{\,5} \left(\frac{b_R}{R_2}\right) \rho\, \omega^2\, K_{B2}} \qquad (37)$$

$$= \eta_{Mu}\, \Phi + \Phi^2 \left[\eta_{Mu}\, \mathrm{Tan}\, \beta_2 - \frac{b_R}{b_s}\, \frac{K_{B2}}{K_{B4}}\, \mathrm{Tan}\, \alpha_4 \right]$$

The general torque equation is

$$T_R - M_{fu} - M_{f\ell} = T_s$$

The torque exerted on the rotor by the fluid minus frictional moment losses is equal to torque exerted on the fluid by the stator.

The dimensionless torque coefficient introduced earlier is again given as

$$\Pi_T = \frac{T}{\rho\omega^2_{MAX} R_2^5} \tag{38}$$

2.0 Energy Relations

The torque and velocity equations developed in the preceeding section remain in terms of the unknown flow coefficient Φ. In this section an algebraic energy equation will be formulated and solved to yield Φ.

For the sake of this development, a total head term H will be defined which differs from the standard definition of total enthalpy H_T which is

$$H_T = h + \frac{V^2}{2} \tag{39}$$

or

$$H_T = u + \frac{p}{\rho} + \frac{V^2}{2} = u + \frac{P_T}{\rho} \tag{40}$$

where h is the static enthalpy

p is the static pressure

u is the internal energy

and P_T is the total pressure.

Since the fluid is treated as incompressible, one can uncouple the thermal effects from the mechanical effects, and define a 'total head' H which does not include thermal effects. This new term is denoted by

$$H = \frac{P_T}{\rho} = \frac{p}{\rho} + \frac{V^2}{2} \qquad (41)$$

Obviously the enthalpies are related by

$$(H_T - u) = H \qquad (42)$$

This new definition of total head H is useful in that constant H and constant P_T lines are coincident. Throughout the remainder of the analysis, useful total head H will be referred to as simply head. Note that this total head has the units of enthalpy (per unit mass).

The process undergone in the absorber is now represented in Figure 8. Obviously the process does not return to the original total enthalpy H_{T1}, although it does return to the original total pressure and head.

From Figure 8 the energy rise across the rotor is shown to be equal to the energy losses across the stator and through the passages, or

$$\Delta H_R - \Delta H_u - \Delta H_\ell - \Delta H_S = 0 \qquad (43)$$

Therefore,

$$(H_2 - H_1) - (H_2 - H_3) - (H_3 - H_4) - (H_4 - H_1) = 0 \qquad (44)$$

where all the above terms are written as positive quantities.

The four terms of eq. 44 will be derived in terms of the flow coefficient and the known geometric parameters as in Section 1.0. Eq. 44 is then straightforwardly solved to yield Φ. Program NORMAL is employed to accomplish this task. Since various loss parameters depend on Φ, an iteration technique must be used.

2.1 Conditions in Rotor

The incidence angle of the rotor blading i_R is defined as

$$i_R = \beta_1 - \beta_{1B} \tag{45}$$

or merely the angle between the tangent to the mean camber line at the leading edge and the relative inlet velocity. The incidence angle i_R is seen to become more negative in the direction corresponding to a greater lift coefficient for the blade.

The relative velocity W_1 can be resolved into two components respectively tangential and normal to the mean camber line. The energy associated with the tangential component W_1' is assumed to be largely recoverable. The energy associated with the normal component is assumed to be totally lost.

The useful relative velocity at the rotor inlet is then

$$W_1' = W_1 \cos i_R \tag{46}$$

and the velocity component lost due to incidence is similarly

$$W_{1i} = W_1 \sin i_R \tag{47}$$

The basic energy equation of turbo-machinery is

$$H_{T2} - H_{T1} = U_2 V_{u2} - U_1 V_{u1} \tag{48}$$

which upon expansion becomes

$$H_{T2} - H_{T1} = \frac{V_2^{\,2} + U_2^{\,2} - W_2^{\,2}}{2} - \frac{V_1^{\,2} + U_1^{\,2} - W_1^{\,2}}{2} \tag{49}$$

Using static enthalpies, regrouping, and cancelling terms in eq. 48 gives

$$h_2 + \frac{W_2^{\,2} - U_2^{\,2}}{2} = h_1 + \frac{W_1^{\,2} - U_1^{\,2}}{2} \tag{50}$$

Substituting for the static enthalpy and rearranging yields

$$\frac{p_2}{\rho} + \frac{W_2^{\,2}}{2} = \frac{p_1}{\rho} + \frac{W_1^{\,2}}{2} - \frac{U_2^{\,2} - U_1^{\,2}}{2} - (u_2 - u_1) \tag{51}$$

Upon resolving $W_1^{\,2}/2$ into its components and regrouping further, one obtains

$$\left(\frac{p_2}{\rho} + \frac{W_2^{\,2}}{2}\right) = \left(\frac{p_1}{\rho} + \frac{W_1^{\,\prime 2}}{2} + \frac{U_2^{\,2} - U_1^{\,2}}{2}\right) - \left(u_2 - u_1 - \frac{W_{1i}^{\,2}}{2}\right) \tag{52}$$

This leads naturally to the definition of the "equivalent relative total pressure" as

$$\frac{P_{E2}}{\rho} = \left(\frac{p_2}{\rho} + \frac{W_2^{\,2}}{2}\right) \tag{53}$$

and

$$\frac{P_{E1}}{\rho} = \left(\frac{p_1}{\rho} + \frac{W_1^{\,\prime 2}}{2} + \frac{U_2^{\,2} - U_1^{\,2}}{2}\right) \tag{54}$$

and to the definition of the rotor blading losses as

$$\frac{\Delta p_f}{\rho} = \left[(u_2 - u_1) - \frac{W_{1\,i}^{\,2}}{2}\right] = \left(\frac{P_{E1} - P_{E2}}{\rho}\right) \tag{55}$$

It also proves useful to express this loss in terms of a dimensionless coefficient defined as

$$Y_R = \left(\frac{P_{E1} - P_{E2}}{\frac{\rho}{2} W_2^2}\right) \qquad (56)$$

Recalling that

$$H_T = H - u \qquad (42)$$

and using the basic energy equation, eq. 48, one obtains the energy rise across the rotor in the form

$$(H_2 - H_1) = U_2 . V_{u2} - U_1 \, V_{u1} - \left\{\sin^2 i_R \frac{W_1^2}{2} + Y_R \frac{W_2^2}{2}\right\} \qquad (57)$$

This equation can be conveniently non-dimensionalized by dividing by U_2^2. The velocity expressions developed in Section 1.0 can not be utilized to simplify eq. 57, and the dimensionless energy rise across the rotor $(\Pi \Delta H)_R$ can be written as

$$(\Pi_{\Delta H})_R = \frac{H_2 - H_1}{\omega^2 R_2^2} = 1 - \frac{(\sin^2 i_R)}{2} \left(\frac{R_1}{R_2}\right)^2$$

$$+ \Phi \left\{\operatorname{Tan} \beta_2 - \left(\frac{K_{B2}}{K_{B4}} \cdot \frac{b_R}{b_s} \eta_{M\ell} \operatorname{Tan} \alpha_4\right) \cos^2 i_R\right\} \qquad (58)$$

$$- \Phi^2 \left\{\frac{\sin^2 i_R}{2} \left(\frac{R_2}{R_1}\right)^2 \left[\left(\frac{K_{B2}}{K_{B1}}\right)^2 + \left(\frac{K_{B2}}{K_{B4}} \frac{b_R}{b_s} \eta_{M\ell} \operatorname{Tan} \alpha_4\right)^2\right]\right.$$

$$\left. + \frac{Y_R}{2\cos^2 \beta_2}\right\}$$

where the dimensionless head coefficient is defined as

$$\Pi_{\Delta H} = \frac{\Delta H}{\omega^2 R_2^2} \tag{59}$$

The loss coefficient Y_R of eqs. 56 and 58 is a function of the deflection $\Delta\beta$, where

$$\Delta \beta_R = \beta_2 - \beta_1$$

and the aspect ration Λ_R, defined by

$$\Lambda_R = \frac{b_R}{R_2 - R_1} \tag{60}$$

This will be further discussed in Section 3.0.

2.2 Performance of Rotor Blading

The rotor is designed for the maximum useful enthalpy rise across the blades. If this were a frictionless process, the useful energy rise would naturally be greater than in an actual process involving friction. Therefore, the rotor efficiency is defined as

$$\eta_R = \frac{H_2 - H_1}{H_{2\,Th} - H_1} \tag{61}$$

where the total heads H_1, H_2, and H_{2Th} are shown on the H-s diagram, Figure 8. Of course the pressure rise through the rotor is related very simply to the corresponding energy rise according to the relation

$$H = \frac{P_T}{\rho} \tag{62}$$

The numerator of eq. 61 is obtained from either eqs. 57 or 58. The denominator of eq. 61 is similarly obtained, but for the theoretical case both the incidence and blading losses are non-existent.

It follows from eq. 58 that

$$(\Pi_{\Delta H_{Th}})_R = \left\{\frac{H_{2Th} - H_1}{\omega^2 R_2^{\,2}}\right\}$$

$$= 1 + \Phi \left\{\mathrm{Tan}\ \beta_2 - \eta_{M\ell} \frac{b_R}{b_s} \frac{K_{B2}}{K_{B4}} \mathrm{Tan}\ \alpha_4\right\} \tag{63}$$

is the theoretical dimensionless energy rise across the rotor. The efficiency can obviously be written as

$$\eta_R = \frac{(\Pi_{\Delta H})_R}{(\Pi_{\Delta H_{Th}})_R} \tag{64}$$

The general definition of power $\mathcal{P}$ is

$$\mathcal{P} = \dot{m}\ \Delta\ H \tag{65}$$

It is convenient to introduce a dimensionless power coefficient as

$$\Pi_{\mathcal{P}} = \frac{\mathcal{P}}{\rho\omega_{MAX}^3\ R_2^{\,5}} \tag{66}$$

Recalling that

$$\Phi = \frac{V_{M2}}{\omega\ R_2} \tag{3}$$

$$\dot{m} = 2\pi\ \rho\ R_2\ b_R\ V_{M2}\ K_{B2} \tag{2}$$

and

$$\Pi_{\Delta\ H} = \frac{\Delta\ H}{\omega^2 R_2^{\,2}} \tag{59}$$

the dimensionless power and head coefficients can now be related as

$$\Pi_{\mathcal{P}} = \left\{ 2\pi \left(\frac{b_R}{R_2} \right) K_B \left(\frac{\omega}{\omega_{MAX}} \right)^3 \right\} \Phi \, \Pi \Delta H \tag{67}$$

The power is related to the torque by the simple expression

$$\Pi_{\mathcal{P}} = \Pi_{TR} \left(\frac{\omega}{\omega_{MAX}} \right) \tag{68}$$

2.3 Energy Losses in the Upper Passage

The energy loss in the upper passage, assumed as only a total pressure loss due to friction between the rotor and stator, is expressed as

$$\Delta H_u = H_2 - H_3 = \frac{P_{T2}}{\rho} - \frac{P_{T3}}{\rho} \tag{69}$$

or

$$\Delta H_u = \left(\frac{p_2}{\rho} + \frac{V_2^2}{2} \right) - \left(\frac{p_3}{\rho} + \frac{V_3^2}{2} \right) . \tag{70}$$

In a frictionless process

$$H_2 = (H_3)_{T\,H} = \frac{p_{3\ TH}}{2} + \frac{V_3^2}{2} . \tag{71}$$

and from eq. 17 with the frictional moment M_{fu} equal to zero

$$(V_{u3})_{TH} = V_{u2} \frac{R_2}{R_3} = \frac{V_{u3}^2}{\eta_{Mu}^2} \tag{72}$$

Resolving $V_3^2/2$ into its components, one can write eq. 71 as

$$H_2 = (H_3)_{TH} = \frac{p_{3TH}}{\rho} + \frac{V_{M3}^2}{2} + \frac{1}{2} \frac{V_{u3}^2}{\eta^2_{Mu}} \tag{73}$$

Similarly for an actual process

$$H_3 = \frac{p_3}{\rho} + \frac{V_{M3}^2}{2} + \frac{V_{u3}^2}{2} \tag{74}$$

the energy loss can now be written using the two previous equations as

$$H_2 - H_3 = \frac{p_{3TH} - p_3}{\rho} + \left(\frac{1}{\eta_{Mu}^2} - 1\right) \frac{V_{u3}^2}{2} \tag{75}$$

A convenient dimensionless pressure loss coefficient can now be denoted as

$$C_u = \frac{p_{3TH} - p_3}{\rho \left(\frac{V_{M3}^2}{2}\right)} \tag{76}$$

where C_u will be shown to depend primarily on the radius ratio $\frac{r_o}{r_i}$ of the upper passage in Figure 2. This is similar to energy loss coefficients developed for bends in smooth pipes.

Eq. 75 is non-dimensionalized, and using eq. 76 one obtains

$$(\Pi\, \Delta H)_u = \frac{C_u}{2} \frac{V_{M3}^2}{\omega^2 R_2^2} + \frac{1}{2} \left(\frac{1}{\eta_{Mu}^2} - 1\right) \frac{V_{u3}^2}{\omega^2 R_2^2} \tag{77}$$

Using previously developed expressions for V_M one obtains an equation similar in form to eq. 58 or

$$(\Pi\, \Delta H)_u = \frac{H_2 - H_3}{\omega^2 R_2^2}$$

$$= \frac{1-\eta_{Mu}^2}{2} \left(\frac{R_2}{R_3}\right)^2 + \Phi \left\{\left(\frac{R_2}{R_3}\right)^2 (1-\eta_{Mu}^2) \operatorname{Tan} \beta_2\right\} \tag{78}$$

$$+ \Phi^2 \left\{\frac{C_u}{2} \left(\frac{R_2}{R_3} \frac{b_R}{b_s} \frac{K_{B2}}{K_{B3}}\right)^2 + \frac{(1-\eta_{Mu}^2)}{2} \left(\frac{R_2}{R_3}\right)^2 \operatorname{Tan} \beta_2\right\}$$

2.4 Performance of Stator Blading

From Figure 4 the stator incidence angle i_s is

$$i_s = \alpha_3 - \alpha_3 B \tag{79}$$

and the useful inlet velocity V_3' is

$$V_3' = V_3 \cos i_s \tag{80}$$

The total head ahead of stator blades is given by

$$H_3 = \frac{p_3}{\rho} + \frac{V_3^2}{2} = \frac{P_{T3}}{\rho} \tag{81}$$

while the useful head is

$$H_3' = \frac{p_3}{\rho} + \frac{(V_3')^2}{2} = \frac{P_T'{}_3}{\rho} \tag{82}$$

The above three equations combine to yield

$$\begin{aligned} H_3' &= H_3 + \frac{(V_3')^2 - (V_3)^2}{2} \\ &= H_3 - \frac{V_3^2}{2} (\sin^2 i_s) \end{aligned} \tag{83}$$

Similar to rotor blading losses, stator blading losses will be defined as

$$Y_s = \frac{P_{T3}' - P_{T4}}{\frac{\rho}{2} V_4^2} = \frac{H_3' - H_4}{(V_4^2/2)} \tag{84}$$

or

$$H_4 = H_3' - Y_s \frac{V_4^2}{2} = H_3 (\sin^2 i_s) \frac{V_3^2}{2} - Y_s \frac{V_4^2}{2} \tag{85}$$

Subtracting H_1 from both sides yields

$$H_4 - H_1 = H_3 - H_1 - (\sin^2 i_s) \frac{V_3^2}{2} - Y_s \frac{V_4^2}{2} \tag{86}$$

The same non-dimensionalizing technique used in Sections 2.1, and 2.3 is again employed and the energy loss in the lower passage is now available in the general form as

$$\frac{H_4 - H_1}{\omega^2 R_2^2} = \frac{H_3 - H_1}{\omega^2 R_2^2} - \frac{\eta_{Mu}^2}{2} \left(\frac{R_2}{R_3}\right)^2 \Bigg\{ (\sin^2 i_s) + \Phi \left[(\sin^2 i_s)\, 2 \operatorname{Tan} \beta_2 \right] + \Phi^2 \left\{ (\sin^2 i_s) \left[\left(\frac{1}{\eta_{Mu}} \frac{b_R}{b_s} \frac{K_{B2}}{K_{B3}} \right)^2 + \operatorname{Tan}^2 \beta_2 \right] + \frac{Y_s}{\eta_{Mu}^2} \left[\frac{R_3}{R_4} \frac{b_R}{b_s} \frac{K_{B2}}{K_{B4}} \frac{1}{\cos \alpha_4} \right]^2 \right\} \Bigg\} \tag{87}$$

The above equation is actually

$$\frac{H_4 - H_1}{\omega^2 R_2^2} = \frac{H_3 - H_1}{\omega^2 R_2^2} - \frac{H_3 - H_4}{\omega^2 R_2^2}$$

This can be further reduced to give

$$\frac{H_4 - H_1}{\omega^2 R_2^2} = \frac{H_2 - H_1}{\omega^2 R_2^2} - \frac{H_2 - H_3}{\omega^2 R_2^2} - \frac{H_3 - H_4}{\omega^2 R_2^2} \tag{88}$$

which gives the energy losses in the lower passage in terms of the energy changes throughout the remainder of the system. The next step is to find the energy loss in the lower passage and solve eq. 44.

Again the loss coefficient Y_s is a function of deflection and the aspect ration, where

$$\Delta\beta_s = \alpha_3 - \alpha_4 \tag{89}$$

and

$$\Lambda_s = \frac{b_s}{R_3 - R_4} \tag{90}$$

2.5 Losses in Lower Passage

The development of the energy loss in the lower passage closely follows the technique of Section 2.3.

The energy loss in the lower passage is

$$\Delta H_\ell = H_4 - H_1 = \frac{p_4}{\rho} + \frac{V_4^{\,2}}{2} - \left(\frac{p_1}{\rho} + \frac{V_1^{\,2}}{2}\right) \tag{91}$$

for a frictionless process

$$(V_{u1})_{Th} = V_{u4}\,\frac{R_4}{R_1} \tag{92}$$

or relating theoretical to actual velocities yields

$$(V_{u1})_{Th} = \frac{V_{u1}}{\eta_{M\ell}} \tag{93}$$

Therefore,

$$H_4 = (H_1)_{Th} = \frac{(p_1)_{Th}}{\rho} + \frac{V_{M1}^{\,2}}{2} + \frac{1}{2}\left(\frac{V_{u1}}{\eta_{M\ell}}\right) \tag{94}$$

while

$$H_1 = \frac{p_1}{\rho} + \frac{V_{M1}^{\,2}}{2} + \frac{V_{u1}^{\,2}}{2} \tag{95}$$

the pressure loss coefficient is

$$\frac{(p_1)_{Th} - p_1}{\rho} = C_\ell \frac{V_{M1}^{\;2}}{2} \qquad (96)$$

The expressions for H_1 and H_4 are now substituted into eq. 1, along with eq. 6 to yield

$$H_4 - H_1 = C_\ell \frac{V_{M1}^{\;2}}{2} + (1 - \eta^2_{M\ell}) \left(\frac{R_4}{R_1}\right)^2 V_{u4}^{\;2} \qquad (97)$$

This is easily put into the dimensionless form used previously or

$$(\Pi\Delta H)_\ell = \frac{\Phi^2}{2} \left(\frac{R_2}{R_1}\right)^2 \left[C_\ell \left(\frac{K_{B2}}{K_{B1}}\right)^2 + \left(1 - \eta_{M\ell}^{\;2}\right)\left(\frac{b_R}{b_s} \frac{K_{B2}}{K_{B4}} \text{Tan } \alpha_4\right)^2\right] \qquad (98)$$

Eq. 97 can now be substituted into eq. 88 and Φ can be solved for straightforwardly. Iteration is necessary, however, since all loss coefficients depend on Φ.

3.0 Loss Coefficient in Rotor

Vavra (3) gives a relation for the losses in axial turbine bladings as

$$\Psi = 0.99 - \frac{2.28}{10^4} \Delta \beta - \frac{4.97}{180 - \Delta\beta} \qquad (99)$$

where $\Delta\beta$ is the flow deflection angle in degrees. The quantity Ψ is the velocity coefficient defined as the ratio of the actual and theoretical discharge velocities, which for the rotor is

$$\Psi_R = \frac{W_2}{W_{2Th}} \qquad (100)$$

and

$$\Delta\beta_R = \beta_2 - \beta_1 \qquad (101)$$

The theoretical case occurs for Y_R equal zero which in accordance to eq. 56 gives $P_{E1} = P_{E2Th}$. Substituting eq. 100 into eq. 53 yields

$$\frac{P_{E1}}{\rho} = \frac{P_{E2Th}}{\rho} = \frac{p_2}{\rho} + \frac{1}{2} \frac{W_2^{\,2}}{\Psi^2} \tag{102}$$

The actual rotor blading losses using eq. 102 can now be written as

$$Y_R = \frac{\left(\frac{p_2}{\rho} + \frac{W_2^{\,2}}{2\Psi^2}\right) - \left(\frac{p_2}{\rho} + \frac{W_2^{\,2}}{2}\right)}{W_2^{\,2}/2} = \frac{1}{\Psi^2} - 1 \tag{103}$$

In accordance with Horlock (Ref. 4) the loss coefficients depend on Reynolds numbers R_{NR} and aspect ratio Λ_R of eq. 60. Hence let Y_R of eq. 103 now denoted as Y_R^* be the loss coefficient across the rotor blading for $\Lambda_R = 3$ and $R_{NR} = 10^5$. The latter term is defined as

$$R_{NR} = \frac{D_{hR}\, W_2}{\nu} \tag{104}$$

where D_{hR} is the hydraulic diameter of the discharge area of the flow channel between adjacent blades. If Δ'_R is the rotor blade spacings at the radius R_2, and a_R is the opening at the discharge as shown in Figure 3, an approximation of the discharge opening is given by

$$a_R \simeq \Delta'_R \cos \beta_2 \tag{105}$$

then

$$D_{hR} = \frac{4\ (\text{flow area})}{\text{wetted perimeter}} = \frac{4\, a_R\, b_R}{2\,(a_R + b_R)} \tag{106}$$

Substituting for a_R and rearranging yields

$$D_{h_R} = \frac{2b_R}{1 + \dfrac{b_R}{s_R \cos \beta_2}} \tag{107}$$

The blade spacing s_R can be found with respect to the radial extension $R_2 - R_1$ by using the blade loading criterion of Zweifel (Ref. 5). For axial bladings this approximation is

$$\frac{s_R}{R_2 - R_1} \simeq \frac{0.425}{(\mathrm{Tan}\ \beta_2 - \mathrm{Tan}\ \beta_{1B}) \cos^2 \beta_2} \tag{108}$$

Substituting this equation into the expression for the hydraulic diameter yields

$$\frac{D_{hR}}{R_2} = \frac{2\left(\dfrac{b_R}{R_2}\right)}{1 + \dfrac{(b_R/R_2)(\mathrm{Tan}\beta_2 - \mathrm{Tan}\beta_{1B})\cos\beta_2}{0.425(1-R_1/R_2)}} \tag{109}$$

Placing the above equation into the expression for the Reynolds number and recalling that

$$W_2 = \frac{\omega R_2\ \Phi}{\cos\ \beta_2} \tag{4}$$

one obtains

$$R_{NR} = \frac{2\left(\dfrac{b_R}{R_2}\right) \Phi\ \omega\ R_2^{\ 2}}{\left[\cos\beta_2 + \dfrac{(b_R/R_2)(\mathrm{Tan}\beta_2 - \mathrm{Tan}\beta_{1B})\ \cos^2\beta_2}{0.425\ (1 - R_1/R_2}\right] \nu} \tag{110}$$

The loss coefficient is dependent on the aspect ratio and Reynolds number through the following relations after Horlock (Ref. 4).

$$Y_R^{\,*} = \frac{1}{\Psi^2} - 1 \tag{111}$$

$$Y_R^{\,'} = \frac{1}{\Psi^2}\,(.975 + \frac{.075}{\Lambda_R}) - 1 \tag{112}$$

and

$$Y_R = Y_R^{\,'}\left(\frac{10^5}{R_{NR}}\right)^{.25} \tag{113}$$

where the coefficient $Y_R^{\,'}$ holds for the actual aspect ration only at a Reynolds number equal to 10^5. By combining the above equations the generalized loss coefficient is simply

$$Y_R = \left\{\frac{1}{\Psi^2}\left(.975 + \frac{.075}{\Lambda_R}\right) - 1\right\}\left(\frac{10^5}{R_{NR}}\right)^{.25} \tag{114}$$

These relations allow the actual loss coefficient of the energy absorber to be determined under varied conditions.

Obviously the Reynolds number is not totally specified by geometric parameters, but depends on the flow coefficient Φ. In iterating for Φ, the process must be assumed to begin at $Y_R^{\,'}$, or a Reynolds number of 10^5, and subsequently correct the loss coefficient as improved values of Φ and R_{NR} are calculated. This procedure must also be employed for the velocity coefficient Ψ which is dependent on Φ through a dependence on the actual inlet angle β_1. The iteration must be continued until convergence is achieved for all values dependent on Φ.

3.1 Loss Coefficient in Stator

This section follows closely the development in Section 3.0. Eq. 99 is again used with

$$\Psi_s = \frac{V_4}{V_{4Th}} \tag{115}$$

and

$$\Delta\beta_s = \alpha_3 - \alpha_4 \tag{116}$$

For a frictionless process in the stator, the total pressure $(P_{T4})_{Th}$ at stator exit would equal total useful inlet pressure P_{T3}', or

$$\frac{(P_{T4})_{Th}}{\rho} = \frac{P_{T3}'}{\rho} = \frac{p_4}{\rho} + \frac{(V_4)^2_{Th}}{2} \tag{117}$$

Substituting eq. 115 into eq. 117 yields

$$\frac{P_{T3}}{\rho} = \frac{p_4}{\rho} + \frac{1}{\Psi_s^2}\,\frac{V_4^2}{2} \tag{118}$$

For an actual flow

$$H_4 = \frac{P_{T4}}{\rho} = \frac{p_4}{\rho} + \frac{V_4^2}{2} \tag{119}$$

which yields through eq. 84

$$Y_s = \frac{1}{\Psi_s^2} - 1 = Y_s^* \tag{120}$$

This was as expected from Section 3.0. The loss coefficient can now be written after eqs. 112, 113, and 114 as

$$Y_s' = \frac{1}{\Psi^2}\left(.975 + \frac{.075}{\Lambda_R}\right) - 1 \tag{121}$$

$$Y_s = Y_s' \left(\frac{10^5}{R_{NS}}\right)^{.25} \tag{122}$$

and finally

$$Y_s = \left\{\frac{1}{\psi^2}\left(.975 + \frac{.075}{\Lambda_s}\right) - 1\right\} \left(\frac{10^5}{R_{Ns}}\right)^{.25} \tag{123}$$

where the aspect ratio is defined by eq. 90 as

$$\Lambda_s = \frac{b_s}{R_3 - R_4}$$

The Reynolds number for the stator is

$$R_{Ns} = \frac{D_{hs} \, V_4}{\nu} \tag{124}$$

where for $a_s \simeq \mathscr{s}_s \cos\alpha_4$, the hydraulic diameter is

$$D_{hs} = \frac{2b_s}{1 + \dfrac{b_s/\mathscr{s}_s}{\cos\,\alpha_4}} \tag{125}$$

The blade spacing according to Zweifel (Ref. 5) is

$$\frac{\mathscr{s}_s}{R_3 - R_4} = \frac{0.425}{(|\,\mathrm{Tan}\;\alpha_4 - \mathrm{Tan}\;\alpha_{3B}\,|)\cos^2\alpha_4} \tag{126}$$

and from eqs. 25 and 26

$$V_4 = \Phi\;\omega\;R_2\;\frac{R_2}{R_4}\;\frac{b_R}{b_s}\;\frac{K_{B2}}{K_{B4}}\;\frac{1}{\cos\;\alpha_4} \tag{127}$$

The Reynolds number can now be expressed using the above four equations as

$$R_{Ns} = \frac{2 \left(\frac{b_R}{R_4}\right) \frac{K_{B2}}{K_{B4}} \Phi \, \omega \, R_2{}^2}{\nu \left[\cos \alpha_4 + \frac{\frac{b_s}{R_2} (| \operatorname{Tan} \alpha_4 - \operatorname{Tan} \alpha_{3B} |) \cos^2 \alpha_4}{0.425 \left(R_3/R_2\right) \left(1 - \frac{R_4}{R_3}\right)} \right]} \tag{128}$$

A series of iterations is again needed to insure proper convergence of all parameters.

4.0 Pressure Loss Coefficients in Upper and Lower Passages

In accordance with eq. 76 the pressure losses in the upper passage are expressed by

$$\frac{(p_3)_{Th} - p_3}{\rho} = C_u \frac{V_{M3}^2}{2} \tag{129}$$

and similarly for the lower passage by eq. 96 as

$$\frac{(p_1)_{Th} - p_1}{\rho} = C_\ell \frac{V_{M1}^2}{2} \tag{130}$$

With Δpb being the pressure drop in the bend, the loss coefficients of these bends defined as

$$\xi = \frac{\Delta pb}{\frac{\rho}{2} V^2} \tag{131}$$

are shown in Figure 15 as functions of the Reynolds number R_N, where similar to eqs. 104 and 124

$$R_N = \frac{V \cdot D_h}{\nu} \tag{132}$$

Vavra (Ref. 2) has developed the set of curves shown in Figure 15. These curves are based on the data of Sprenger (Ref. 6). Interpolation

was to obtain values for ratios of r_i/b different than those found in Sprenger.

The hydraulic diameter D_h is again

$$D_h = \frac{4 \text{ flow area}}{\text{wetted perimeter}} \tag{133}$$

For a ring channel with flow area of 2π R b the wetted perimeter is $2(2\pi R)$, or

$$D_h = \frac{4(2\pi\ R)b}{2(2\pi\ R)} = 2b \tag{134}$$

Hence at the rotor inlet there is

$$D_h = 2b_R \tag{135}$$

and at the stator inlet

$$D_h = 2b_s \tag{136}$$

These above two values are introduced into eq. 132, with V equal to the corresponding value of V_M, that is, V_{M1} before the rotor and V_{M3} before the stator. The result is

$$R_{Nu} = \frac{V_{M3}\ 2b_s}{\nu} \tag{137}$$

$$R_{N\ell} = \frac{V_{M1}\ 2b_R}{\nu} \tag{138}$$

The Reynolds number is then used to obtain the loss coefficients ξ of Figure 15.

The loss coefficients ξ of Figure 15 have been obtained from the measured pressure drops by subratcting the pressure drops that would

occur in a straight duct at the corresponding Reynolds number and surface roughness.

There are several conclusions which can be drawn from Figure 15 and from additional data in Sprenger (Ref. 6). In general, the loss coefficients for bends made up of two concentric radii increase with decreasing $^{r}i/b$ ratios. The curves ξ versus R_N that exhibit a minimum indicate the flow separations occur at the inner radius, and should be avoided. Finally, Sprenger (Ref. 6) shows that two bends with $^{r}i/b = 0.5$ arranged in series to form a 180° bend have a loss coefficient of 1.66ξ at $R_N = 10^5$ where ξ is the loss coefficient of one of the 90° bends. This data will be a first approximation in choosing the loss coefficient for the 180° bends in the energy absorber.

4.1 Estimate of the Pressure Loss Coefficients in the Upper and Lower Passage

The losses in the upper and lower passages will be assumed due to two components, passage bending and friction. The losses due to duct bending were discussed in the previous section. An arbitrary assumption is to take these loss coefficients equal to 2.0 and 2.5 for the upper and lower passage respectively. The values of ξ are given in Figure 15 for various value of $^{r}i/b$. It is recommended that $^{r}i/b$ be chosen between 0.5 and 1.0. Any bend with a value of $^{r}i/b$ larger than 1.0 will be assumed to have the same losses as a bend with $^{r}i/b$ equal 1.0.

To the above losses must be added the frictional losses in a straight duct of hydraulic diameter D_h and average length L, where

$$L = \frac{L_i + L_o}{2} \qquad (139)$$

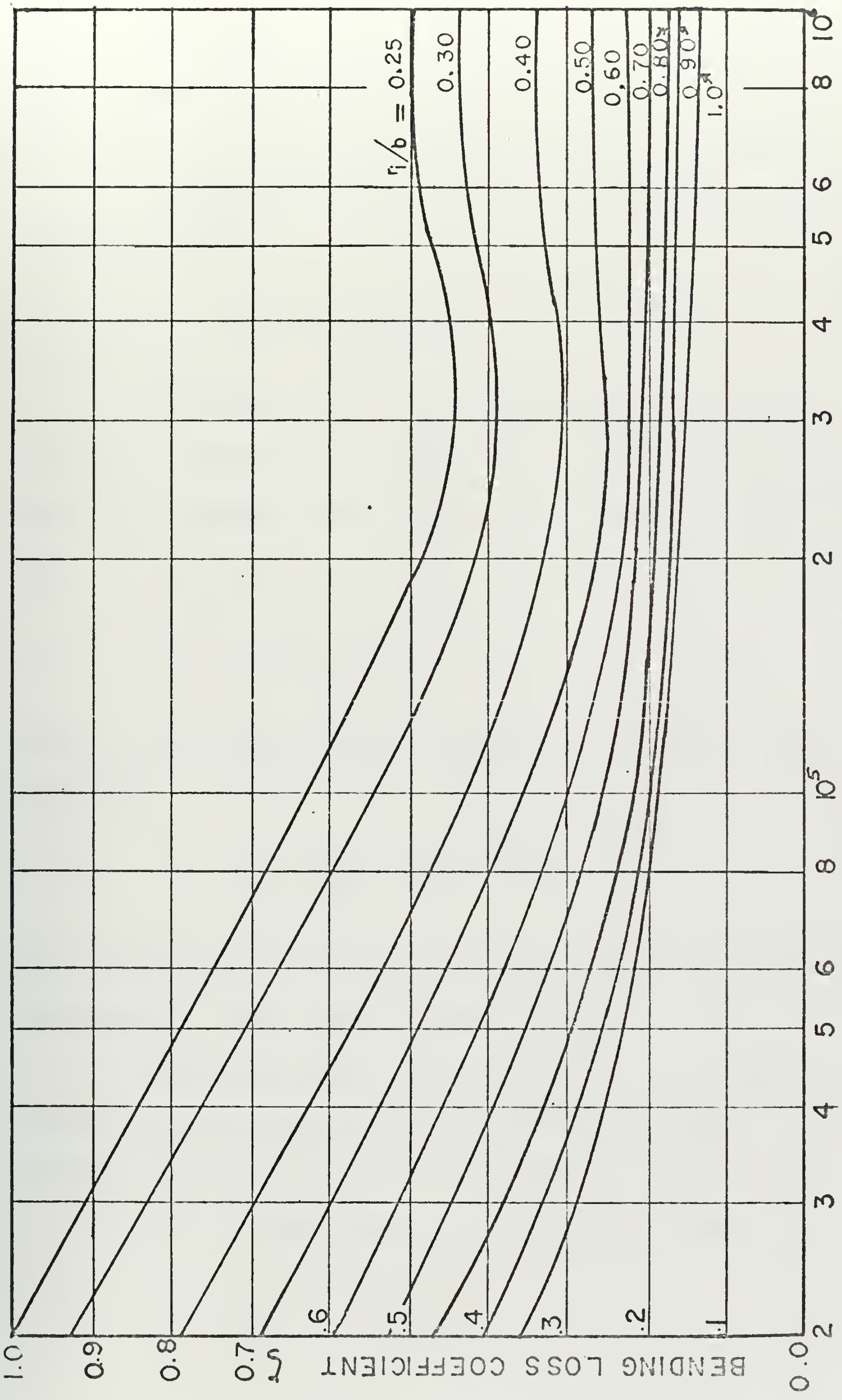

Figure 15 Estimate of Loss Coefficient ξ (Vavra Ref. 2)

and L_i is the distance along the inner contour and L_o that along the outer contour in the meridional plane from the trailing edges of one blade row to the leading edges of the other row. (See Figure 2)

In accordance with eqs. 132 and 136 this general frictional pressure loss is

$$\Delta p_f' = \lambda_f \frac{L}{2b} \frac{\rho}{2} V_M^2 \qquad (140)$$

The friction factor λ_f is a function of both Reynolds number and surface roughness. The value of λ_f is obtained from the curve of Figure 16, also from Vavra (Ref. 2), for a relative surface roughness of

$$\frac{K_r}{D_h} = \frac{1}{10^4} \qquad (141)$$

where K_r is the peak-to-valley roughness of the surface. Hence, for this case

$$K_r = \frac{2b}{10^4} = 200 \text{ b u - in.} \qquad (142)$$

If it is assumed that the rms roughness be one-half K_r, the surface finish must be better than 100 b micro-inches.

The applicability of this data to the three dimensional flow channels of the energy absorbed is obviously questionable. The losses defined below must , at best, be considered as first estimates only.

The loss coefficient C_u of eq. 129 will be taken as

$$C_u = 2.0\ \xi + \frac{L_u}{2b_R} \lambda_f \qquad (143)$$

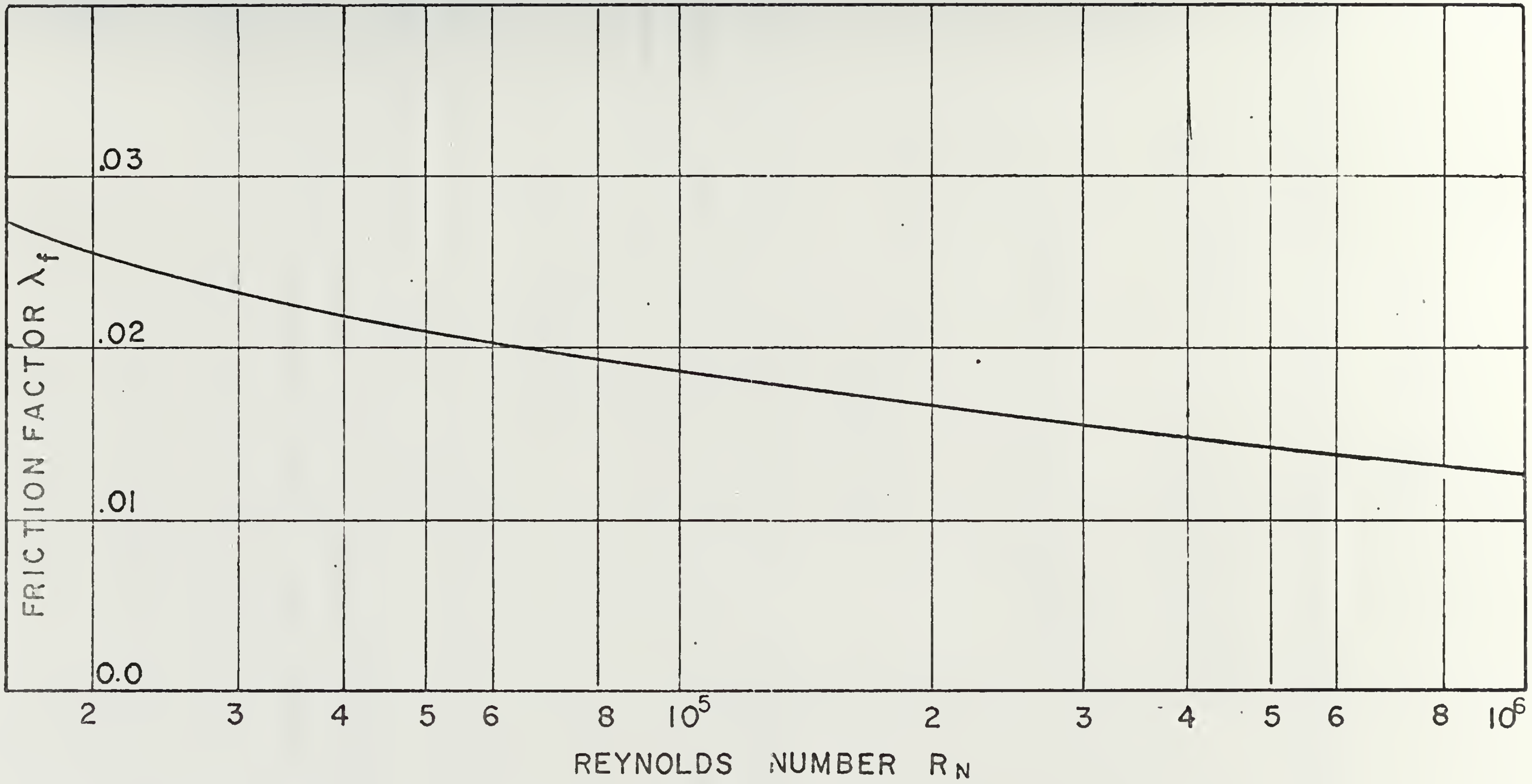

Figure 16 Estimated Channel Wall Friction Factor λ_f (Vavra Ref. 2)

and C_ℓ of eq. 130 is

$$C_\ell = 2.5\,\xi + \frac{L_\ell}{2b_s}\,\lambda_f \tag{144}$$

where ξ is obtained from Figure 15 and λ_f from Figure 16 for

$$R_{Nu} = \frac{2b_s\, V_{M3}}{\nu} = \left(\Phi\ \omega\ R_2\ \frac{R_2}{R_3}\ \frac{K_{B2}}{K_{B3}}\ \frac{b_R}{b_s}\right) \frac{2b_s}{\nu} \tag{145}$$

and

$$R_{N\ell} = \frac{2b_R\, V_{M1}}{\nu} = \left(\Phi\ \omega\ R_2\ \frac{R_2}{R_1}\ \frac{K_{B2}}{K_{B1}}\right) \frac{2b_R}{\nu} \tag{146}$$

In eq. 4 the length L_u is given by

$$L_u = \frac{(L_u)_i + (L_u)_o}{2}$$

where $(L_u)_i$ and $(L_u)_o$ are the lengths of the inner and outer meridional contours, respectively, of the walls of the upper passage between stations 2 and 3. Similarly in eq. 133

$$L_\ell = \frac{(L_\ell)_i + (L_\ell)_o}{2} \tag{147}$$

where $(L_\ell)_i$ and $(L_\ell)_o$ are the counterparts of $(L_i)_u$ and $(L_u)_o$ for the lower passage between stations 4 and 1.

5.0 Losses of Angular Momentum in Upper and Lower Passages

The frictional moments along the upper and lower passages were introduced by eqs. 18 and 22 respectively as

$$M_{fu} = \lambda_u\ \dot{m}\ R_2\ V_{u2} \tag{148}$$

and

$$M_{f\ell} = \lambda_\ell\ \dot{m}\ R_4\ V_{u4} \tag{149}$$

No data is presently available for the losses of angular momentum in passages of the type needed between the rotor and stator of the present absorber. A very crude approximation of these moments is obtained, however, by assuming that the shear stresses Ψ_o on the walls are merely those acting on a flat plate with a peripheral velocity V_u at R being the velocity outside the boundary layer. This over-simplification ignores the effect of the meridional velocity components which may cause large increases in the frictional moments.

For fully turbulent boundary layers along rough walls the shear stress is

$$\Psi_o = c_f \frac{\rho}{2} V_u^2 \tag{150}$$

where c_f is assumed to be invarient with the Reynolds number of the flow. On the element of wall area 2π Rd L of Figure 2 there acts a frictional moment

$$dM_f = 2\pi \, RdL \, \Psi_o \, R$$

which becomes when using eq. 3

$$dM_f = \pi \, \rho \, c_f \, (R \, V_u)^2 \, d \, L \tag{151}$$

It is assumed that the passages have been designed such that the flow is not separated from the walls, and all stresses external to the boundary layer are an order of magnitude smaller than stresses along the walls, and therefore negligible. This results in the product (RV_u) being constant outside of the boundary layers and equal to R_2V_{u2}, the value at the rotor discharge, for the upper passage. Integrating eq. 151 from station 2 to station 3 yields

$$M_{fu} = \int_{(2)}^{(3)} \pi \rho c_f (R_2 V_{u2})^2 dL \tag{152}$$

$$M_{fu} = \pi \rho c_f (R_2 V_{u2})^2 \left[(L_u)_i + (L_u)_o\right] \tag{153}$$

where the inner wall is of length $(L_u)_i$ and the outer wall is of length $(L_u)_o$. Hence by eq. 148

$$\lambda_u = \frac{\pi \rho c_f R_2 V_{u2} \left[(L_u)_i + (L_u)_o\right]}{\dot{m}} \tag{154}$$

Substitution of the mass flow equation and velocity relations into eq. 154 gives

$$\lambda_u = c_f \frac{1 + \Phi \operatorname{Tan} \beta_2}{\Phi} \frac{\left[(L_u)_i + (L_u)_o\right]}{2 b_R K_{B2}} \tag{155}$$

from eq. 19

$$\eta_{Mu} = 1 - c_f \frac{1 + \Phi \operatorname{Tan} \beta_2}{\Phi} \frac{\left[(L_u)_i + (L_u)_o\right]}{2 b_R K_{B2}} \tag{156}$$

For the lower passage a similar procedure and derivation leads to

$$\lambda_\ell = \frac{c_f \operatorname{Tan} \alpha_4}{K_{B4}} \frac{\left[(L_\ell)_i + (L_\ell)_o\right]}{2 b_s} \tag{157}$$

and

$$\eta_{M\ell} = 1 - \frac{c_f \operatorname{Tan} \alpha_4 \left[(L_\ell)_i + (L_\ell)_o\right]}{2 K_{B4} b_s} \tag{158}$$

In eqs. 155 through 158, the absolute value of the flow angles must be introduced since the loss is a function of absolute deflection.

For fully turbulent boundary layers, as in the present case, the local skin friction coefficients c_f depend on the surface roughness ration K_s/x, where K_s is the peak to average value roughness and x is length along the plate.

$$c_f \simeq .004 \text{ for } K_s/x = 10^{-4}$$

and

$$c_f \simeq .006 \text{ for } K_s/x = 10^{-3}$$

Since there will be flow irregularities and possible flow separations, it is advisable to use a larger value for c_f. A $c_f = .016$ was chosen since it gives best agreement with M-21 test data.

APPENDIX B

DETAILED ANALYSIS OF THE ENERGY ABSORBER WITH THE FLUID CIRCULATING IN THE REVERSE DIRECTION, MODES 3 AND 4

A separate set of equations must be derived for the reverse flow modes. The reason, mentioned earlier, is that the relative flow exit angles which are assumed constant are now different.

This development follows very closely to the previous analysis. Therefore, the intermediate steps of this derivation are omitted.

1. Assumptions

a. β_1 = constant

α_3 = constant

The remaining assumptions are identical to the normal flow case.

2. Analysis

The geometric relations employed are obtainable from Figures 6 and 7. A new flow coefficient Φ' is conveniently defined as

$$\Phi' = \frac{V_{M1}}{\omega R_1} = \Phi \left(\frac{V_{M1}}{V_{M2}}\right) \left(\frac{R_2}{R_1}\right) \qquad . \quad . \qquad (1)$$

The torque exerted on the fluid by the rotor when acting in the direction of rotation is

$$T_R = \dot{m} \left(R_1 V_{u1} - R_2 V_{u2}\right) \qquad (2)$$

where the mass flow equations are identical to those for the normal case.

The frictional moments acting from stations 1 to 4 and stations 3 to 2 are respectively

$$\begin{aligned} M_{f\ell} &= \lambda_\ell \, \dot{m} \, R_1 \, V_{u1} \\ M_{fu} &= \lambda_u \, \dot{m} \, R_3 \, V_{u3} \end{aligned} \tag{3}$$

where

$$\begin{aligned} \dot{m} \, R_4 \, V_{u4} &= \dot{m} \, R_1 \, V_{u1} - M_{f\ell} \\ \dot{m} \, R_2 \, V_{u2} &= \dot{m} \, R_3 \, V_{u3} - M_{fu} \end{aligned} \tag{4}$$

The relative flow inlet angles are

$$\mathrm{Tan}\ \beta_2 = \eta_{Mu} \frac{b_R}{b_s} \frac{K_{B2}}{K_{B3}} \mathrm{Tan}\ \alpha_3 - \left(\frac{R_2}{R_1}\right)^2 \frac{K_{B2}}{K_{B1}} 1/\Phi' \tag{5}$$

and

$$\mathrm{Tan}\ \alpha_4 = \frac{\eta_{M\ell} \left(1 + \Phi' \ \mathrm{Tan}\ \beta_1\right)}{\Phi' \dfrac{K_{B1}}{K_{B4}} \dfrac{b_R}{b_s}} \tag{6}$$

The torque is now reduced to

$$T_R = 2 \pi \rho R_1^{\ 5} \left(\frac{b_R}{R_1}\right) K_{B1} \, \omega^2 \, \tau_R \tag{7}$$

where

$$\tau_R = \Phi + \Phi'^2 \left[\mathrm{Tan}\ \beta_1 - \frac{K_{B1}}{K_{B3}} \frac{b_R}{b_s} \eta_{Mu} \ \mathrm{Tan}\ \alpha_3\right] \tag{8}$$

Proceeding to the rotor, one can write,

$$W_2{}' = W_2 \cos i_R$$

$$i_R = \beta_{2B} - \beta_2$$

$$Y_R = \frac{P_{E2} - P_{E1}}{\frac{\rho}{2} W_1{}^2}$$

and finally

$$\frac{\Delta H_R}{\omega^2 R_1{}^2} \quad \frac{H_1 - H_2}{\omega^2 R_1{}^2} = 1 - \frac{\sin^2 i_R}{2} \left(\frac{R_2}{R_1}\right)$$

$$+ \Phi' \left\{ \operatorname{Tan} \beta_1 - \left(\frac{K_{B1}}{K_{B3}} \frac{b_R}{b_s} \eta_{Mu} \operatorname{Tan} \alpha_3 \right) \cos^2 i_R \right\} \qquad (9)$$

$$- \Phi'^2 \left\{ \frac{\sin^2 i_R}{2} \left(\frac{R_1}{R_2}\right)^2 \left[\left(\frac{K_{B1}}{K_{B2}}\right)^2 + \left(\frac{K_{B1}}{K_{B3}} \frac{b_R}{b_s} \eta_{Mu} \operatorname{Tan} \alpha_3 \right)^2 \right] + \frac{Y_R}{2 \cos^2 \beta_1} \right\}$$

where

$$\Delta\beta_R = \beta_1 - \beta_2$$

$$\Lambda_R = \frac{b_R}{R_2 - R_1}$$

for this case

$$\Pi_{\Delta H} = \frac{\Delta H}{\omega^2 R_1{}^2} \qquad (10)$$

In the lower passage

$$C_\ell = \frac{p_{4Th} - p_4}{\frac{\rho}{2} V_{M4}{}^2} \qquad (11)$$

and the energy drop is

$$\frac{H_1 - H_4}{\omega^2 R_1^{\,2}} = \frac{(1 - \eta^2_{M\ell})}{2}\left(\frac{R_1}{R_4}\right)^2 + \Phi'\left\{(1 - \eta^2_{M\ell})\left(\frac{R_1}{R_4}\right)^2 \text{Tan}\ \beta_1\right\} + \Phi'^2\left\{\frac{C_\ell}{2}\left(\frac{K_{B1}}{K_{B4}}\ \frac{b_R}{b_s}\ \frac{R_1}{R_4}\right)^2 + \frac{(1 - \eta^2_{M\ell})}{2}\left(\frac{R_1}{R_4}\right)^2 \text{Tan}^2\beta_1\right\} \qquad (12)$$

Nor for the stator

$$V_4' = V_4 \cos i_s$$

$$i_s = \alpha_{4B} - \alpha_4$$

$$Y_s = \frac{P_{T4} - P_{T3}}{\frac{\rho}{2} V_3^{\,2}}$$

$$\Lambda_s = \frac{b_s}{R_3 - R_4}$$

$$\Delta\beta_s = \alpha_3 - \alpha_4$$

and the energy drop across the stator is

$$\frac{H_4 - H_3}{\omega^2\ R_1^{\,2}} = \frac{\sin^2 i_s}{2}\,\eta^2_{M\ell}\left(\frac{R_1}{R_4}\right)^2 + \Phi'\left\{(\sin^2 i_s)\eta^2_{M\ell}\left(\frac{R_1}{R_4}\right)^2 \text{Tan}\ \beta_1\right\} + \Phi'^2\,\frac{\sin^2 i_s}{2}\left(\frac{R_1}{R_4}\,\eta_{M\ell}\right)^2\left\{\left(\frac{1}{\eta_{M\ell}}\ \frac{K_{B1}}{K_{B4}}\ \frac{b_R}{b_s}\right)^2 + \text{Tan}^2\ \beta_1\right\} + \frac{\Phi'^2}{2\cos^2\alpha_3}\ Y_s\left(\frac{R_1}{R_3}\ \frac{b_R}{b_s}\ \frac{K_{B1}}{K_{B3}}\right)^2 \qquad (13)$$

In the upper passage

$$C_u = \frac{p_{2Th} - p_2}{\rho \frac{V_{M2}}{2}} \tag{14}$$

and

$$\frac{H_3 - H_2}{\omega^2 R_1^2} = \frac{\Phi'^2}{2} \left(\frac{R_1}{R_2}\right)^2 \left\{C_u \left(\frac{K_{B1}}{K_{B2}}\right)^2 + (1 - \eta^2_{Mu})\left(\frac{b_R}{b_s} \frac{K_{B1}}{K_{B3}} \text{Tan } \alpha_3\right)^2\right\} \tag{15}$$

The loss coefficients are now given as

$$C_u = 2.0 \xi + \frac{L_u}{2b_s} \lambda_f \tag{16}$$

$$C_\ell = 2.5 \xi + \frac{L_\ell}{2b_R} \lambda_f$$

$$\lambda_u = c_f \text{ Tan } \alpha_3 \frac{L_u}{b_s K_{B4}} \tag{17}$$

$$\lambda_\ell = c_f \text{ Tan } \beta_1 \frac{L_\ell}{b_R K_{B1}}$$

The Reynolds numbers ot obtain ξ and λ_f graphically are

$$R_{Nu} = \frac{2b_s}{\nu} \left(\Phi' \omega \frac{R_1^2}{R_3} \frac{K_{B1}}{K_{B3}}\right) \tag{18}$$

$$R_{N\ell} = \frac{2b_R}{\nu} \Phi' \omega_R R_1$$

The expressions for Ψ, Y_R, and Y_s remain the same as in the previous analysis, but the Reynolds numbers are now

$$R_{NR} = \frac{2\left(\frac{b_R}{R_1}\right) \frac{\Phi' \, \omega \, R_1^2}{\nu}}{\cos\beta_1 + \frac{(b_R/R_1 \left[\mathrm{Tan}\ \beta_1 - \mathrm{Tan}\ \beta_{2B}\right] \cos^2 \beta_1}{0.425 \left(\frac{R_2}{R_1} - 1\right)}}$$

$$R_{NS} = \frac{2\left(\frac{b_R}{R_3}\right) \left(\frac{K_{B1}}{K_{B3}}\right) \frac{\Phi' \, \omega \, R_1^2}{\nu}}{\cos\alpha_3 + \frac{\frac{b_s}{R_1} \left[\mathrm{Tan}\ \alpha_{4B} - \mathrm{Tan}\ \alpha_3\right] \cos^2\alpha_3}{0.425 \left(\frac{R_4}{R_1}\right) \left(\frac{R_3}{R_4} - 1.0\right)}} \tag{19}$$

The equation which is finally solved to obtain Φ is

$$\Delta H_R = \Delta H_u + \Delta H_s + \Delta H_\ell$$

or

$$H_1 - H_2 - (H_4 - H_3) - (H_3 - H_2) - (H_1 - H_4) = 0 \tag{20}$$

The equation is solved by the program. An iteration technique must be carried out until all parameters dependent on Φ' converge.

APPENDIX C

PROGRAM NORMAL

Program NORMAL is essentially a modification of the program developed by NAEC.

Program NORMAL solves the equations governing normal circulation, Modes 1 and 2, for a given design. The solution is based on an iteration technique which is repeated until the flow coefficient Φ converges to within a specific accuracy. A starting value of Φ is picked as are initial values of the various Reynolds numbers which are also Φ dependent. The initial iteration step occurs with all losses based on standard initial Reynolds numbers. This subsequent value of Φ is then used to improve the estimates of the Reynolds numbers and consequential losses. The technique is carried out until Φ converges to the proper value.

If the design parameters and angular speed are input data, the program will compute the flow coefficient, torque, velocities, losses, energy changes over each component, and the dimensionless torque, power, speed, and energy. The flow chart of Table IV depicts this process.

The method of data input is clearly indicated in the program itself. The program is felt to be self-explanatory in that comment cards have been extensively used. The Fortran symbols employed are given in the list of symbols.

Subroutines have been used liberally. Each subroutine accomplishes one individual task such as determining a loss coefficient, or

enthalpy change across the stator, etc. The subroutines Fig. 15 and Fig. 16 are closest point approximations of the curves depicted in Figures 15 and 16 of the analysis. Thses points are given by Block data which is called by each subroutine.

Table IV FLOW CHART FOR COMPUTER PROGRAMS NORMAL AND REVERSE

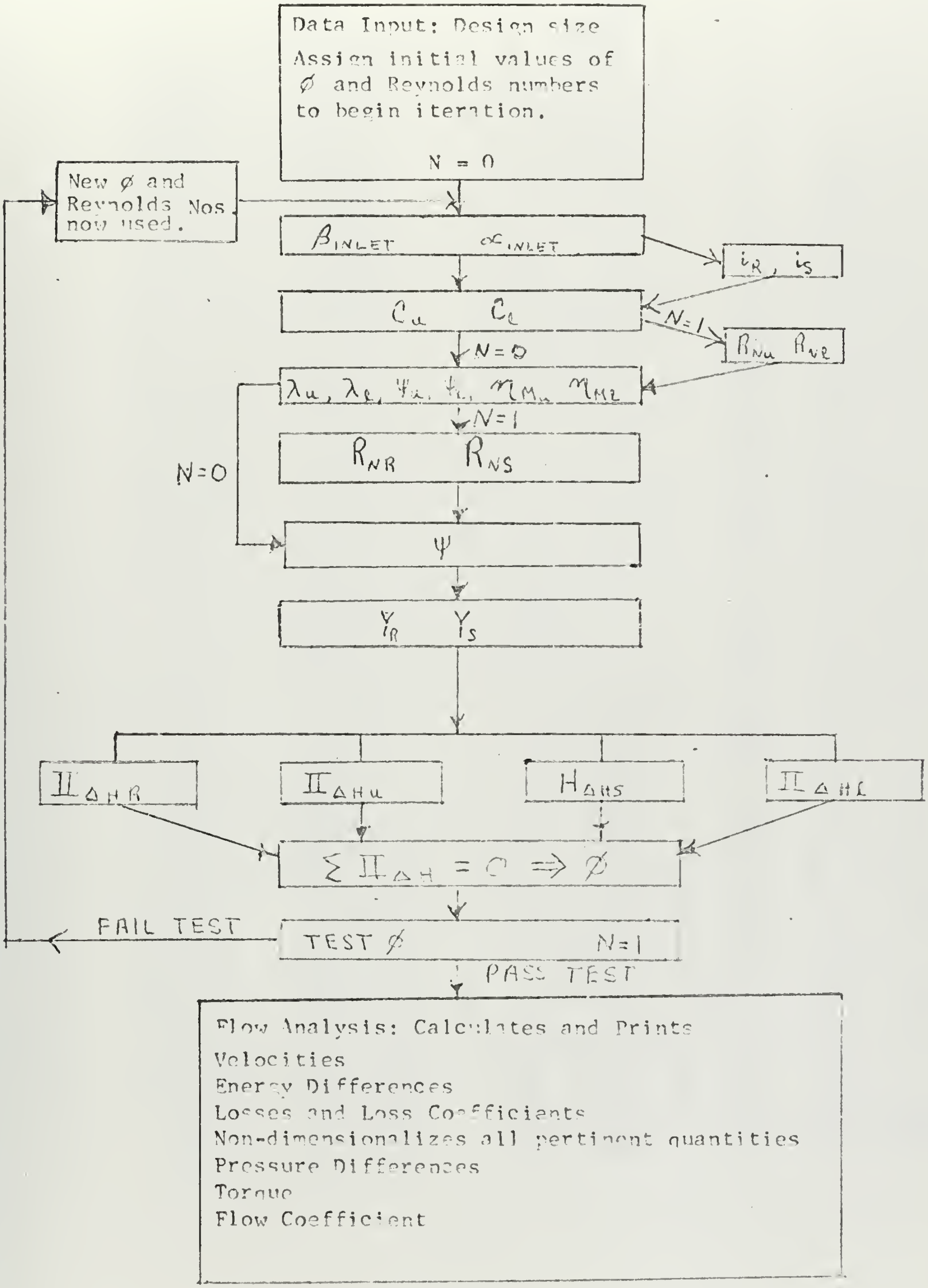

Data Input: Design size
Assign initial values of ∅ and Reynolds numbers to begin iteration.
N = 0

New ∅ and Reynolds Nos. now used.

Flow Analysis: Calculates and Prints
Velocities
Energy Differences
Losses and Loss Coefficients
Non-dimensionalizes all pertinent quantities
Pressure Differences
Torque
Flow Coefficient

PROGRAM NORMAL

```
C          THIS PROGRAM SOLVES THE SET OF EQUATIONS PRESENTED IN APPENDIX A.
C     AN ITERATION TECHNIQUE IS NECESSARY TO SOLVE FOR PHI SINCE VARIOUS LOSS
C     COEFFICIENTS ARE PHI DEPENDENT.  A STRAIGHT QUADRATIC EQUATION SOLVES
C     THE ENERGY BALANCE EQUATION GIVEN BY EQUATION A44..  AFTER CONVERGENCE
C     IS ACHIEVED, THE FLOW ANALYSIS AND NON-DIMENSIONALIZATION WILL BE ACCOM-
C     PLISHED.
C
C          IT MUST BE REMEMBERED THAT THIS SOLUTION IS ONLY VALID FOR THE CON-
C     DITION OF NORMAL CIRCULATION, MODES 1 OR 2.  THE ACTUAL DIFFERENCE BETWEEN
C     THE MODES IS THE DIRECTION OF SHAFT ROTATION.  THE FLOW EXIT ANGLES AT
C     THE ROTOR AND STATOR MUST REMAIN CONSTANT, HOWEVER, THE SIGNS WILL BE
C     CHANGED DUE TO THE SIGN CONVENTION EMPLOYED IN THE ANALYSIS.THAT IS ALL
C     ANGLES ARE POSITIVE IF THEIR PERIPHERAL COMPONENT OF VELOCITY IS IN THE
C     DIRECTION OF ROTATION.
C
C
C          THE DATA IS INPUTTED ON SEVEN(7) DATA CARDS.
C
C     CARD ONE:  THE MONTH, DAY, AND YEAR ARE PLACED IN CCLUMNS1-5,6-10, AND 11-15
C     RESPECTIVELY.  NOTE THAT THESE INTEGERS MUST BE RIGHT HAND ADJUSTED
C
C     CARD TWO:  COLUMNS 1 -5 THE RUN NUMBER, RIGHT ADJUSTED.  COLUMNS6-15 AND
C     16-25,THE RADIUS OF THE ROTOR INLET AND OUTLET(IN INCHES), RESPECTIVELY.
C     COLUMNS 26-35, THE INCREMENT OF ANGULAR SPEED(RAD/SECOND). COLUMNS 36-45,
C     VALUE OF PHI TO BEGIN ITERATIONS.  COLUMS 46-55, THE INITIAL ANGULAR SPEED.
C
C     CARD THREE:  THE BLOCKAGE FACTORS AT STATIONS 1,2,3, AND 4 ARE PLACED IN
C     COLUMNS 1-10,11-20,21-30,31-40.
C
C     CARD FOUR:  THE RELATIVE EXIT ANGLES AT ROTOR AND STATOR(IN DEGREES) GO IN
C     COLUMNS 1-10, AND 11-20.  THE ANGLE TO THE MEAN CAMBER LINE(IN DEGREES) FOR
C     ROTCR AND STATOR GO IN COLUMNS 21-30, AND 31-40, RESPECTIVELY.
C
C     CARD FIVE:  IN COLUMNS 1-10,11-20,21-30, AND 31-40 ARE PLACED THE COEFFI-
C     CIENT OF FRICTION, THE SPECIFIC HEAT OF THE FLUID, THE FLUID DENSITY(SLUGS
C     PER CUBIC FOOT), AND THE KINEMATIC VISCOSITY( FEET**2 PER SECOND)
C     CARD SIX:  THE RATIO OF THE AVERAGE LENGTH OF THE UPPER PASSAGE TO ROTOR
C     BLADE HIEGHT, THE RATIO OF THE AVERAGE LENGHT OF THE LOWER PASSAGE TO STATOR
C     BLADE HIEGHT, THE RADIUS OF THE INNER CONTOUR TO ROTOR BLADE HIEGHT, AND THE
C     RATIO OF THE ROTOR TO STATOR BLADE HIEGHT  GO IN COLUMNS 1-10,11-20,21-30,
C     AND 31-40, RESPECTIVELY.
C
```

```
C    CARD SEVEN:  THE RADIUS OF STATIONS 3 AND 4 AND THE BLADE HIEGHT OF THE
C    ROTOR AND STATOR(ALL VALUES ARE IN INCHES) ARE PLACED IN COLUMNS 1-10,11-20,
C    21-30,AND 31-40, RESPECTIVELY.
C
C
C
C    BLOCK DATA IS USED FOR CONVENIENCE DUE TO THE LARGE NUMBER OF SUBROUTINES.
C
      REAL KB1,KB2,KB3,KB4,IR,IS,NU,LAMDAU,LAMDAL,LUBR,LLBS,LMBDU,LMBDL
      CCMMON   R1,R2,R3,R4,KB1,KB2,KB3,KB4,RHO,ETAMU,ETAML,PHIO,B1B,A3B,
     1         BETA1,BETA2,ALPHA1,ALPHA2,ALPHA3,ALPHA4,B2B,A4B,BR,BS,
     2         IR,IS,PSIU,PSIL,RER,RES,REU,REL,PHI,ARR,ARS,YR,YS,CU,CL,
     3         CH2MH1,CH2MH3,CH3MH4,CH4MH1,AH2MH1,AH2MH3,AH3MH4,AH4MH1,
     4      BH2MH1,BH2MH3,BH3MH4,BH4MH1,CSUM,BSUM,ASUM,ROOT,PHIPR,PHIMR
      COMMON R2R1,R3R2,R4R2,BRR2,BRBS,NU,R1R2,R2R3,R2R4,R4R3,BSR2,BSR3,
     1         TORQUE,TAUR,OM,DELOM,LAMDAU,LAMDAL,LMBDU,LMBDL,LLBS,LUBR,
     2         ZETAU,ZETAL
      CCMMON   CP,CF
      CCMMON JJ,JJJ,K
      COMMON TORREF,POWREF,PIOM,PITORQ,PIPOWR,OMMAX
      COMMON/  ZETARE / YZ(9,11),XRZ(11),YSTRZ,NZR,IZ
      COMMON/  LMDARE / YL(12),XRL(12),YSTRL,NRL
C
C
C        *** DATA INPUT***
      READ 498,IMON,IDAY,IYEAR
      READ 499,IRUN,R1,R2,DELOM,PHIO,OMO
      READ 500,KB1,KB2,KB3,KB4
      READ 500,BETA2,ALPHA4,B1B,A3B
      READ 500,CF,CP,RHO,NU
      READ 500,LUBR,LLBS,RIBR,BRBS
      READ 500,R3,R4,BR,BS
      K = 0
C****    LIST DATA INPUT
   10 PRINT 509
      PRINT 540
      PRINT 510,IMON,IDAY,IYEAR
      CM = OMO
      PRINT 521
      PRINT 523,IRUN,R1,R2,DELOM,PHIO,OMO
  20  PRINT 513
      PRINT 501,KB1,KB2,KB3,KB4
      PRINT 514
      PRINT 501,BETA2,ALPHA4,B1B,A3B
      PRINT 515
      PRINT 530,CF,CP,RHO,NU
      PRINT 517
      PRINT 501,LUBR,LLBS,RIBR,BRBS
```

```
498   FORMAT(3I5)
 499  FORMAT(I5,5F10.3)
 500  FORMAT(3F10.5,F10.8)
501   FORMAT(1H ,4F10.3)
509   FORMAT(1H1,'          ROLEK, LEO S.      ')
 510  FORMAT(1H0,'DATE =',3I5)
513   FORMAT(1H0,7X,'KB1',7X,'KB2',7X,'KB3',7X,'KB4')
514   FORMAT(1H0,5X,'BETA2',4X,'ALPHA4',7X,'B1B',7X,'A3B')
515   FORMAT(1H0,8X,'CF',8X,'CP',7X,'RHO',13X,'NU')
516   FORMAT(1H0,6X,'R1R2',6X,'R3R2',6X,'R4R2',6X,'BRR2')
517   FORMAT(1H0,6X,'LUBR',6X,'LLBS',6X,'RIBR',6X,'BRBS')
521   FORMAT(1H0,3X,'IRUN',8X,'R1',9X,'R2',9X,'DELOM',8X,'PHIO',6X,'OMO'
     1)
523   FORMAT(1H0,I5,5F12.3)
530   FORMAT(1H0,2F10.3,F15.5,F15.8)
 540  FORMAT(1H0,10X,'FLOW EXITS AT STATION 2, NORMAL ROTATION')
 550  FORMAT(1H0,7X,'R1',8X,'R2',8X,'R3',8X,'R4',8X,'BR',8X,'BS')
 551  FORMAT(1H0,6F10.3)
C
C*****                 INITIALIZATION
C
      R1R2 = R1/R2
      R3R2 = R3/R2
      R4R2 = R4/R2
      BRR2 =  BR/R2
      R1INCH = R1
      R2INCH = R2
      R3INCH = R3R2*R2INCH
      R4INCH = R4R2*R2INCH
      BRINCH = BRR2*R2INCH
      BSINCH =  BRINCH/BRBS
      PRINT 516
      PRINT 501,R1R2,R3R2,R4R2,BRR2
      PRINT 550
      PRINT 551,R1INCH,R2INCH,R3INCH,R4INCH,BRINCH,BSINCH
      OMMAX = 800.*3.1416/30.0
      OM = OMMAX * 0.1
      R1 = R1/12.
      R2 = R2/12.0
      BR= BRR2*R2
      BS= BR/BRBS
      AB2 = BETA2
      AA4 = ALPHA4
      BETA2 = 3.1416/180. * BETA2
      ALPHA4 = 3.1416/180. * ALPHA4
      B1B = 3.1416/180.*B1B
      A3B = 3.1416/180.*A3B
      R2R1 = 1./R1R2
```

```
      R2R3 = 1./R3R2
      R2R4 = 1./R4R2
      R4R3 = R4R2 * R2R3
      BSR2 = BRR2/BRBS
      BSR3 = BSR2*R2R3
      ARR = BRR2/(1. -R1R2)
      ARS = BSR3/(1.-R4R3)
C    THE VALUE OF RIBR IS INITIALIZED HERE AND WILL BE USED IN SUBROUTINE FIG TO
C   OBTAIN VALUES OF THE BENDING LOSSES FROM FIGURE 15.
      IZ = 0
      IF (RIBR .LE. 0.25) IZ=1
      IF (RIBR .GE. 1.0)  IZ=9
      IF (IZ .NE. 0) GO TO 22
      REALIZ = RIBR*10.0 - 1.0
      IZ = REALIZ
C
C     INITIAL VALUES OF THE REYNOLDS NUMBERS ARE GIVEN TO BEGIN THE ITERATIONS.
  22  RER = 10.0**5
      RES = 10.0**5
      REU = 10.0**5
      REL = 10.0**5
      PHI = PHIO
      TORREF = RHO*(OMMAX**2)*(R2**5)
      POWREF = TORREF * OMMAX
      PRINT 410,POWREF
      PRINT 415,TORREF
 410  FORMAT(1HO,6X,'THE REFERENCE POWER IS',F13.3)
 415  FORMAT(1HO,6X,'THE REFERENCE TORQUE IS',F13.3)
      IF ( PHI .GT. 0.0 ) GO TO 30
C
      IR=0.
      IS = 0.0
      BETA1 = B1B
      ALPHA3 = A3B
       GO TO 40
C
C*****      CALCULATE PHI
C
 25   RER =ENRER ( PHI )
      RES =ENRES ( PHI )
C
 30   CALL EQG1
      CALL EQG2
      CALL EQH5
      CALL EQH6
      TANB1 = (ETAML*KB1/KB4*TAN(ALPHA4))- (R1R2**2)*(KB1/KB2)/PHI
      BETA1 = ATAN(TANB1)
      IR = BETA1 - B1B
```

```
      TANA3 = ETAMU*(1. + PHI*TAN(BETA2))/(PHI*KB2/KB3)
      ALPHA3 = ATAN(TANA3)
      IS = ALPHA3 - A3B
C
 40   YR = EQI8(RER,ARR,BETA2,BETA1)
      YS = EQI8(RES,ARS,ALPHA4,ALPHA3)
      CALL EQE28
      CALL EQF12
      CALL EQE13A
      CALL EQD9
      CALL PHITES
C
C***           TESTING PHI
C
 100  IF ( K .GE. 1 ) GO TO 110
      K = 2
      PHIO = PHI
      GO TO 25
C
 110  TEST = ABS( (PHI - PHIO)/((PHI + PHIO)/2.) )
      IF  ( TEST .LE. 0.0005 ) GO TO 120
C
      K = K + 1
C***           SAFETY OUTLET
      IF ( K .GT. 20 ) GO TO 120
      PHIO = PHI
       GO TO 25
C
C*****      OUTPUT AND FLOW CALCULATIONS
C
 120  TAUR = EQB19( PHI )
      CALL EQB20
      DELBET = BETA2-BETA1
      DELALP = ALPHA4-ALPHA3
      DELBET = DELBET*180./3.1416
      DELALP = DELALP*180./3.1416
      DBETA1 = BETA1 *180.0/3.1416
      CALPH3= ALPHA3 * 180./3.1416
      DIR = IR * 180./3.1416
      DIS = IS * 180./3.1416
      PRINT 300
      PRINT 299,K,PHI,TORQUE,TAUR,OM
      PRINT 311
      PRINT 302,DBETA1,DALPH3,DIR,DIS
      PRINT 312
      PRINT 313,DELBFT,DELALP
      PRINT 325
      PRINT 308
```

```
      PRINT 302,YR,YS,CU,CL
      PRINT 309
      PRINT 302,ETAMU,ETAML,PSIU,PSIL
      PRINT 310
      PRINT 303,RER,RES,REU,REL
C
      CALL NONDEM
      CALL VALUE
      DELOM = OMMAX * 0.1
      OM = OM + DELOM
      PHIO = PHI
       K = 1
      IF ( OM.LE. OMMAX )  GO TO 25
C
  299 FORMAT(1H ,8X,I5,F15.4,F15.2,F15.5,F15.2)
  300 FORMAT(1H1,11X,' K ',10X,'PHI',10X,'TORQUE',10X,'TAUR',10X,'OM')
  302 FORMAT(1H ,13X,4F15.3)
  303 FORMAT(1H ,13X,4E15.5)
  308 FORMAT(1H0,26X,'YR',13X,'YS',13X,'CU',13X,'CL')
 309  FORMAT(1H0,23X,'ETAMU',11X,'ETAML',11X,'PSIU',11X,'PSIL')
 310  FORMAT(1H0,25X,'RER',12X,'RES',12X,'REU',12X'REL')
 311  FORMAT(1H0,22X,'BETA1',11X,'ALPHA3',10X,'IR   ',10X,'IS    ')
  312 FORMAT(1H0,20X,'DELTA BETA', 3X,'DELTA ALPHA')
  313 FORMAT(1H ,12X,2F15.3)
  325 FORMAT(1H0,30X,'FLOW LOSS COEFFICIENTS')
      STOP
      END


      SUBROUTINE EQG1
C
C  FINDS CU AND REU
C
      REAL KB1,KB2,KB3,KB4,IR,IS,NU,LAMDAU,LAMDAL,LUBR,LLBS,LMBDU,LMBDL
      COMMON  R1,R2,R3,R4,KB1,KB2,KB3,KB4,RHO,ETAMU,ETAML,PHIO,B1B,A3B,
     1        BETA1,BETA2,ALPHA1,ALPHA2,ALPHA3,ALPHA4,B2B,A4B,BR,BS,
     2        IR,IS,PSIU,PSIL,RER,RES,REU,REL,PHI,ARR,ARS,YR,YS,CU,CL,
     3        CH2MH1,CH2MH3,CH3MH4,CH4MH1,AH2MH1,AH2MH3,AH3MH4,AH4MH1,
     4      BH2MH1,BH2MH3,BH3MH4,BH4MH1,CSUM,BSUM,ASUM,ROOT,PHIPR,PHIMR
      CCMMON R2R1,R3R2,R4R2,BRR2,BRBS,NU,R1R2,R2R3,R2R4,R4R3,BSR2,BSR3,
     1        TORQUE,TAUR,OM,DELOM,LAMDAU,LAMDAL,LMBDU,LMBDL,LLBS,LUBR,
     2        ZETAU,ZETAL
      COMMON  CP,CF
      CCMMON JJ,JJJ,K
      CCMMON/ ZETARE / YZ(9,11),XRZ(11),YSTRZ,NZR,IZ
      COMMON/ LMDARE / YL(12),XRL(12),YSTRL,NRL
C
      REU = 2.*BS*R2R3*KB2/KB3*PHI*R2*OM/NU
```

```
      ZETAU = FIG(REU)
      LMBDU  = FIG2(REU)
      CU = 2.0*ZETAU+ .5*LUBR*LMBDU
      RETURN
      END


      SUBROUTINE EQG2
C
C******     CALCULATES CL AND REL
C
      REAL KB1,KB2,KB3,KB4,IR,IS,NU,LAMDAU,LAMDAL,LUBR,LLBS,LMBDU,LMBDL
      COMMON  R1,R2,R3,R4,KB1,KB2,KB3,KB4,RHO,ETAMU,ETAML,PHIO,B1B,A3B,
     1        BETA1,BETA2,ALPHA1,ALPHA2,ALPHA3,ALPHA4,B2B,A4B,BR,BS,
     2        IR,IS,PSIU,PSIL,RER,RES,REU,REL,PHI,ARR,ARS,YR,YS,CU,CL,
     3        CH2MH1,CH2MH3,CH3MH4,CH4MH1,AH2MH1,AH2MH3,AH3MH4,AH4MH1,
     4      BH2MH1,BH2MH3,BH3MH4,BH4MH1,CSUM,BSUM,ASUM,ROOT,PHIPR,PHIMR
      COMMON R2R1,R3R2,R4R2,BRR2,BRBS,NU,R1R2,R2R3,R2R4,R4R3,BSR2,BSR3,
     1        TORQUE,TAUR,OM,DELOM,LAMDAU,LAMDAL,LMBDU,LMBDL,LLBS,LUBR,
     2        ZETAU,ZETAL
      COMMON  CP,CF
      COMMON JJ,JJJ,K
      COMMON/ ZETARE / YZ(9,11),XRZ(11),YSTRZ,NZR,IZ
      COMMON/ LMDARE / YL(12),XRL(12),YSTRL,NRL
      REL = 2.*BR*R2R1*KB2/KB1*PHI*R2*OM/NU
      LMBDL  = FIG2(REL)
      ZETAL = FIG(REL)
      CL = 2.5*ZETAL+ .5 * LLBS * LMBDL
      RETURN
      END


      SUBROUTINE EQH5
C
C****    FINDS LAMBDA, ETA, AND PSI FOR THE LOWER PASSAGES
C
      REAL KB1,KB2,KB3,KB4,IR,IS,NU,LAMDAU,LAMDAL,LUBR,LLBS,LMBDU,LMBDL
      COMMON  R1,R2,R3,R4,KB1,KB2,KB3,KB4,RHO,ETAMU,ETAML,PHIO,B1B,A3B,
     1        BETA1,BETA2,ALPHA1,ALPHA2,ALPHA3,ALPHA4,B2B,A4B,BR,BS,
     2        IR,IS,PSIU,PSIL,RER,RES,REU,REL,PHI,ARR,ARS,YR,YS,CU,CL,
     3        CH2MH1,CH2MH3,CH3MH4,CH4MH1,AH2MH1,AH2MH3,AH3MH4,AH4MH1,
     4      BH2MH1,BH2MH3,BH3MH4,BH4MH1,CSUM,BSUM,ASUM,ROOT,PHIPR,PHIMR
      COMMON R2R1,R3R2,R4R2,BRR2,BRBS,NU,R1R2,R2R3,R2R4,R4R3,BSR2,BSR3,
     1        TORQUE,TAUR,OM,DELOM,LAMDAU,LAMDAL,LMBDU,LMBDL,LLBS,LUBR,
     2        ZETAU,ZETAL
      COMMON  CP,CF
      COMMON JJ,JJJ,K
C
```

```
C***** TAKING INTO ACCOUNT ABSOLUTE VALUE
      AAAA4 = ABS(ALPHA4)
      LAMDAL = CF*TAN(AAAA4)*LLBS/KB4
       ETAML = 1.0 - LAMDAL
      PSIL = 1.0 -(ETAML**2)
      RETURN
      END


      SUBROUTINE EQH6
C
C**** FINDS LAMBDA, ETA, AND PSI FOR THE UPPER PASSAGES.
C
      REAL KB1,KB2,KB3,KB4,IR,IS,NU,LAMDAU,LAMDAL,LUBR,LLBS,LMBDU,LMBDL
      COMMON   R1,R2,R3,R4,KB1,KB2,KB3,KB4,RHO,ETAMU,ETAML,PHIO,B1B,A3B,
     1         BETA1,BETA2,ALPHA1,ALPHA2,ALPHA3,ALPHA4,B2B,A4B,BR,BS,
     2         IR,IS,PSIU,PSIL,RER,RES,REU,REL,PHI,ARR,ARS,YR,YS,CU,CL,
     3         CH2MH1,CH2MH3,CH3MH4,CH4MH1,AH2MH1,AH2MH3,AH3MH4,AH4MH1,
     4       BH2MH1,BH2MH3,BH3MH4,BH4MH1,CSUM,BSUM,ASUM,ROOT,PHIPR,PHIMR
      COMMON R2R1,R3R2,R4R2,BRR2,BRBS,NU,R1R2,R2R3,R2R4,R4R3,BSR2,BSR3,
     1         TORQUE,TAUR,OM,DELOM,LAMDAU,LAMDAL,LMBDU,LMBDL,LLBS,LUBR,
     2         ZETAU,ZETAL
      COMMON   CP,CF
      COMMON JJ,JJJ,K
C
C***** ACCOUNTING FOR SIGNS BY ASSIGNING ABSOLUTE VALUES
      BBBB2 = ABS(BETA2)
      LAMDAU = (CF*(1. + PHI*TAN(BBBB2)) * LUBR)/(PHI *KB2)
      ETAMU = 1.0 - LAMDAU
      PSIU = 1.0 -(ETAMU**2)
      RETURN
      END


      FUNCTION EQI8 (RE,AR,ANG1,ANG2)
C
C   CALCULATES THE LOSS COEFFICIENTS YR AND YS.
C
      REAL KB1,KB2,KB3,KB4,IR,IS,NU,LAMDAU,LAMDAL,LUBR,LLBS,LMBDU,LMBDL
      COMMON   R1,R2,R3,R4,KB1,KB2,KB3,KB4,RHO,ETAMU,ETAML,PHIO,B1B,A3B,
     1         BETA1,BETA2,ALPHA1,ALPHA2,ALPHA3,ALPHA4,B2B,A4B,BR,BS,
     2         IR,IS,PSIU,PSIL,RER,RES,REU,REL,PHI,ARR,ARS,YR,YS,CU,CL,
     3         CH2MH1,CH2MH3,CH3MH4,CH4MH1,AH2MH1,AH2MH3,AH3MH4,AH4MH1,
     4       BH2MH1,BH2MH3,BH3MH4,BH4MH1,CSUM,BSUM,ASUM,ROOT,PHIPR,PHIMR
      COMMON R2R1,R3R2,R4R2,BRR2,BRBS,NU,R1R2,R2R3,R2R4,R4R3,BSR2,BSR3,
     1         TORQUE,TAUR,OM,DELOM,LAMDAU,LAMDAL,LMBDU,LMBDL,LLBS,LUBR,
     2         ZETAU,ZETAL
      COMMON   CP,CF
```

```
      COMMON JJ,JJJ,K
C***** TAKING INTO ACCOUNT ABSOLUTE VALUE
      DELANG = ABS((ANG1 -ANG2))
      DELBE = DELANG*180./3.1416
      PSI = .99 - 2.28 * DELBE/(10.0**4) -4.97/(180.- DELBE)
      EQI8 = ((.975+.075/AR)/(PSI**2)-1.) * (((10.**5)/RE)**.25)
      RETURN
      END


      FUNCTION ENRER (PHII)
C
C     CALCULATES THE REYNOLDS NUMBER OF THE ROTOR
C
      REAL KB1,KB2,KB3,KB4,IR,IS,NU,LAMDAU,LAMDAL,LUBR,LLBS,LMBDU,LMBDL
      COMMON  R1,R2,R3,R4,KB1,KB2,KB3,KB4,RHO,ETAMU,ETAML,PHIO,B1B,A3B,
     1        BETA1,BETA2,ALPHA1,ALPHA2,ALPHA3,ALPHA4,B2B,A4B,BR,BS,
     2        IR,IS,PSIU,PSIL,RER,RES,REU,REL,PHI,ARR,ARS,YR,YS,CU,CL,
     3        CH2MH1,CH2MH3,CH3MH4,CH4MH1,AH2MH1,AH2MH3,AH3MH4,AH4MH1,
     4      BH2MH1,BH2MH3,BH3MH4,BH4MH1,CSUM,BSUM,ASUM,ROOT,PHIPR,PHIMR
      COMMON R2R1,R3R2,R4R2,BRR2,BRBS,NU,R1R2,R2R3,R2R4,R4R3,BSR2,BSR3,
     1        TORQUE,TAUR,OM,DELOM,LAMDAU,LAMDAL,LMBDU,LMBDL,LLBS,LUBR,
     2        ZETAU,ZETAL
      CCMMON  CP,CF
      COMMON JJ,JJJ,K
C***** TAKING INTO ACCOUNT ABSOLUTE VALUE
C
      ADELB2  = ABS(TAN(BETA2) - TAN(B1B))
      X1 = BRR2*ADELB2*COS(BETA2)**2
      X2 = 0.425*(1. - R1R2)
      X3 = PHII*OM*(R2**2)/NU
      ENRER = X3*(2.0*BRR2 ) / (COS(BETA2) + X1/X2 )
      RETURN
      END


      FUNCTION ENRES (PHII )
C
C     CALCULATES THE REYNOLDS NUMBER OF THE STATOR
C
      REAL KB1,KB2,KB3,KB4,IR,IS,NU,LAMDAU,LAMDAL,LUBR,LLBS,LMBDU,LMBDL
      COMMON  R1,R2,R3,R4,KB1,KB2,KB3,KB4,RHO,ETAMU,ETAML,PHIO,B1B,A3B,
     1        BETA1,BETA2,ALPHA1,ALPHA2,ALPHA3,ALPHA4,B2B,A4B,BR,BS,
     2        IR,IS,PSIU,PSIL,RER,RES,REU,REL,PHI,ARR,ARS,YR,YS,CU,CL,
     3        CH2MH1,CH2MH3,CH3MH4,CH4MH1,AH2MH1,AH2MH3,AH3MH4,AH4MH1,
     4      BH2MH1,BH2MH3,BH3MH4,BH4MH1,CSUM,BSUM,ASUM,ROOT,PHIPR,PHIMR
      CCMMON R2R1,R3R2,R4R2,BRR2,BRBS,NU,R1R2,R2R3,R2R4,R4R3,BSR2,BSR3,
     1        TORQUE,TAUR,OM,DELOM,LAMDAU,LAMDAL,LMBDU,LMBDL,LLBS,LUBR,
```

```
     2         ZETAU,ZETAL
      CCMMON   CP,CF
      COMMON JJ,JJJ,K
C***** TAKING INTO ACCOUNT ABSOLUTE VALUE
      ADELA4 = ABS(TAN(A3B) - TAN(ALPHA4))
C
      X1 = BSR2 *ADELA4*(COS(ALPHA4)**2)
      X2 = 0.425*R3R2*(1. -R4R3)
      X3 = PHII*OM*(R2**2)/NU
       ENRES = X3*(2.*BRR2/R4R2*KB2/KB4)/(COS(ALPHA4) + X1/X2)
      RETURN
      END


      SUBROUTINE EQE28
C
C******  CALCULATES COEFFECIENTS OF (H2 - H1)/(OMEGA * R2)**2
C
      REAL KB1,KB2,KB3,KB4,IR,IS,NU,LAMDAU,LAMDAL,LUBR,LLBS,LMBDU,LMBDL
      COMMON   R1,R2,R3,R4,KB1,KB2,KB3,KB4,RHO,ETAMU,ETAML,PHIO,B1B,A3B,
     1         BETA1,BETA2,ALPHA1,ALPHA2,ALPHA3,ALPHA4,B2B,A4B,BR,BS,
     2         IR,IS,PSIU,PSIL,RER,RES,REU,REL,PHI,ARR,ARS,YR,YS,CU,CL,
     3         CH2MH1,CH2MH3,CH3MH4,CH4MH1,AH2MH1,AH2MH3,AH3MH4,AH4MH1,
     4      BH2MH1,BH2MH3,BH3MH4,BH4MH1,CSUM,BSUM,ASUM,ROOT,PHIPR,PHIMR
      COMMON R2R1,R3R2,R4R2,BRR2,BRBS,NU,R1R2,R2R3,R2R4,R4R3,BSR2,BSR3,
     1         TORQUE,TAUR,OM,DELOM,LAMDAU,LAMDAL,LMBDU,LMBDL,LLBS,LUBR,
     2         ZETAU,ZETAL
      COMMON   CP,CF
      CCMMON JJ,JJJ,K
      X1 = COS(IR)**2
      X2 = (1.-X1)/2.
      X3 = ( KB2/KB4*ETAML*TAN(ALPHA4))
      CH2MH1 = 1. -X2*((R1R2)**2)
      BH2MH1 = TAN(BETA2) -(X1*X3)
        AH2MH1 = -X2*( (R2R1)**2)*(((KB2/KB1)**2) + (X3**2) ) - YR/(2.*(
     1      COS(BETA2)**2))
      RETURN
      END


      SUBROUTINE EQF12
C
C     CALCULATES COEFFICIENTS OF (H2 - H3)/(OMEGA * R2)**2
C
      REAL KB1,KB2,KB3,KB4,IR,IS,NU,LAMDAU,LAMDAL,LUBR,LLBS,LMBDU,LMBDL
      COMMON   R1,R2,R3,R4,KB1,KB2,KB3,KB4,RHO,ETAMU,ETAML,PHIO,B1B,A3B,
     1         BETA1,BETA2,ALPHA1,ALPHA2,ALPHA3,ALPHA4,B2B,A4B,BR,BS,
     2         IR,IS,PSIU,PSIL,RER,RES,REU,REL,PHI,ARR,ARS,YR,YS,CU,CL,
```

```
3          CH2MH1,CH2MH3,CH3MH4,CH4MH1,AH2MH1,AH2MH3,AH3MH4,AH4MH1,
4        BH2MH1,BH2MH3,BH3MH4,BH4MH1,CSUM,BSUM,ASUM,ROOT,PHIPR,PHIMR
 COMMON R2R1,R3R2,R4R2,BRR2,BRBS,NU,R1R2,R2R3,R2R4,R4R3,BSR2,BSR3,
1          TORQUE,TAUR,OM,DELOM,LAMDAU,LAMDAL,LMBDU,LMBDL,LLBS,LUBR,
2          ZETAU,ZETAL
 CCMMON  CP,CF
 COMMON JJ,JJJ,K
C
 X1 = (R2R3)**2
 CH2MH3 = PSIU*X1/2.
 BH2MH3 = PSIU*X1*TAN(BETA2)
 AH2MH3 = X1/2. * (PSIU*(TAN(BETA2)**2) + CU*((KB2/KB3)**2))
 RETURN
 END


 SUBROUTINE EQE13A
C
C   CALCULATES COEFFICIENTS OF (H3 - H4)/(OMEGA * R2)**2
C
 REAL KB1,KB2,KB3,KB4,IR,IS,NU,LAMDAU,LAMDAL,LUBR,LLBS,LMBDU,LMBDL
 COMMON  R1,R2,R3,R4,KB1,KB2,KB3,KB4,RHO,ETAMU,ETAML,PHIO,B1B,A3B,
1          BETA1,BETA2,ALPHA1,ALPHA2,ALPHA3,ALPHA4,B2B,A4B,BR,BS,
2          IR,IS,PSIU,PSIL,REP,RES,REU,REL,PHI,ARR,ARS,YR,YS,CU,CL,
3          CH2MH1,CH2MH3,CH3MH4,CH4MH1,AH2MH1,AH2MH3,AH3MH4,AH4MH1,
4        BH2MH1,BH2MH3,BH3MH4,BH4MH1,CSUM,BSUM,ASUM,ROOT,PHIPR,PHIMR
 COMMON R2R1,R3R2,R4R2,BRR2,BRBS,NU,R1R2,R2R3,R2R4,R4R3,BSR2,BSR3,
1          TORQUE,TAUR,OM,DELOM,LAMDAU,LAMDAL,LMBDU,LMBDL,LLBS,LUBR,
2          ZETAU,ZETAL
 COMMON  CP,CF
 COMMON JJ,JJJ,K
 X1 = ((1.-(COS(IS)**2))/2.)* ((R2R3)**2)
 X2 = (R2R4*(KB1/KB4)/(COS(ALPHA4)))**2
 CH3MH4 = X1*(ETAMU**2)
 BH3MH4 = CH3MH4*2.*TAN(BETA2)
 AH3MH4 =X1*(((KB2/KB3)**2)  +  ((ETAMU*TAN(BETA2))**2)) + YS*X2*.5
 RETURN
 END


 SUBROUTINE EQD9
C
C   CALCULATES COEFFICIENTS OF (H4 - H1)/(OMEGA * R2)**2
C
 REAL KB1,KB2,KB3,KB4,IR,IS,NU,LAMDAU,LAMDAL,LUBR,LLBS,LMBDU,LMBDL
 COMMON  R1,R2,R3,R4,KB1,KB2,KB3,KB4,RHO,ETAMU,ETAML,PHIO,B1B,A3B,
1          BETA1,BETA2,ALPHA1,ALPHA2,ALPHA3,ALPHA4,B2B,A4B,BR,BS,
2          IR,IS,PSIU,PSIL,RER,RES,REU,REL,PHI,ARR,ARS,YR,YS,CU,CL,
```

```
     3      CH2MH1,CH2MH3,CH3MH4,CH4MH1,AH2MH1,AH2MH3,AH3MH4,AH4MH1,
     4     BH2MH1,BH2MH3,BH3MH4,BH4MH1,CSUM,BSUM,ASUM,ROOT,PHIPR,PHIMR
      COMMON R2R1,R3R2,R4R2,BRR2,BRBS,NU,R1R2,R2R3,R2R4,R4R3,BSR2,BSR3,
     1      TORQUE,TAUR,OM,DELOM,LAMDAU,LAMDAL,LMBDU,LMBDL,LLBS,LUBR,
     2      ZETAU,ZETAL
      COMMON  CP,CF
      COMMON JJ,JJJ,K
C
      X1 = KB2/KB4*TAN(ALPHA4)
      CH4MH1 = 0.0
      BH4MH1 = 0.0
      AH4MH1 = .5*((R2R1)**2)*( CL*((KB2/KB1)**2) + PSIL*(X1**2))
      RETURN
      END


      SUBROUTINE PHITES
C
C    ACCOMPLISHES THE FINAL ITERATION STEP IN DETERMINING PHI
C
      REAL KB1,KB2,KB3,KB4,IR,IS,NU,LAMDAU,LAMDAL,LUBR,LLBS,LMBDU,LMBDL
      COMMON  R1,R2,R3,R4,KB1,KB2,KB3,KB4,RHO,ETAMU,ETAML,PHIO,B1B,A3B,
     1      BETA1,BETA2,ALPHA1,ALPHA2,ALPHA3,ALPHA4,B2B,A4B,BR,BS,
     2      IR,IS,PSIU,PSIL,RER,RES,REU,REL,PHI,ARR,ARS,YR,YS,CU,CL,
     3      CH2MH1,CH2MH3,CH3MH4,CH4MH1,AH2MH1,AH2MH3,AH3MH4,AH4MH1,
     4     BH2MH1,BH2MH3,BH3MH4,BH4MH1,CSUM,BSUM,ASUM,ROOT,PHIPR,PHIMR
      COMMON R2R1,R3R2,R4R2,BRR2,BRBS,NU,R1R2,R2R3,R2R4,R4R3,BSR2,BSR3,
     1      TORQUE,TAUR,OM,DELOM,LAMDAU,LAMDAL,LMBDU,LMBDL,LLBS,LUBR,
     2      ZETAU,ZETAL
      COMMON  CP,CF
      COMMON JJ,JJJ,K
C
C    THE PREVIOUS FOUR SUBROUTINES ARE NOW ADDED
      CSUM = CH2MH1 - CH2MH3 - CH3MH4 - CH4MH1
      BSUM = BH2MH1 - BH2MH3 - BH3MH4 - BH4MH1
      ASUM = AH2MH1 - AH2MH3 - AH3MH4 - AH4MH1
C
C   THE QUADRATIC EQUATION IS NOW SOLVED TO YIELD THE NEW VALUE OF PHI.
      ROOT = SQRT((BSUM**2)- 4.0*ASUM * CSUM)
      PHIPR = (-BSUM + ROOT)/ (2.0*ASUM)
      PHIMR = (-BSUM - ROOT)/ (2.0*ASUM)
      JJ = 0
      JJJ= 0
C
C    DETERMINING THE PROPER ROOT
      IF (PHIMR. LT. 0.0 ) GO TO 2
      IF ( PHIMR. GT. 0.0) GO TO 5
    2 IF ( PHIPR .LT. 0.0 ) GO TO 15
```

```
      IF (PHIPR .GT. 0.0 ) GO TO 6
 5    PHI = PHIMR
      GO TO 80
 15   PRINT 20
 6    PHI = PHIPR
 20   FORMAT(1H0,' BOTH ROOTS OF PHI ARE NEGATIVE, AND THE PROGRAM WILL BE
     1 DUMPED*************************')
 80   IF ( PHI .LT. 0.0 ) JJ = 1
      IF ( JJ .EQ. 1 ) GO TO 10
      IF (JJJ .EQ. 1 ) GO TO 10
      RETURN
10    PRINT 11,JJ,JJJ
11    FORMAT(1H0,'JJ = ',I5,'JJJ = ',I5)
      RETURN
      END


      FUNCTION EQB19( PHII )
      REAL KB1,KB2,KB3,KB4,IR,IS,NU,LAMDAU,LAMDAL,LUBR,LLBS,LMBDU,LMBDL
      COMMON   R1,R2,R3,R4,KB1,KB2,KB3,KB4,RHO,ETAMU,ETAML,PHIO,B1B,A3B,
     1         BETA1,BETA2,ALPHA1,ALPHA2,ALPHA3,ALPHA4,B2B,A4B,BR,BS,
     2         IR,IS,PSIU,PSIL,RER,RES,REU,REL,PHI,ARR,ARS,YR,YS,CU,CL,
     3         CH2MH1,CH2MH3,CH3MH4,CH4MH1,AH2MH1,AH2MH3,AH3MH4,AH4MH1,
     4      BH2MH1,BH2MH3,BH3MH4,BH4MH1,CSUM,BSUM,ASUM,ROOT,PHIPR,PHIMR
      COMMON R2R1,R3R2,R4R2,BRR2,BRBS,NU,R1R2,R2R3,R2R4,R4R3,BSR2,BSR3,
     1         TORQUE,TAUR,OM,DELOM,LAMDAU,LAMDAL,LMBDU,LMBDL,LLBS,LUBR,
     2         ZETAU,ZETAL
      COMMON   CP,CF
      COMMON JJ,JJJ,K
C
      X1 = TAN(BETA2) - ETAML*(KB2/KB4)*TAN(ALPHA4)
      EQB19 = PHII + (PHII **2)*X1
      RETURN
      END


      SUBROUTINE EQB20
      REAL KB1,KB2,KB3,KB4,IR,IS,NU,LAMDAU,LAMDAL,LUBR,LLBS,LMBDU,LMBDL
      COMMON   R1,R2,R3,R4,KB1,KB2,KB3,KB4,RHO,ETAMU,ETAML,PHIO,B1B,A3B,
     1         BETA1,BETA2,ALPHA1,ALPHA2,ALPHA3,ALPHA4,B2B,A4B,BR,BS,
     2         IR,IS,PSIU,PSIL,RER,RES,REU,REL,PHI,ARR,ARS,YR,YS,CU,CL,
     3         CH2MH1,CH2MH3,CH3MH4,CH4MH1,AH2MH1,AH2MH3,AH3MH4,AH4MH1,
     4      BH2MH1,BH2MH3,BH3MH4,BH4MH1,CSUM,BSUM,ASUM,ROOT,PHIPR,PHIMR
      COMMON R2R1,R3R2,R4R2,BRR2,BRBS,NU,R1R2,R2R3,R2R4,R4R3,BSR2,BSR3,
     1         TORQUE,TAUR,OM,DELOM,LAMDAU,LAMDAL,LMBDU,LMBDL,LLBS,LUBR,
     2         ZETAU,ZETAL
      COMMON   CP,CF
      COMMON JJ,JJJ,K
```

```
      TORQUE = 2.*3.1416*RHO*(R2**5)*BRR2*KB2*TAUR*(OM**2)
      RETURN
      END


      SUBROUTINE NONDEM
C
C    ACCOMPLISHES THE NON-DIMENSIONALIZATION
C
      REAL KB1,KB2,KB3,KB4,IR,IS,NU,LAMDAU,LAMDAL,LUPR,LLBS,LMBDU,LMBDL
      COMMON  R1,R2,R3,R4,KB1,KB2,KB3,KB4,RHO,ETAMU,ETAML,PHIO,B1B,A3B,
     1        BETA1,BETA2,ALPHA1,ALPHA2,ALPHA3,ALPHA4,B2B,A4B,BR,BS,
     2        IR,IS,PSIU,PSIL,RER,RES,REU,REL,PHI,ARR,ARS,YR,YS,CU,CL,
     3        CH2MH1,CH2MH3,CH3MH4,CH4MH1,AH2MH1,AH2MH3,AH3MH4,AH4MH1,
     4      BH2MH1,BH2MH3,BH3MH4,BH4MH1,CSUM,BSUM,ASUM,ROOT,PHIPR,PHIMR
      COMMON R2R1,R3R2,R4R2,BRR2,BRBS,NU,R1R2,R2R3,R2R4,R4R3,BSR2,BSR3,
     1        TORQUE,TAUR,OM,DELOM,LAMDAU,LAMDAL,LMBDU,LMBDL,LLBS,LUBR,
     2        ZETAU,ZETAL
      COMMON  CP,CF
      CCMMON JJ,JJJ,K
      COMMON TORREF,POWREF,PIOM,PITORQ,PIPOWR,OMMAX
C
      PIOM = OM/OMMAX
      PITORQ = TORQUE/TORREF
      PIPOWR = (OM*TORQUE)/POWREF
      PIPHI = PHI*PIOM
      PRINT 600,PIOM
      PRINT 605,PIPOWR
      PRINT 609,PITORQ
      PRINT 611,PIPHI
  600 FORMAT(1H0,15X,'THE DIMENSIONLESS ROTATIONAL SPEED=',F6.3)
  605 FORMAT(1H0,15X,'THE DIMENSIONLESS POWER =',F16.3)
  609 FORMAT(1H0,15X,'THE DIMENSIONLESS TORQUE =',F15.3)
  611 FORMAT(1H0,15X,'THE REVISED FLOW COEFFICIENT =',F9.3)
      RETURN
      END


      FUNCTION FIG( RE )
C
C   THE BENDING LOSS COEFFICIENT IS APPROXIMATED FOR IN THIS SUBROUTINE
C   AN ALTERNATE CHOICE TO EMPLOY WOULD BE TO USE A CURVE FIT ON FIGURE 15.
C
      COMMCN/ ZETARE / YZ(9,11),XRZ(11),YSTRZ,NZR,IZ
C
      J = 1
      IF(RE .LE. XRZ(J)) GO TO 20
      J = NZR
```

```
      IF(RE .GE. XRZ(J)) GO TO 20
      J = 1
 10   IF(RE .EQ. XRZ(J)) GO TO 20
      IF(RE .LT. XRZ(J+1)) GO TO 25
      J = J + 1
      IF( J .LT. NZR ) GO TO 10
  20  Y    =    YZ(IZ,J)
      GO TO 30
 25      Y = YZ(IZ,J) + (YZ(IZ,J+1) - YZ(IZ,J))*(RE - XRZ(J))/
     1   (XRZ(J+1) - XRZ(J))
  30  FIG          = Y*YSTRZ
      RETURN
      END


      FUNCTION FIG2( RE )
C
C   THE FRICTION FACTOR IS APPROXIMATED IN THIS SUBROUTINE.  THE VALUES ARE
C   GIVEN IN THE BLOCK DATA OBTAINED FROM FIGURE 16.  THIS IS APPROXIMATE
C   SINCE IT IS ONLY TO THE NEAREST VALUE OF REYNOLDS NUMBERS.
C   AN ALTERNATE CHOICE TO EMPLOY WOULD BE TO USE A CURVE FIT ON FIGURE 16.
C
      COMMON/ LMDARE / YL(12),XRL(12),YSTRL,NRL
C
      J = 1
      IF(RE .LE. XRL(J)) GO TO 20
      J = NRL
      IF(RE .GE. XRL(J)) GO TO 20
      J = 1
 10   IF(RE .EQ. XRL(J)) GO TO 20
      IF(RE .LT. XRL(J+1)) GO TO 25
      J = J + 1
      IF( J .LT. NRL) GO TO 10
 20   Y = YL(J)
      GO TO 30
 25   Y = YL(J) + (YL(J+1)- YL(J))*(RE - XRL(J))/(XRL(J+1) - XRL(J))
 30   FIG2 = Y*YSTRL
      RETURN
      END


      SUBROUTINE VALUE
C
C        THIS SUBROUTINE ACCOMPLISHES THE FLOW ANALYSIS.  ANY MODIFICATIONS TO
C   THE DESIRED OUTPUT SHOULD PROBABLY BE MADE IN THIS SUBROUTINE.
C   SINCE THE FLOW COEFFICIENT IS ALREADY KNOWN, ANY VALUES IN TERMS OF
C   PHI OR GEOMETRIC PARAMETERS CAN NOW BE EVALUATED
C
```

```
      REAL KB1,KB2,KB3,KB4,IR,IS,NU,LAMDAU,LAMDAL,LUBR,LLBS,LMBDU,LMBDL
      COMMON  R1,R2,R3,R4,KB1,KB2,KB3,KB4,RHO,ETAMU,ETAML,PHIO,B1B,A3B,
     1        BETA1,BETA2,ALPHA1,ALPHA2,ALPHA3,ALPHA4,B2B,A4B,BR,BS,
     2        IR,IS,PSIU,PSIL,RER,RES,REU,REL,PHI,ARR,ARS,YR,YS,CU,CL,
     3        CH2MH1,CH2MH3,CH3MH4,CH4MH1,AH2MH1,AH2MH3,AH3MH4,AH4MH1,
     4      BH2MH1,BH2MH3,BH3MH4,BH4MH1,CSUM,BSUM,ASUM,ROOT,PHIPR,PHIMR
      COMMON R2R1,R3R2,R4R2,BRR2,BRBS,NU,R1R2,R2R3,R2R4,R4R3,BSR2,BSR3,
     1        TORQUE,TAUR,OM,DELOM,LAMDAU,LAMDAL,LMBDU,LMBDL,LLBS,LUBR,
     2        ZETAU,ZETAL
      COMMON  CP,CF
      CCMMON JJ,JJJ,K
      COMMON TORREF,POWREF,PIOM,PITORQ,PIPOWR,OMMAX
C
C           VELOCITIES
C
      VM2 = PHI*OM*R2
      VU2 = VM2 * TAN(BETA2) + (R2*OM)
      V2  = SQRT(VU2**2 + VM2**2)
      VM1 = VM2 * R2R1 * KB2/KB1
      VU1 = VM1 * TAN(BETA1) + OM *R1
      V1 = SQRT(VU1**2 + VM1**2)
      VM3 = VM2 * R2R3 * BRBS * KB2/KB3
      VU3 = VU2 * R2R3 *ETAMU
      V3 = SQRT(VU3**2 + VM3**2)
      VM4 = VM2 * R2R4 * BRBS * KB2/KB4
      VU4 = VM4*TAN(ALPHA4)
      V4 = SQRT(VU4**2 + VM4**2)
      W1 = VM1/COS(BETA1)
      W2 = VM2/COS(BETA2)
C
C           ENERGY DIFFERENCES
C
C   ABSOLUTE ENERGY CHANGES
      ROM = (R2**2)*(OM**2)
      H2M1 = (CH2MH1 + PHI*BH2MH1 +(PHI**2)*AH2MH1)*ROM
      H2M3 = (CH2MH3 + PHI*BH2MH3 +(PHI**2)*AH2MH3)*ROM
      H3M4 = (CH3MH4 + PHI*BH3MH4 +(PHI**2)*AH3MH4)*ROM
      H4M1 = (CH4MH1 + PHI*BH4MH1 +(PHI**2)*AH4MH1)*ROM
C
C    DIMENSIONLESS ENERGY CHANGES AND INFUT
C
      H2M1N= (CH2MH1 + PHI*BH2MH1 +(PHI**2)*AH2MH1)
      H2M3N= (CH2MH3 + PHI*BH2MH3 +(PHI**2)*AH2MH3)
      H3M4N= (CH3MH4 + PHI*BH3MH4 +(PHI**2)*AH3MH4)
      H4M1N= (CH4MH1 + PHI*BH4MH1 +(PHI**2)*AH4MH1)
      ENERIN = OM *(R2*VU2 - R1*VU1)
      H2M1TH = ENERIN/ROM
      ROTLOS = H2M1TH - H2M1N
```

```
C
C           TOTAL PRESSURE DIFFERENCES
C
      RHOIN = RHO/144.
      TP2M1 = H2M1*RHOIN
      TP2M3 = H2M3*RHOIN
      TP3M4 = H3M4*RHOIN
      TP4M1 = H4M1*RHOIN
C
C           STATIC PRESSURE DIFFERENCES
C
      SP2M1 = TP2M1 + ((V1**2) - (V2**2))*RHOIN/2.
      SP2M3 = TP2M3 + ((V3**2) - (V2**2))*RHOIN/2.
      SP3M4 = TP3M4 + ((V4**2) - (V3**2))*RHOIN/2.
      SP4M1 = TP4M1 + ((V1**2) - (V4**2))*RHOIN/2.
C
C           LOSSES ENCOUNTERED
C
      ENLYR = YR*(W2**2)/(2.*ENERIN)
      ENLIR = (1.-(COS(IR)**2))*(W1**2)/(2.*ENERIN)
      ENLCU = CU*(VM3**2)/(2.*ENERIN)
      ENLEU = ((1./(ETAMU**2)) - 1.)*(VU3**2)/(2.*ENERIN)
      ENLYS = YS*(V4**2)/(2.*ENERIN)
      ENLIS = (1.- (COS(IS)**2))*(V3**2)/(2.*ENERIN)
      ENLCL = CL*(VM1**2)/(2.*ENERIN)
      ENLEL = ((1./(ETAML**2)) - 1.)*(VU1**2)/ (2.*ENERIN)
C
      PRINT 700
      PRINT 701,VM1,VM2,VM3,VM4
      PRINT 702,VU1,VU2,VU3,VU4
      PRINT 703,V1,V2,V3,V4
      PRINT 704,W1,W2
      PRINT 750,ENERIN
      PRINT 752
      PRINT 755
      PRINT 756,H2M1,H2M3,H3M4,H4M1
      PRINT 757
      PRINT 758,H2M1N
      PRINT 759,H2M3N
      PRINT 760,H3M4N
      PRINT 761,H4M1N
      PRINT 763,H2M1TH
      PRINT 764,ROTLOS
      PRINT 770
      PRINT 772
      PRINT 774,TP2M1,TP2M3,TP3M4,TP4M1
      PRINT 776
      PRINT 778
```

```
      PRINT 774,SP2M1,SP2M3,SP3M4,SP4M1
  700 FORMAT(1H0,23X,'1',11X,'2',11X,'3',11X,'4')
  701 FCRMAT( 1H ,' VM (FT/SEC)',4F12.1)
  702 FCRMAT( 1H ,' VU (FT/SEC)',4F12.1)
  703 FCRMAT( 1H ,' V  (FT/SEC)',4F12.1)
  704 FCRMAT( 1H ,' W  (FT/SEC)',4F12.1)
  750 FORMAT(1H0,'ENERGY INPUTED(FT-LB/SLUG)',F13.2)
  752 FORMAT(1H0,'  THE ENERGY CHANGES OVER EACH COMPONENT')
  755 FORMAT(1H0,23X,'H2-H1'7X'H2-H3',9X'H3-H4',8X'H1-H4')
  756 FORMAT(1H0,' H(FT-LBS/SLUG)', 4F12.1)
  757 FORMAT(1H0,'   THE DIMENSIONLESS ENERGY CHANGES OVER EACH COMPONEN
     1T')
  758 FORMAT(1H0,'(H2-H1)/(OM*R2)**2 = ', F13.2)
  759 FORMAT(1H ,'(H2-H3)/(OM*R2)**2 = ', F13.2)
  760 FORMAT(1H ,'(H3-H4)/(OM*R2)**2 = ', F13.2)
  761 FORMAT(1H ,'(H4-H1)/(OM*R2)**2 = ', F13.2)
  763 FORMAT(1H ,'DIMENSIONLESS ENERGY INPUT =',F6.2)
  764 FORMAT(1H ,'DIMENSIONLESS ROTOR LOSS =',F9.2)
  770 FORMAT(1H0,'   THE TOTAL PRESSURE CHANGES OVER EACH COMPONENT')
  772 FORMAT(1H0,22X,'TP2-TP1',5X,'TP2-TP3','TP3-TP4',6X,'TP1-TP4')
  774 FORMAT(1H0,' P(LBS/SQ.IN)', 4F12.1)
  776 FORMAT(1H0,'   THE STATIC PRESSURE CHANGES OVER EACH COMPONENT')
  778 FORMAT(1H0,22X,'SP2-SP1',5X,'SP2-SP3','SP3-SP4',6X,'SP1-SP4')
      RETURN
      END


      BLOCK DATA
C
C    THIS DATA IS OBTAINED FROM FIGURE 15. IT REPRESENTS THE VALUE OF THE
C    BENDING LOSS COEFFICIENT FOR VARIOUS VALUES OF TURNING RATIOS AND
C    REYNOLDS NUMBERS
C
      CCMMON/ ZETARE / YZ(9,11),XRZ(11),YSTRZ,NZR,IZ
      DATA YZ/1.00,.925,.780,.680,.600,.530,.470,.410,.362,
     1          .844,.760,.624,.540,.450,.384,.333,.288,.254,
     2          .747,.663,.532,.455,.375,.321,.275,.238,.212,
     3          .680,.595,.472,.394,.330,.285,.243,.213,.190,
     4          .632,.542,.429,.350,.296,.260,.225,.198,.179,
     5          .545,.456,.364,.289,.250,.227,.201,.180,.165,
     6          .483,.415,.330,.264,.235,.213,.195,.175,.160,
     7          .445,.390,.309,.250,.225,.204,.185,.170,.155,
     8         .450,.400,.315,.258,.225,.200,.180,.167,.151,
     9          .490,.430,.332,.270,.230,.200,.180,.167,.151,
     A          .500,.440,.340,.272,.232,.200,.180,.167,.151/,
     B          XRZ/2.E04,4.E04,6.E04,8.E04,1.E05,1.5E05,2.E05,3.E05,
     C          4.E05,6.E05,8.E05/,YSTRZ/1.0/,NZR/11/
      END
```

```
      BLOCK DATA
C
C     THIS DATA IS OBTAINED FROM FIGURE 16, AND ARE THE VALUES OF THE FRICTION
C     FACTOR AT VARIOUS REYNOLDS NUMBERS.
C
      COMMON/ LMDARE / YL(12),XRL(12),YSTRL,NRL
      DATA YL/.0265,.0233,.0218,.0204,.0193,.0185,.0173,.0165,.0155,
     1         .0148,.0141,.0137/,XRL/2.E04,3.E04,4.E04,6.E04,8.E04,
     2         1.E05,1.5E05,2.E05,3.E05,4.E05,6.E05,8.E05/,
     3         YSTRL/1.0/,NRL/12/
      END
```

APPENDIX D

PROGRAM REVERSE

Program REVERSE solves the equations for reverse circulation, Modes 3 and 4. The program is very similar to program NORMAL, and the flow chart of Table IV is the same. Further discussion would be mere repetition of Appendix C.

PROGRAM REVERSE

```
C
C           THIS PROGRAM SOLVES THE SET OF EQUATIONS PRESENTED IN APPENDIX B.
C     AN ITERATION TECHNIQUE IS NECESSARY TO SOLVE FOR PHI SINCE VARIOUS LOSS
C     COEFFICIENTS ARE PHI DEPENDENT.  A STRAIGHT QUADRATIC EQUATION SOLVES
C     THE ENERGY BALANCE EQUATION GIVEN BY EQUATION B2C.   AFTER CONVERGENCE
C     IS ACHIEVED, THE FLOW ANALYSIS AND NON-DIMENSIONALIZATION WILL BE ACCOM-
C     PLISHED.
C
C           IT MUST BE REMEMBERED THAT THIS SOLUTION IS ONLY VALID FOR THE CON-
C     DITION OF REVERSE CIRCULATION, MODES 3 AND 4.  THE ACTUAL DIFFERENCE BETWEEN
C     THE MODES IS THE DIRECTION OF SHAFT ROTATION.  THE FLOW EXIT ANGLES AT
C     THE ROTOR AND STATOR MUST REMAIN CONSTANT, HOWEVER, THE SIGNS WILL BE
C     CHANGED DUE TO THE SIGN CONVENTION EMPLOYED IN THE ANALYSIS.THAT IS ALL
C     ANGLES ARE POSITIVE IF THEIR PERIPHERAL COMPONENT OF VELOCITY IS IN THE
C     DIRECTION OF ROTATION.
C
C
C           THE DATA IS INPUTTED ON SEVEN(7) DATA CARDS.
C
C     CARD ONE:  THE MONTH, DAY, AND YEAR ARE PLACED IN COLUMNS1-5,6-10, AND 11-15
C     RESPECTIVELY.  NOTE THAT THESE INTEGERS MUST BE RIGHT HAND ADJUSTED.
C
C     CARD TWO:  COLUMNS 1 -5 THE RUN NUMBER, RIGHT ADJUSTED.  COLUMNS6-15 AND
C     16-25,THE RADIUS OF THE ROTOR INLET AND OUTLET(IN INCHES), RESPECTIVELY.
C     COLUMNS 26-35, THE INCREMENT OF ANGULAR SPEED(RAD/SECOND). COLUMNS 36-45,
C     VALUE OF PHI TO BEGIN ITERATIONS.  COLUMS 46-55, THE INITIAL ANGULAR SPEED.
C
C     CARD THREE:  THE BLOCKAGE FACTORS AT STATIONS 1,2,3, AND 4 ARE PLACED IN
C     COLUMNS 1-10,11-20,21-30,31-40.
C
C     CARD FOUR:  THE RELATIVE EXIT ANGLES AT ROTOR AND STATOR(IN DEGREES) GO IN
C     COLUMNS 1-10, AND 11-20.  THE ANGLE TO THE MEAN CAMBER LINE(IN DEGREES) FOR
C     ROTOR AND STATOR GO IN COLUMNS 21-30, AND 31-40, RESPECTIVELY.
C
C     CARD FIVE:  IN COLUMNS 1-10,11-20,21-30, AND 31-40 ARE PLACED THE COEFFI-
C     CIENT OF FRICTION, THE SPECIFIC HEAT OF THE FLUID, THE FLUID DENSITY(SLUGS
C     PER CUBIC FOOT), AND THE KINEMATIC VISCOSITY( FEET**2 PER SECOND)
C
C     CARD SIX:  THE RATIO OF THE AVERAGE LENGTH OF THE UPPER PASSAGE TO ROTOR
C     BLADE HIEGHT, THE RATIO OF THE AVERAGE LENGHT OF THE LOWER PASSAGE TO STATOR
```

```
C     BLADE HIEGHT, THE RADIUS OF THE INNER CONTOUR TO ROTOR BLADE HIEGHT, AND THE
C     RATIO OF THE ROTOR TO STATOR BLADE HIEGHT  GO IN COLUMNS 1-10,11-20,21-30,
C     AND 31-40, RESPECTIVELY.
C
C     CARD SEVEN:  THE RADIUS OF STATIONS 3 AND 4 AND THE BLADE HIEGHT OF THE
C     ROTOR AND STATOR(ALL VALUES ARE IN INCHES) ARE PLACED IN COLUMNS 1-10,11-20,
C     21-30,AND 31-40, RESPECTIVELY.
C
C
C     BLOCK DATA IS USED FOR CONVENIENCE DUE TO THE LARGE NUMBER OF SUBROUTINES.
C
      REAL KB1,KB2,KB3,KB4,IR,IS,NU,LAMDAU,LAMDAL,LUBS,LLBR,LMBDU,LMBDL
      COMMON   R1,R2,R3,R4,KB1,KB2,KB3,KB4,RHO,ETAMU,ETAML,PHIO,
     1         BETA1,BETA2,ALPHA1,ALPHA2,ALPHA3,ALPHA4,B2B,A4B,BR,BS,
     2         IR,IS,PSIU,PSIL,RER,RES,REU,REL,PHI,ARR,ARS,YR,YS,CU,CL,
     3         CH1MH2,CH3MH2,CH4MH3,CH1MH4,AH1MH2,AH3MH2,AH4MH3,AH1MH4,
     4      BH1MH2,BH3MH2,BH4MH3,BH1MH4,CSUM,BSUM,ASUM,ROOT,PHIPR,PHIMR
      COMMON R2R1,R3R1,R4R1,BRR1,BRBS,NU,R1R2,R1R3,R1R4,R3R4,BSR1,BSR4,
     1   TORQUE,TAUR,OM,DELOM,LAMDAU,LAMDAL,LUBS,LLBR,ZETAU,ZETAL,
     2   LMBDU,LMBDL
      COMMON   CP,CF
      COMMON JJ,JJJ,K
      CCMMON TORREF,POWREF,PIOM,PITORQ,PIPOWR,OMMAX
      COMMON/ ZETARE / YZ(9,11),XRZ(11),YSTRZ,NZR,IZ
      COMMON/ LMDARE / YL(12),XRL(12),YSTRL,NRL
C
C
C          ****DATA INPUT***
C
      READ 498,IMON,IDAY,IYEAR
      READ 499,IRUN,R1,R2,DELOM,PHIO,OMO
      READ 500,KB1,KB2,KB3,KB4
      READ 500,BETA1,ALPHA3,B2B,A4B
      READ 500,CF,CP,RHO,NU
      READ 500,LUBS,LLBR,RIBR,BRBS
      READ 500,R3,R4,BR,BS
      K = 0
C
C***        LIST DATA INPUT
C
      PRINT 509
      PRINT 540
      PRINT 510,IMON,IDAY,IYEAR
      OM = OMO
      PRINT 524
      PRINT 521
      PRINT 523,IRUN,R1,R2,DELOM,PHIO,OMO
   20 PRINT 513
```

```
      PRINT 501,KB1,KB2,KB3,KB4
      PRINT 514
      PRINT 501,BETA1,ALPHA3,B2B,A4B
      PRINT 515
      PRINT 530,CF,CP,RHO,NU
      PRINT 517
      PRINT 501,LUBS,LLBR,RIBR,BRBS
      PRINT 518
C
 498  FORMAT(3I5)
  499 FORMAT(I5,5F10.2)
  500 FORMAT(3F10.5,F10.8)
 501  FORMAT(1H ,4F10.3)
  503 FORMAT(1H ,4F10.4)
 509  FORMAT(1H1,'       ROLEK, LEO S.     ')
  510 FORMAT(1H0,'DATA =',3I5)
 513  FORMAT(1H0,7X,'KB1',7X,'KB2',7X,'KB3',7X,'KB4')
 514  FORMAT(1H0,5X,'BETA1',4X,'ALPHA3',7X,'B2B',7X,'A4B')
 515  FORMAT(1H0,7X,'CF',8X,'CP',7X,'RHO',13X,'NU')
 516  FORMAT(1H0,6X,'R2R1',6X,'R3R1',6X,'R4R1',6X,'BRR1')
 517  FORMAT(1H0,6X,'LUBS',6X,'LLBR',6X,'RIBR',6X,'BRBS')
 518  FORMAT(1H0,6X,'LMBDF',6X,'ZETA',6X,'  BR  ',6X,'  BS  ')
 521  FORMAT(1H0,3X,'IRUN',8X,'R1',9X,'R2',9X,'DELOM',8X,'PHIO',6X,'OMO'
     1)
 523  FORMAT(1H0,I5,5F12.2)
 524  FORMAT(1H0,'  CASE A.. FLOW IS RADIALLY INWARD AT ROTOR  ')
 530  FORMAT(1H0,2F10.3,F15.5,F15.8)
  540 FORMAT(1H0,10X,'FLOW EXITS ROTOR AT STATION 1, RETRACTION')
  550 FORMAT(1H0,7X,'R1',9X,'R2',9X,'R3',9X,'R4',9X,'BR',9X,'BS')
  551 FORMAT(1H0,6F12.2)
C
C*****                INITIALIZATION
C
      R2R1 = R2/R1
      R3R1 = R3/R1
      R4R1 = R4/R1
      BRR1 =  BR/R1
      R1INCH = R1
      R2INCH = R2
      R3INCH = R3R1*R1INCH
      R4INCH = R4R1*R1INCH
      BRINCH = BRR1*R1INCH
      BSINCH =  BRINCH/BRBS
      PRINT 516
      PRINT 503,R2R1,R3R1,R4R1,BRR1
      PRINT 550
      PRINT 551,R1INCH,R2INCH,R3INCH,R4INCH,BRINCH,BSINCH
      OMMAX = 800.*3.1416/30.0
```

```
      OM = OMMAX*0.1
      R1 = R1/12.
      R2 = R2/12.0
      BR= BRR1*R1
      BS= BR/BRBS
      AB1 = BETA1
      AA3 = ALPHA3
      BETA1 = 3.1416/180. * BETA1
      ALPHA3 = 3.1416/180. * ALPHA3
      B2B = 3.1416/180.*B2B
      A4B = 3.1416/180.*A4B
      R1R2 = 1./R2R1
      R1R3 = 1./R3R1
      R1R4 = 1./R4R1
      R3R4 = R3R1*R1R4
      BSR1 = BRR1/BRBS
      BSR4 = BSR1*R1R4
      ARR= BRR1/(R2R1-1.0)
      ARS = BSR4/(R3R4-1.0)
C    THE VALUE OF RIBR IS INITIALIZED HERE AND WILL BE USED IN SUBROUTINE FIG TO
C   OBTAIN VALUES OF THE BENDING LOSSES FROM FIGURE 15.
      IZ = 0
      IF (RIBR .LE. 0.25) IZ=1
      IF (RIBR .GE. 1.0)  IZ=9
      IF (IZ .NE. 0) GO TO 22
      REALIZ = RIBR*10.0 - 1.0
      IZ = REALIZ
C
C    INITIAL VALUES OF THE REYNOLDS NUMBERS ARE GIVEN TO BEGIN THE ITERATIONS.
   22 RER = 10.0**5
      RES = 10.0**5
      REU = 10.0**5
      REL = 10.0**5
      PHI = PHI0
      TORREF = RHO*(OMMAX**2)*(R2**5)
      POWREF = TORREF * OMMAX
      PRINT 410,POWREF
      PRINT 415,TORREF
  410 FORMAT(1H0,6X,'THE REFERENCE POWER IS',F13.3)
  415 FORMAT(1H0,6X,'THE REFERENCE TORQUE IS',F13.3)
      IF ( PHI .GT. 0.0 ) GO TO 30
C
      IR=0.
      IS = 0.0
      BETA2 = B2B
      ALPHA4 = A4B
      GO TO 30
C
```

```
C*****       CALCULATE PHI
C
 25    RER =ENRER ( PHI )
       RES =ENRES ( PHI )
 30    CALL EQG1
       CALL EQG2
       CALL EQH5
       CALL EQH6
       IF(PHI. LE. 0.0) GO TO 40
       TANB2 = (ETAMU*KB2/KB3*TAN(ALPHA3))- (R2R1**2)*(KB2/KB1)/PHI
       BETA2 = ATAN(TANB2)
       IR = B2B -BETA2
       TANA4 = (ETAML/(PHI*(KB1/KB4)))*(1. + PHI*TAN(BETA1))
       ALPHA4 = ATAN(TANA4)
       IS = A4B - ALPHA4
C
 40    YR = EQI8(RER,ARR,BETA1,BETA2)
       YS = EQI8(RES,ARS,ALPHA3,ALPHA4)
       CALL EQE28
       CALL EQF12
       CALL EQE13A
       CALL EQD9
       CALL PHITES
C
C   **** TESTING PHI
C
 100   IF ( K .GE. 1 ) GO TO 110
       K = 2
       PHIO = PHI
       GO TO 25
C
  110  TEST = ABS( (PHI - PHIO)/((PHI + PHIO)/2.) )
       IF ( TEST .LE. .0005 ) GO TO 120
C
       K = K + 1
C***            SAFETY OUTLET
       IF ( K .GT. 20 ) GO TO 120
         PHIO = PHI
        GO TO 25
C
C****** OUTPUT AND FLOW CALCULATIONS
C
 120   TAUR = EQB19( PHI )
       CALL EQB20
       DELBET = BETA1-BETA2
       DELALP = ALPHA3-ALPHA4
       DELALP = DELALP*180./3.1416
       DELBET = DELBET*180./3.1416
```

```
      DBETA2 = BETA2 *180.0/3.1416
      DALPH4 = ALPHA4*180.0/3.1416
      DIR = IR * 180.0/3.1416
      DIS = IS * 180.0/3.1416
      PRINT 300
      PRINT 299,K,PHI,TORQUE,TAUR,OM
      PRINT 325
      PRINT 308
      PPINT 302,YR,YS,CU,CL
      PRINT 309
      PRINT 302,ETAMU,ETAML,PSIU,PSIL
      PRINT 310
      PRINT 303,RER,RES,REU,REL
      PRINT 307
      PRINT 305,DBETA2,DALPH4,DIR,DIS
      PRINT 312
      PRINT 313,DELBET,DELALP
      CALL NONDEM
      CALL VALUE
      DELOM = OMMAX * 0 .1
      OM = OM + DELOM
      PHIO = PHI
       K = 1
      IF ( OM .LE. OMMAX ) GO TO 25
299   FORMAT(1H ,8X,I5,F15.4,F15.2,F15.5,F15.2)
 300  FORMAT(1H1,11X,' K ',10X,'PHI',10X,'TORQUE',10X,'TAUR',10X,'OM')
302   FORMAT(1H ,13X,4F15.3)
 303  FORMAT(1H ,20X,4E15.5)
305   FORMAT(1H0,22X,F10.4,10X,F10.4,10X,F10.4,10X,F10.4)
307   FORMAT(1H0,22X,'BETA2',11X,'ALPHA4',10X,' DIR ',11X,' DIS ')
 308  FORMAT(1H0,26X,'YR',13X,'YS',13X,'CU',13X,'CL')
309   FORMAT(1H0,23X,'ETAMU',11X,'ETAML',11X,'PSIU',11X,'PSIL')
310   FORMAT(1H0,25X,'RER',12X,'RES',12X,'REU',12X'REL')
 312  FORMAT(1H0,20X,'DELTA BETA', 3X,'DELTA ALPHA')
 313  FORMAT(1H ,12X,2F15.3)
 325  FORMAT(1H0,30X,'FLOW LOSS COEFFICIENTS')
      STOP
      END

      SUBROUTINE EQG1
C
C  FINDS CU AND REU
C
      REAL KB1,KB2,KB3,KB4,IR,IS,NU,LAMDAU,LAMDAL,LUBS,LLBR,LMBDU,LMBDL
      COMMON  P1,R2,R3,R4,KB1,KB2,KB3,KB4,RHO,ETAMU,ETAML,PHIO,
     1        BETA1,BETA2,ALPHA1,ALPHA2,ALPHA3,ALPHA4,B2B,A4B,BR,BS,
     2        IR,IS,PSIU,PSIL,RER,RES,REU,REL,PHI,ARR,ARS,YR,YS,CU,CL,
```

```
     3        CH1MH2,CH3MH2,CH4MH3,CH1MH4,AH1MH2,AH3MH2,AH4MH3,AH1MH4,
     4      BH1MH2,BH3MH2,BH4MH3,BH1MH4,CSUM,BSUM,ASUM,ROOT,PHIPR,PHIMR
      COMMON R2R1,R3R1,R4R1,BRR1,BRBS,NU,R1R2,R1R3,R1R4,R3R4,BSR1,BSR4,
     1   TORQUE,TAUR,OM,DELOM,LAMDAU,LAMDAL,LUBS,LLBR,ZETAU,ZETAL,
     2   LMBDU,LMBDL
      CCMMON  CP,CF
      COMMON JJ,JJJ,K
      CCMMCN/ ZETARE / YZ(9,11),XRZ(11),YSTRZ,NZR,IZ
      COMMON/ LMDARE / YL(12),XRL(12),YSTRL,NRL
C
      REU = (2.*BS/NU)*R1R3*(KB1/KB3)*OM*R1*PHI
      ZETAU = FIG(REU)
      LMBDU = FIG2(REU)
      CU = 2.0*ZETAU+ .5*LUBS*LMBDU
      RETURN
      END


      SUBROUTINE EQG2
C
C     FINDS CL AND REL
C
      REAL KB1,KB2,KB3,KB4,IR,IS,NU,LAMDAU,LAMDAL,LUBS,LLBR,LMBDU,LMBDL
      COMMON  R1,R2,R3,R4,KB1,KB2,KB3,KB4,RHO,ETAMU,ETAML,PHIO,
     1        BETA1,BETA2,ALPHA1,ALPHA2,ALPHA3,ALPHA4,B2B,A4B,BR,BS,
     2        IR,IS,PSIU,PSIL,RER,RES,REU,REL,PHI,ARR,ARS,YR,YS,CU,CL,
     3        CH1MH2,CH3MH2,CH4MH3,CH1MH4,AH1MH2,AH3MH2,AH4MH3,AH1MH4,
     4      BH1MH2,BH3MH2,BH4MH3,BH1MH4,CSUM,BSUM,ASUM,ROOT,PHIPR,PHIMR
      COMMON R2R1,R3R1,R4R1,BRR1,BRBS,NU,R1R2,R1R3,R1R4,R3R4,BSR1,BSR4,
     1   TORQUE,TAUR,OM,DELOM,LAMDAU,LAMDAL,LUBS,LLBR,ZETAU,ZETAL,
     2   LMBDU,LMBDL
      COMMON  CP,CF
      COMMON JJ,JJJ,K
      CCMMON/ ZETARE / YZ(9,11),XRZ(11),YSTRZ,NZR,IZ
      COMMON/ LMDARE / YL(12),XRL(12),YSTRL,NRL
C
      REL = (2.*BR/NU)*OM*R1*PHI
      LMBDL = FIG2(REL)
      ZETAL = FIG(REL)
      CL = 2.5*ZETAL+ .5 * LLBR * LMBDL
      RETURN
      END
```

```
      SUBROUTINE EQH5
C
C****    FINDS LAMBDA, ETA, AND PSI FOR THE LOWER PASSAGES
C
      REAL KB1,KB2,KB3,KB4,IR,IS,NU,LAMDAU,LAMDAL,LUBS,LLBR,LMBDU,LMBDL
      COMMON  R1,R2,R3,R4,KB1,KB2,KB3,KB4,RHO,ETAMU,ETAML,PHIO,
     1        BETA1,BETA2,ALPHA1,ALPHA2,ALPHA3,ALPHA4,B2B,A4B,BR,BS,
     2        IR,IS,PSIU,PSIL,RER,RES,REU,REL,PHI,ARR,ARS,YR,YS,CU,CL,
     3        CH1MH2,CH3MH2,CH4MH3,CH1MH4,AH1MH2,AH3MH2,AH4MH3,AH1MH4,
     4      BH1MH2,BH3MH2,BH4MH3,BH1MH4,CSUM,BSUM,ASUM,ROOT,PHIPR,PHIMR
      COMMON R2R1,R3R1,R4R1,BRR1,BRBS,NU,R1R2,R1R3,R1R4,R3R4,BSR1,BSR4,
     1   TORQUE,TAUR,OM,DELOM,LAMDAU,LAMDAL,LUBS,LLBR,ZETAU,ZETAL,
     2   LMBDU,LMBDL
      COMMON  CP,CF
      COMMON JJ,JJJ,K
C
C***** TAKING INTO ACCOUNT ABSOLUTE VALUE
      BBBB1 = ABS(BETA1)
      LAMDAL = CF*(TAN(BBBB1))*LLBR/KB1
      ETAML = 1.0 - LAMDAL
      PSIL = 1.0 -(ETAML**2)
      RETURN
      END


      SUBROUTINE EQH6
C
C*****   FINDS LAMBDA, ETA, AND PSI FOR THE UPPER PASSAGES
C
      REAL KB1,KB2,KB3,KB4,IR,IS,NU,LAMDAU,LAMDAL,LUBS,LLBR,LMBDU,LMBDL
      COMMON  R1,R2,R3,R4,KB1,KB2,KB3,KB4,RHO,ETAMU,ETAML,PHIO,
     1        BETA1,BETA2,ALPHA1,ALPHA2,ALPHA3,ALPHA4,B2B,A4B,BR,BS,
     2        IR,IS,PSIU,PSIL,RER,RES,REU,REL,PHI,ARR,ARS,YR,YS,CU,CL,
     3        CH1MH2,CH3MH2,CH4MH3,CH1MH4,AH1MH2,AH3MH2,AH4MH3,AH1MH4,
     4      BH1MH2,BH3MH2,BH4MH3,BH1MH4,CSUM,BSUM,ASUM,ROOT,PHIPR,PHIMR
      COMMON R2R1,R3R1,R4R1,BRR1,BRBS,NU,R1R2,R1R3,R1R4,R3R4,BSR1,BSR4,
     1   TORQUE,TAUR,OM,DELOM,LAMDAU,LAMDAL,LUBS,LLBR,ZETAU,ZETAL,
     2   LMBDU,LMBDL
      COMMON  CP,CF
      COMMON JJ,JJJ,K
      AAAAA3 = ABS(ALPHA3)
      LAMDAU = CF*TAN(AAAAA3)*LLBR/KB4
      ETAMU = 1.0 - LAMDAU
      PSIU = 1.0 -(ETAMU**2)
      RETURN
      END
```

```
      FUNCTION EQI8 (RE,AR,ANG1,ANG2)
C
C     CALCULATES THE LOSS CEFFICIENTS YR AND YS
C
      REAL KB1,KB2,KB3,KB4,IR,IS,NU,LAMDAU,LAMDAL,LUBS,LLBR,LMBDU,LMBDL
      COMMON   R1,R2,R3,R4,KB1,KB2,KB3,KB4,RHO,ETAMU,ETAML,PHIO,
     1         BETA1,BETA2,ALPHA1,ALPHA2,ALPHA3,ALPHA4,B2B,A4B,BR,BS,
     2         IR,IS,PSIU,PSIL,RER,RES,REU,REL,PHI,ARR,ARS,YR,YS,CU,CL,
     3         CH1MH2,CH3MH2,CH4MH3,CH1MH4,AH1MH2,AH3MH2,AH4MH3,AH1MH4,
     4       BH1MH2,BH3MH2,BH4MH3,BH1MH4,CSUM,BSUM,ASUM,ROOT,PHIPR,PHIMR
      COMMON R2R1,R3R1,R4R1,BRR1,BRBS,NU,R1R2,R1R3,R1R4,R3R4,BSR1,BSR4,
     1   TORQUE,TAUR,OM,DELOM,LAMDAU,LAMDAL,LUBS,LLBR,ZETAU,ZETAL,
     2   LMBDU,LMBDL
      COMMON   CP,CF
      COMMON JJ,JJJ,K
C
C***** TAKING INTO ACCOUNT ABSOLUTE VALUE
      DELANG = ABS(ANG1 - ANG2)
      DELBE = DELANG* 180./3.1416
      PSI = .99 - 2.28 * DELBE/(10.0**4) -4.97/(180.- DELBE)
      EQI8 = ((.975+.075/AR)/(PSI**2)-1.) * (((10.**5)/RE)**.25)
      RETURN
      END


      FUNCTION ENRER (PHII)
C
C****    CALCULATES THE REYNOLDS NUMBER OF THE ROTOR
C
      REAL KB1,KB2,KB3,KB4,IR,IS,NU,LAMDAU,LAMDAL,LUBS,LLBR,LMBDU,LMBDL
      COMMON   R1,R2,R3,R4,KB1,KB2,KB3,KB4,RHO,ETAMU,ETAML,PHIO,
     1         BETA1,BETA2,ALPHA1,ALPHA2,ALPHA3,ALPHA4,B2B,A4B,BR,BS,
     2         IR,IS,PSIU,PSIL,RER,RES,REU,REL,PHI,ARR,ARS,YR,YS,CU,CL,
     3         CH1MH2,CH3MH2,CH4MH3,CH1MH4,AH1MH2,AH3MH2,AH4MH3,AH1MH4,
     4       BH1MH2,BH3MH2,BH4MH3,BH1MH4,CSUM,BSUM,ASUM,ROOT,PHIPR,PHIMR
      COMMON R2R1,R3R1,R4R1,BRR1,BRBS,NU,R1R2,R1R3,R1R4,R3R4,BSR1,BSR4,
     1   TORQUE,TAUR,OM,DELOM,LAMDAU,LAMDAL,LUBS,LLBR,ZETAU,ZETAL,
     2   LMBDU,LMBDL
      COMMON   CP,CF
      COMMON JJ,JJJ,K
C
      X1 = (2.*BRR1*PHII*OM*R1**2)/NU
C***** TAKING INTO ACCOUNT ABSOLUTE VALUE
      ABB1 = ABS(TAN(BETA1) -TAN(B2B))
      X2 = BRR1*ABB1* (COS(BETA1)**2)
      X3 = .425*(R2R1 -1.0)
      ENRER = X1/(COS(BETA1) + X2/X3)
      RETURN
```

```
      END

      FUNCTION ENRES (PHII )
C
C        CALCULATES THE REYNOLDS NUMBER OF THE STATOR
C
      REAL KB1,KB2,KB3,KB4,IR,IS,NU,LAMDAU,LAMDAL,LUBS,LLBR,LMBDU,LMBDL
      COMMON  R1,R2,R3,R4,KB1,KB2,KB3,KB4,RHO.ETAMU.ETAML,PHIO,
     1        BETA1,BETA2,ALPHA1,ALPHA2,ALPHA3,ALPHA4,B2B,A4B,BR,BS,
     2        IR,IS,PSIU,PSIL,RER,RES,REU,REL,PHI,ARR,ARS,YR,YS,CU,CL,
     3        CH1MH2,CH3MH2,CH4MH3,CH1MH4,AH1MH2,AH3MH2,AH4MH3,AH1MH4,
     4      BH1MH2,BH3MH2,BH4MH3,BH1MH4,CSUM,BSUM,ASUM,ROOT,PHIPR,PHIMR
      COMMON R2R1,R3R1,R4R1,BRR1,BRBS,NU,R1R2,R1R3,R1R4,R3R4,BSR1,BSR4,
     1   TORQUE,TAUR,OM,DELOM,LAMDAU,LAMDAL,LUBS,LLBR,ZETAU,ZETAL,
     2   LMBDU,LMBDL
      COMMON  CP,CF
      CCMMON JJ,JJJ,K
C
      X1 = (2.*BS*CM*PHII*R1*R1R3*KB1/KB3)/NU
C***** TAKING INTO ACCOUNT ABSOLUTE VALUE
      AA43B = ABS(TAN(A4B) - TAN(ALPHA3))
      X2 = BS*AA43B*(COS(ALPHA3)**2)
      X3 = .425*R4R1*R1*(R3R4-1.0)
      ENRES = X1/(COS(ALPHA3) + X2/X3)
      RETUPN
      END


      SUBROUTINE EQE28
C
C     CALCULATES COEFFICIENTS OF (H1 - H2)/(OMEGA * R1)**2
C
      REAL KB1,KB2,KB3,KB4,IR,IS,NU,LAMDAU,LAMDAL,LUBS,LLBR,LMBDU,LMBDL
      COMMON  R1,R2,R3,R4,KB1,KB2,KB3,KB4,RHO,ETAMU.ETAML,PHIO,
     1        BETA1,BETA2,ALPHA1,ALPHA2,ALPHA3,ALPHA4,B2B,A4B,BR,BS,
     2        IR,IS,PSIU,PSIL,RER,RES,REU,REL,PHI,ARR,ARS,YR,YS,CU,CL,
     3        CH1MH2,CH3MH2,CH4MH3,CH1MH4,AH1MH2,AH3MH2,AH4MH3,AH1MH4,
     4      BH1MH2,BH3MH2,BH4MH3,BH1MH4.CSUM,BSUM,ASUM,ROOT,PHIPR,PHIMR
      COMMON R2R1,R3R1,R4R1,BRR1,BRBS,NU,R1R2,R1R3,R1R4,R3R4,BSR1,BSR4,
     1   TORQUE,TAUR,OM,DELOM,LAMDAU,LAMDAL,LUBS,LLBR,ZETAU,ZETAL,
     2   LMBDU.LMBDL
      COMMON  CP,CF
      CCMMON JJ,JJJ,K
C
      X1 = (1.0 - (COS(IR)**2))/(COS(BETA2)**2)
      CH1MH2 = 1.0
      BH1MH2 = TAN(BETA1) -(KB1/KB3)*ETAMU*TAN(ALPHA3)
```

```
      AH1MH2 = -YR/(2.*COS(BETA1)**2) -((R1R2*KB1/KB2)**2)*X1*0.5
      RETURN
      END

      SUBROUTINE EQF12
C
C    CALCULATES COEFFICIENTS OF (H3 - H2)/(OMEGA * R1)**2
C
C
      REAL KB1,KB2,KB3,KB4,IR,IS,NU,LAMDAU,LAMDAL,LUBS,LLBR,LMBDU,LMBDL
      COMMON   R1,R2,R3,R4,KB1,KB2,KB3,KB4,RHO,ETAMU,ETAML,PHIO,
     1         BETA1,BETA2,ALPHA1,ALPHA2,ALPHA3,ALPHA4,B2B,A4B,BR,BS,
     2         IR,IS,PSIU,PSIL,RER,RES,REU,REL,PHI,ARR,ARS,YR,YS,CU,CL,
     3         CH1MH2,CH3MH2,CH4MH3,CH1MH4,AH1MH2,AH3MH2,AH4MH3,AH1MH4,
     4       BH1MH2,BH3MH2,BH4MH3,BH1MH4,CSUM,BSUM,ASUM,ROOT,PHIPR,PHIMR
      COMMON R2R1,R3R1,R4R1,BRR1,BRBS,NU,R1R2,R1R3,R1R4,R3R4,BSR1,BSR4,
     1   TORQUE,TAUR,OM,DELOM,LAMDAU,LAMDAL,LUBS,LLBR,ZETAU,ZETAL,
     2   LMBDU,LMBDL
      COMMON   CP,CF
      COMMON JJ,JJJ,K
C
      X1 = (KB1/KB3)*TAN(ALPHA3)
      CH3MH2 = 0.0
      BH3MH2 = 0.0
      AH3MH2 = 0.5*(R1R2**2)*(CU * ((KB1/KB2)**2)+PSIU*(X1**2))
      RETURN
      END

      SUBROUTINE EQE13A
C
C    CALCULATES COEFFICIENTS OF (H4 - H3)/(OMEGA * R1)**2
C
      REAL KB1,KB2,KB3,KB4,IR,IS,NU,LAMDAU,LAMDAL,LUBS,LLBR,LMBDU,LMBDL
      COMMON   R1,R2,R3,R4,KB1,KB2,KB3,KB4,RHO,ETAMU,ETAML,PHIO,
     1         BETA1,BETA2,ALPHA1,ALPHA2,ALPHA3,ALPHA4,B2B,A4B,BR,BS,
     2         IR,IS,PSIU,PSIL,RER,RES,REU,REL,PHI,ARR,ARS,YR,YS,CU,CL,
     3         CH1MH2,CH3MH2,CH4MH3,CH1MH4,AH1MH2,AH3MH2,AH4MH3,AH1MH4,
     4       BH1MH2,BH3MH2,BH4MH3,BH1MH4,CSUM,BSUM,ASUM,ROOT,PHIPR,PHIMR
      COMMON R2R1,R3R1,R4R1,BRR1,BRBS,NU,R1R2,R1R3,R1R4,R3R4,BSR1,BSR4,
     1   TORQUE,TAUR,OM,DELOM,LAMDAU,LAMDAL,LUBS,LLBR,ZETAU,ZETAL,
     2   LMBDU,LMBDL
      COMMON   CP,CF
      COMMON JJ,JJJ,K
C
      X1 = ((1.-(COS(IS)**2))/2.)* ((R1R4)**2)
      X2 = (R1R3*(KB1/KB3)/(COS(ALPHA3)))**2
```

```
      CH4MH3 = X1*(ETAML**2)
      BH4MH3 = X1*2.*TAN(BETA1)*(ETAML**2)
      AH4MH3 = X1*(((KB1/KB4)**2)+(TAN(BETA1)**2))+.5*YS*X2
      RETURN
      END


      SUBROUTINE EQD9
C
C    CALCULATES COEFFICIENTS OF (H1 - H4)/(OMEGA * R1)**2
C
      REAL KB1,KB2,KB3,KB4,IR,IS,NU,LAMDAU,LAMDAL,LUBS,LLBR,LMBDU,LMBDL
      CCMMON  R1,R2,R3,R4,KB1,KB2,KB3,KB4,RHO,ETAMU,ETAML,PHIO,
     1        BETA1,BETA2,ALPHA1,ALPHA2,ALPHA3,ALPHA4,B2B,A4B,BR,BS,
     2        IR,IS,PSIU,PSIL,RER,RES,REU,REL,PHI,ARR,ARS,YR,YS,CU,CL,
     3        CH1MH2,CH3MH2,CH4MH3,CH1MH4,AH1MH2,AH3MH2,AH4MH3,AH1MH4,
     4     BH1MH2,BH3MH2,BH4MH3,BH1MH4,CSUM,BSUM,ASUM,ROOT,PHIPR,PHIMR
      COMMON R2R1,R3R1,R4R1,BRR1,BRBS,NU,R1R2,R1R3,R1R4,R3R4,BSR1,BSR4,
     1   TORQUE,TAUR,OM,DELOM,LAMDAU,LAMDAL,LUBS,LLBR,ZETAU,ZETAL,
     2   LMBDU,LMBDL
      COMMON  CP,CF
      COMMON JJ,JJJ,K
C
      X1 = (R1R4)**2
      CH1MH4 = .5*PSIL*X1
      BH1MH4 = PSIL*X1*TAN(BETA1)
      AH1MH4 = X1*.5*((CL*((KB1/KB4)*2)+PSIL*(TAN(BETA1)**2) ))
      RETURN
      END


      SUBROUTINE PHITES
C
C   ACCOMPLISHES THE FINAL ITERATION STEP IN DETERMINING PHI
C
      REAL KB1,KB2,KB3,KB4,IR,IS,NU,LAMDAU,LAMDAL,LUBS,LLBR,LMBDU,LMBDL
      COMMON  R1,R2,R3,R4,KB1,KB2,KB3,KP4,RHO,ETAMU,ETAML,PHIO,
     1        BETA1,BETA2,ALPHA1,ALPHA2,ALPHA3,ALPHA4,B2B,A4B,BR,BS,
     2        IR,IS,PSIU,PSIL,RER,RES,REU,REL,PHI,ARR,ARS,YR,YS,CU,CL,
     3        CH1MH2,CH3MH2,CH4MH3,CH1MH4,AH1MH2,AH3MH2,AH4MH3,AH1MH4,
     4     BH1MH2,BH3MH2,BH4MH3,BH1MH4,CSUM,BSUM,ASUM,ROOT,PHIPR,PHIMR
      COMMON R2R1,R3R1,R4R1,BRR1,BRBS,NU,R1R2,R1R3,R1R4,R3R4,BSR1,BSR4,
     1   TORQUE,TAUR,OM,DELOM,LAMDAU,LAMDAL,LUBS,LLBR,ZETAU,ZETAL,
     2   LMBDU,LMBDL
      CCMMON  CP,CF
      COMMON JJ,JJJ,K
C
C    THE PREVIOUS FOUR SUBROUTINES ARE NOW ADDED
```

```
      CSUM = CH1MH2 - CH3MH2 - CH4MH3 - CH1MH4
      BSUM = BH1MH2 - BH3MH2 - BH4MH3- BH1MH4
      ASUM = AH1MH2 - AH3MH2 - AH4MH3 - AH1MH4
C    THE QUADRATIC EQUATION IS NOW SOLVED TO YIELD THE NEW VALUE OF PHI.
      ROOT = SQRT((BSUM**2)- 4.0*ASUM * CSUM)
      PHIPR = (-BSUM + ROOT)/ (2.0*ASUM)
      PHIMR = (-BSUM - ROOT)/ (2.0*ASUM)
C*** IF PHI IS NEGATIVE, CASE A IS NOT TAKING PLACE
C    TESTING FOR THE PROPER ROOT
      JJ = 0
      JJJ= 0
      IF (PHIMR. LT. 0.0 ) GO TO 2
      IF ( PHIMR. GT. 0.0) GO TO 5
  2   IF ( PHIPR .LT. 0.0 ) GO TO 15
      IF (PHIPR .GT. 0.0 ) GO TO 6
  5   PHI = PHIMR
      GO TO 80
 15   PRINT 20
  6   PHI = PHIPR
 80   PRINT 90,PHI,PHIMR,PHIPR
 90   FORMAT(1H0,3X,'PHI=',F1C.5,3X,'PHIMR=',F10.5,' PHIPR = ',F10.5)
 20   FORMAT(1H0,' BOTH ROOTS OF PHI ARE NEGATIVE, AND THE PROGRAM WILL BE
     1 CUMPED************************')
      IF ( PHI .LT. 0.0 ) JJ = 1
      IF ( JJ .EQ. 1 ) GO TO 10
      IF (JJJ .EQ. 1 ) GO TO 10
      RETURN
 10   PRINT 11,JJ,JJJ
 11   FORMAT(1H0,'JJ = ',I5,'JJJ = ',I5)
      RETURN
      END


      FUNCTION EQB19 (PHII)
C******     CALCULATES TAUR COEFFICIENTS
C
      REAL KB1,KB2,KB3,KB4,IR,IS,NU,LAMDAU,LAMDAL,LUBS,LLBR,LMBDU,LMBDL
      CCMMON   R1,R2,R3,R4,KB1,KB2,KB3,KB4,RHO,ETAMU,ETAML,PHIO,
     1         BETA1,BETA2,ALPHA1,ALPHA2,ALPHA3,ALPHA4,B2B,A4B,BR,BS,
     2         IR,IS,PSIU,PSIL,RER,RES,REU,REL,PHI,ARR,ARS,YR,YS,CU,CL,
     3         CH1MH2,CH3MH2,CH4MH3,CH1MH4,AH1MH2,AH3MH2,AH4MH3,AH1MH4,
     4       BH1MH2,BH3MH2,BH4MH3,BH1MH4,CSUM,BSUM,ASUM,ROOT,PHIPR,PHIMR
      COMMON R2R1,R3R1,R4R1,BRR1,BRBS,NU,R1R2,R1R3,R1R4,R3R4,BSR1,BSR4,
     1   TORQUE,TAUR,OM,DELOM,LAMDAU,LAMDAL,LUBS,LLBR,ZETAU,ZETAL,
     2   LMBDU,LMBDL
      CCMMON   CP,CF
      COMMON JJ,JJJ,K
C
```

```
      EQB19 = PHII + (PHII**2)*(TAN(BETA1)- ETAMU * KB1/KB3*TAN(ALPHA3))
      RETURN
      END


      SUBROUTINE EQB20
C*******      CALCULATES TORQUE
C
      REAL KB1,KB2,KB3,KB4,IR,IS,NU,LAMDAU,LAMDAL,LUBS,LLBR,LMBDU,LMBDL
      CCMMON  R1,R2,R3,R4,KB1,KB2,KB3,KB4,RHO,ETAMU,ETAML,PHIO,
     1        BETA1,BETA2,ALPHA1,ALPHA2,ALPHA3,ALPHA4,B2B,A4B,BR,BS,
     2        IR,IS,PSIU,PSIL,RER,RES,REU,REL,PHI,ARR,ARS,YR,YS,CU,CL,
     3        CH1MH2,CH3MH2,CH4MH3,CH1MH4,AH1MH2,AH3MH2,AH4MH3,AH1MH4,
     4      BH1MH2,BH3MH2,BH4MH3,BH1MH4,CSUM,BSUM,ASUM,ROOT,PHIPR,PHIMR
      COMMON R2R1,R3R1,R4R1,BRR1,BRBS,NU,R1R2,R1R3,R1R4,R3R4,BSR1,BSR4,
     1   TORQUE,TAUR,OM,DELOM,LAMDAU,LAMDAL,LUBS,LLBR,ZETAU,ZETAL,
     2   LMBDU,LMBDL
      CCMMON  CP,CF
      COMMON JJ,JJJ,K
C
      TORQUE = 2.*3.1416*RHO*(OM**2)*(R1**5)*(BRR1)*      TAUR
      RETURN
      END


      SUBROUTINE NONDEM
C
C     ACCOMPLISHES THE NON-DIMENSIONALIZATION
C
      REAL KB1,KB2,KB3,KB4,IR,IS,NU,LAMDAU,LAMDAL,LUBS,LLBR,LMBDU,LMBDL
      CCMMON  R1,R2,R3,R4,KB1,KB2,KB3,KB4,RHO,ETAMU,ETAML,PHIO,
     1        BETA1,BETA2,ALPHA1,ALPHA2,ALPHA3,ALPHA4,B2B,A4B,BR,BS,
     2        IR,IS,PSIU,PSIL,RER,RES,REU,REL,PHI,ARR,ARS,YR,YS,CU,CL,
     3        CH1MH2,CH3MH2,CH4MH3,CH1MH4,AH1MH2,AH3MH2,AH4MH3,AH1MH4,
     4      BH1MH2,BH3MH2,BH4MH3,BH1MH4,CSUM,BSUM,ASUM,ROOT,PHIPR,PHIMR
      CCMMON R2R1,R3R1,R4R1,BRR1,BRBS,NU,R1R2,R1R3,R1R4,R3R4,BSR1,BSR4,
     1   TORQUE,TAUR,OM,DELOM,LAMDAU,LAMDAL,LUBS,LLBR,ZETAU,ZETAL,
     2   LMBDU.LMBDL
      CCMMON  CP,CF
      COMMON JJ,JJJ,K
      CCMMON TORREF,POWREF,PIOM,PITORQ,PIPOWR,OMMAX
      PIOM = OM/OMMAX
      PITORQ = TORQUE/TORREF
      PIPOWR = (OM*TORQUE)/POWREF
      PIPHI = PHI*PIOM
      PRINT 600,PIOM
      PRINT 605,PIPOWR
      PRINT 609,PITORQ
```

```
      PRINT 611,PIPHI
  600 FORMAT(1H0,15X,'THE DIMENSIONLESS ROTATIONAL SPEED=',F6.3)
  605 FORMAT(1H0,15X,'THE DIMENSIONLESS POWER =',F16.3)
  609 FORMAT(1H0,15X,'THE DIMENSIONLESS TORQUE =',F15.3)
  611 FORMAT(1H0,15X,'THE REVISED FLOW COEFFICIENT =',F9.3)
      RETURN
      END


      FUNCTION FIG( RE )
C
      COMMON/ ZETARE / YZ(9,11),XRZ(11),YSTRZ,NZR,IZ
C
C   THE BENDING LOSS COEFFICIENT IS APPROXIMATED FOR IN THIS SUBROUTINE
C   AN ALTERNATE CHOICE TO EMPLOY WOULD BE TO USE A CURVE FIT ON FIGURE 15.
C
      J = 1
      IF(RE .LE. XRZ(J)) GO TO 20
      J = NZR
      IF(RE .GE. XRZ(J)) GO TO 20
      J = 1
  10  IF(RE .EQ. XRZ(J)) GO TO 20
      IF(RE .LT. XRZ(J+1)) GO TO 25
      J = J + 1
      IF( J .LT. NZR ) GO TO 10
   20 Y   =    YZ(IZ,J)
      GO TO 30
  25     Y = YZ(IZ,J) + (YZ(IZ,J+1) - YZ(IZ,J))*(RE - XRZ(J))/
     1   (XRZ(J+1) - XRZ(J))
   30 FIG        = Y*YSTRZ
      RETURN
      END


      FUNCTION FIG2( RE )
C
C   THE FRICTION FACTOR IS APPROXIMATED IN THIS SUBROUTINE.  THE VALUES ARE
C   GIVEN IN THE BLOCK DATA OBTAINED FROM FIGURE 16.  THIS IS APPROXIMATE
C   SINCE IT IS ONLY TO THE NEAREST VALUE OF REYNOLDS NUMBERS.
C   AN ALTERNATE CHOICE TO EMPLOY WOULD BE TO USE A CURVE FIT ON FIGURE 16.
C
      COMMON/ LMDARE / YL(12),XRL(12),YSTRL,NRL
C
C
      J = 1
      IF(RE .LE. XRL(J)) GO TO 20
      J = NRL
      IF(RE .GE. XRL(J)) GO TO 20
```

```
      J = 1
   10 IF(RE .EQ. XRL(J)) GO TO 20
      IF(RE .LT. XRL(J+1)) GO TO 25
      J = J + 1
      IF( J .LT. NRL) GO TO 10
   20 Y = YL(J)
      GO TO 30
   25 Y = YL(J) + (YL(J+1)- YL(J))*(RE - XRL(J))/(XRL(J+1) - XRL(J))
   30 FIG2 = Y*YSTRL
      RETURN
      END


      SUBROUTINE VALUE
C
C        THIS SUBROUTINE ACCOMPLISHES THE FLOW ANALYSIS.  ANY MODIFICATIONS TO
C   THE DESIRED OUTPUT SHOULD PROBABLY BE MADE IN THIS SUBROUTINE.
C   SINCE THE FLOW COEFFICIENT IS ALREADY KNOWN, ANY VALUES IN TERMS OF
C   PHI OR GEOMETRIC PARAMETERS CAN NOW BE EVALUATED.
C
      REAL KB1,KB2,KB3,KB4,IR,IS,NU,LAMDAU,LAMDAL,LUBS,LLBR,LMBDU,LMBDL
      COMMON  R1,R2,R3,R4,KB1,KB2,KB3,KB4,RHO,ETAMU,ETAML,PHIO,
     1        BETA1,BETA2,ALPHA1,ALPHA2,ALPHA3,ALPHA4,B2B,A4B,BR,BS,
     2        IR,IS,PSIU,PSIL,RER,RES,REU,REL,PHI,ARR,ARS,YR,YS,CU,CL,
     3        CH1MH2,CH3MH2,CH4MH3,CH1MH4,AH1MH2,AH3MH2,AH4MH3,AH1MH4,
     4      BH1MH2,BH3MH2,BH4MH3,BH1MH4,CSUM,BSUM,ASUM,ROOT,PHIPR,PHIMR
      COMMON R2R1,R3R1,R4R1,BRR1,BRBS,NU,R1R2,R1R3,R1R4,R3R4,BSR1,BSR4,
     1   TORQUE,TAUR,OM,DELOM,LAMDAU,LAMDAL,LUBS,LLBR,ZETAU,ZETAL,
     2   LMBDU,LMBDL
C
C             VELOCITIES
C
      R2R3 = R2R1*R1R3
      R3R2 = 1./R2R3
      VM1 = OM*R1*PHI
      VU1 = OM*R1*(1. + PHI * TAN(BETA1))
      V1  = SQRT(VU1**2 + VM1**2)
      VM4 = VM1 * R1R4*BRBS*KB1/KB4
      VU4 = ETAML*R1R4* VU1
      V4  = SQRT(VU4**2 + VM4**2)
      VM3 = VM1 * R1R2*BRBS*KB1*R2R3/KB3
      VU3 = VM3*TAN(ALPHA3)
      V3  = SQRT(VU3**2 + VM3**2)
      VM2 = VM1 * R1R2*KB1/KB2
      VU2 = ETAMU*R3R2*VU3
      V2  = SQRT(VU2**2 + VM2**2)
      W1 = VM1/COS(BETA1)
      W2 = VM2/COS(BETA2)
```

```
C
C   ENERGY DIFFERENCES
      ROM = (R1**2)*(OM**2)
C    ABSOLUTE ENERGY DIFFERENCES
C
      H1M2 = (CH1MH2 + PHI*BH1MH2 +(PHI**2)*AH1MH2)*ROM
      H1M4 = (CH1MH4 + PHI*BH1MH4 +(PHI**2)*AH1MH4)*ROM
      H4M3 = (CH4MH3 + PHI*BH4MH3 +(PHI**2)*AH4MH3)*ROM
      H3M2 = (CH3MH2 + PHI*BH3MH2 +(PHI**2)*AH3MH2)*ROM
C
C    DIMENSIONLESS ENERGY DIFFERENCES OVER THE VARIOUS COMPONENTS
C   THE FOLLOWINT TERMS ARE DELTA H/OMEGA**2 * R2**2
C  NON DIMENSIONALIZATION IS IN TERMS OF R2
C
      AD = (R1R2**2)
      H1M2N= (CH1MH2 + PHI*BH1MH2 +(PHI**2)*AH1MH2)*AD
      H1M4N= (CH1MH4 + PHI*BH1MH4 +(PHI**2)*AH1MH4)*AD
      H4M3N= (CH4MH3 + PHI*BH4MH3 +(PHI**2)*AH4MH3)*AD
      H3M2N= (CH3MH2 + PHI*BH3MH2 +(PHI**2)*AH3MH2)*AD
      ENERIN = OM*(R1*VU1 -R2*VU2)
      H1M2TH =(ENERIN/ROM)*AD
      ROTLOS = H1M2TH -H1M2N
C
      PRINT 700
      PRINT 701,VM1,VM2,VM3,VM4
      PRINT 702,VU1,VU2,VU3,VU4
      PRINT 703,V1,V2,V3,V4
      PRINT 704,W1,W2
  700 FORMAT(1H0,23X,'1',11X,'2',11X,'3',11X,'4')
  701 FORMAT( 1H ,' VM (FT/SEC)',4F12.2)
  702 FORMAT( 1H ,' VU (FT/SEC)',4F12.2)
  703 FCRMAT( 1H ,' V  (FT/SEC)',4F12.2)
  704 FORMAT( 1H ,' W  (FT/SEC)',4F12.2)
      PRINT 750,ENERIN
      PRINT 752
      PRINT 755
      PRINT 756,H1M2,H1M4,H4M3,H3M2
      PRINT 757
      PRINT 758,H1M2N
      PRINT 759,H1M4N
      PRINT 760,H4M3N
      PRINT 761,H3M2N
      PRINT 763,H1M2TH
       PPINT 764,ROTLOS
  750 FORMAT(1H0,'ENERGY INPUTED(FT-LB/SLUG)',F13.2)
  752 FORMAT(1H0,'  THE ENERGY CHANGES OVER EACH COMPONENT')
  755 FORMAT(1H0,23X,'H1-H2'7X'H1-H4',9X'H4-H3',8X'H3-H2')
  756 FORMAT(1H0,' H(FT-LBS/SLUG)', 4F12.1)
```

```
  757 FORMAT(1HO,'   THE DIMENSIONLESS ENERGY CHANGES OVER EACH COMPONEN
     1T')
  758 FORMAT(1HO,'(H1-H2)/(OM*R2)**2 = ', F13.2)
  759 FORMAT(1H ,'(H1-H4)/(OM*R2)**2 = ', F13.2)
  760 FORMAT(1H ,'(H4-H3)/(OM*R2)**2 = ', F13.2)
  761 FORMAT(1H ,'(H3-H2)/(OM*R2)**2 = ', F13.2)
  763 FORMAT(1H ,'DIMENSIONLESS ENERGY INPUT =',F6.2)
  764 FORMAT(1H ,'DIMENSICNLESS ROTOR LOSS =',F9.2)
      RETURN
      END

      BLOCK DATA
C
C   THIS DATA IS OBTAINED FROM FIGURE 15. IT REPRESENTS THE VALUE OF THE
C   BENDING LOSS COEFFICIENT FOR VARIOUS VALUES OF TURNING RATIOS AND
C   REYNOLDS NUMBERS
C
      COMMON/ ZETARE / YZ(9,11),XRZ(11),YSTRZ,NZR,IZ.
      DATA YZ/1.00,.925,.780,.680,.600,.530,.470,.410,.362,
     1        .844,.760,.624,.540,.450,.384,.333,.288,.254,
     2        .747,.663,.532,.455,.375,.321,.275,.238,.212,
     3        .680,.595,.472,.394,.330,.285,.243,.213,.190,
     4        .632,.542,.429,.350,.296,.260,.225,.198,.179,
     5        .545,.456,.364,.289,.250,.227,.201,.180,.165,
     6        .483,.415,.330,.264,.235,.213,.195,.175,.160,
     7        .445,.390,.309,.250,.225,.204,.185,.170,.155,
     8       .450,.400,.315,.258,.225,.200,.180,.167,.151,
     9        .490,.430,.332,.270,.230,.200,.180,.167,.151,
     A        .500,.440,.340,.272,.232,.200,.180,.167,.151/,
     B        XRZ/2.E04,4.EC4,6.E04,8.EC4,1.E05,1.5E05,2.E05,3.E05,
     C        4.EC5,6.E05,8.E05/,YSTRZ/1.0/,NZR/11/
      END

      BLOCK DATA
C
C   THIS DATA IS OBTAINED FROM FIGURE 16, AND ARE THE VALUES OF THE FRICTION
C   FACTOR AT VARIOUS REYNOLDS NUMBERS.
C
      COMMON/ LMDARE / YL(12),XRL(12),YSTRL,NRL
      DATA YL/.0265,.0233,.0218,.0204,.C193,.0185,.0173,.0165,.0155,
     1        .0148,.0141,.0137/,XRL/2.E04,3.E04,4.E04,6.E04,8.E04,
     2        1.E05,1.5E05,2.E05,3.E05,4.EC5,6.E05,8.E05/,
     3        YSTRL/1.0/,NRL/12/
      END
```

REFERENCES

1. Naval Air Engineering Center, Engineering Department (SI) Report Misc-08998, Theoretical Performance of Programmed Drum Arresting Gear, by William Clark, 1 July 1970.

2. Vavra, M. H., Energy Absorber, April 1970.

3. Vavra, M. H., Aero-Thermodynamics and Flow in Turbomachines. New York: John Wiley and Sons, 1960.

4. Horlock, J.H., Journal of the Institute of Mechanical Science, Vol. 2, p. 48-75, 1960.

5. Zweifel, O., "The Spacing of Turbomachine Bladings", Brown Boveri Company Review, December, 1945.

6. Sprenger, H., Schweiz Bauzeitung, 87th year, no. 13, p. 223-231, 1969.

7. Biolley, A., Schweiz Bauzeitung, Vol. 118, no. 8, p. 85-86, 1941.

INITIAL DISTRIBUTION LIST

		No. Copies
1.	Defense Documentation Center Cameron Station Alexandria, Virginia 22314	2
2.	Library, Code 0212 Naval Postgraduate School Monterey, California 93940	2
3.	Professor T. H. Gawain, Code 57Gn Department of Aeronautics Naval Postgraduate School Monterey, California 93940	2
4.	Chairman, Code 57 Department of Aeronautics Naval Postgraduate School Monterey, California 93940	1
5.	Assoc. Professor R. D. Zucker, Code 57Zu Department of Aeronautics Naval Postgraduate School Monterey, California 93940	1
6.	Professor M. H. Vavra, Code 57Va Department of Aeronautics Naval Postgraduate School Monterey, California 93940	5
7.	ENS Leo S. Rolek, Jr. USN 9808 Avenue J Chicago, Illinois 60617	1

DOCUMENT CONTROL DATA - R & D

(Security classification of title, body of abstract and indexing annotation must be entered when the overall report is classified)

RIGINATING ACTIVITY *(Corporate author)* Naval Postgraduate School Monterey, California 93940	2a. REPORT SECURITY CLASSIFICATION Unclassified 2b. GROUP

EPORT TITLE

Performance Analysis of a Turbo-Type Energy Absorber for an Aircraft Carrier Arresting Gear

ESCRIPTIVE NOTES *(Type of report and inclusive dates)*

Master's Thesis; June 1971

UTHOR(S) *(First name, middle initial, last name)*

Leo S. Rolek, Jr.

EPORT DATE June 1971	7a. TOTAL NO. OF PAGES 132	7b. NO. OF REFS 7
CONTRACT OR GRANT NO. PROJECT NO.	9a. ORIGINATOR'S REPORT NUMBER(S) 9b. OTHER REPORT NO(S) *(Any other numbers that may be assigned this report)*	

DISTRIBUTION STATEMENT

Approved for public release; distribution unlimited.

SUPPLEMENTARY NOTES	12. SPONSORING MILITARY ACTIVITY Naval Postgraduate School Monterey, California 93940

ABSTRACT

The increasing weight and speed of carrier based aircraft are taxing the limit of conventional piston type energy absorbers which are used for arresting gear. Turbo-type absorbers have been proposed as an alternative. This study investigates a turbo-type energy absorber for an aircraft arresting gear under development by the Naval Air Engineering Center. A mathematical analysis, computer simulation and performance prediction are given for each mode of operation. It was initially expected that the absorber could operate in just two modes, forward and reverse, but the analysis shows that four distinct modes are possible, since not only shaft rotation but the path of fluid flow can be reversed. Theoretical performance predictions are also compared with test data from an existing smaller scale version of the absorber. The agreement is excellent. An approximation of scaling effects on power absorption is also presented. It is concluded that the turbo-type absorber is basically adequate to meet the demands of carrier operation for the forseeable future.

KEY WORDS	LINK A		LINK B		LINK C	
	ROLE	WT	ROLE	WT	ROLE	WT
urbo-type energy absorber						
rresting gear						

128616
Thesis
R68945 Rolek
c.1 Performance analysis
of a turbo-type energy
absorber for an air-
craft carrier arresting
gear.

128616
Thesis
R68945 Rolek
c.1 Performance analysis
of a turbo-type energy
absorber for an air-
craft carrier arresting
gear.

thesR68945
Performance analysis of a turbo-type ene
3 2768 001 98109 5
DUDLEY KNOX LIBRARY